FAULT DETECTION AND IDENTIFICATION USING WIGNER-VILLE DISTRIBUTION

By

M.S. SAFIZADEH, A.A. LAKIS and M. THOMAS

Department of Mechanical Engineering
École Polytechnique de Montréal

1999

No. EPM/RT-99/6

NOMENCLATURE

$s(t)$	Magnitude of the vibration signal with zero mean
$S(\omega)$	Spectrum of the signal $s(t)$
$P(t,\omega)$	The joint distribution function of time and frequency
$\Omega(t)$	The first order moment of the $P(t,\omega)$ with respect to frequency
$T(\omega)$	The first order moment of the $P(t,\omega)$ with respect to time
$v(t)$	Amplitude of the signal $s(t)$
$\varphi(t)$	Phase of the signal $s(t)$
$A(\omega)$	Spectral amplitude of the signal $S(\omega)$
$\psi(\omega)$	Spectral phase of the signal $S(\omega)$
	Wigner distribution
$R(t,\tau)$	Instantaneous auto correlation function
$s_I(t)$	Imaginary part of the signal
$s_R(t)$	Real part of the signal
$WVD(t,\omega)$	Wigner-Ville distribution
$PWD(t,\omega)$	pseudo-Wigner distribution
$SWD(t,\omega)$	smoothed Wigner distribution
$e(t,\omega)$	Energy density in time and frequency
$\varphi(\theta,\tau)$	Kernel function
$CWD(t,\omega)$	Choi-Williams distribution
$RID(t,\omega)$	reduced interference distribution
$BJC(t,\omega)$	Born-Jordan-Cohen distribution

LEGENDS OF FIGURES

ABSTRACT

Time-frequency analysis is relatively new in the field of mechanical signal processing and has yet to be applied to its full potential. This method of analysis is effective in the detection of faults in machinery and, in certain instances, is the most efficient method available. In this paper, some of the methods of time-frequency analysis such as the Wigner Distribution. the Choi-Williams Distribution, and the RID Distribution, are briefly reviewed and the advantages and disadvantages of each are considered. The efficacy of each method is tested by the practical application of an in-house software program developed for all time-frequency methods. Firstly. computer-generated signals are used to determine the effectiveness of a method. Secondly, the signal recorded from an experimental set-up is applied in order to verify performance. Finally, the various methods are evaluated using real-life signals recorded from a defective gearbox and a defective dryer machine. This paper demonstrates the effectiveness of time-frequency analysis in presenting a clear and exact representation of a signal, and compares the results with those obtained using the Short-Time Fourier Transform and traditional methods of analyzing signals measured on a rotating machine.

1. INTRODUCTION

The primary objective of all research into signal processing has been to find an efficient method which would generate results rapidly and clearly and in a manner which could be relatively easily interpreted.

The Short-Time Fourier Transform (STFT), used as a time-frequency representation of the signal energy, was one of the first attempts to see a signal in three dimensions and obtain rapid calculation and clear interpretation. The STFT is obtained by applying a fixed-length moving window to the non-stationary data sequence prior to computing the spectrum. The result is a time average of the signal spectrum over the window width. However, although this method provides a time-frequency representation of the signal, both the time and the frequency resolution are completely dependent upon the choice of the window length and the method does not satisfy certain prerequisites for a joint time-frequency distribution.

Use of the STFT in the solution of problems in signal processing was followed by the development of time-frequency methods. Researchers tried to find a way to show the distribution of signal energy as a joint function of time and frequency which. on the one hand, satisfied certain conditions and, on the other hand, reduced the time-frequency resolution dependence on the window.

The Wigner Distribution (WD), first used in quantum mechanics [1], has been used to overcome the problem of the STFT. It was employed in signal processing by Ville in 1948 [2]. The WD has very desirable properties which have been extensively investigated by Classen and Mecklenbrauker [3]. The major draw-back of the WD is the presence of cross terms between frequency components in the time-frequency plane. Cross terms and their properties have been

studied by Hlawatsch and Flandrin [4-5].

Some smoothing of the Wigner Distribution is needed to suppress the cross terms. A windowed-Wigner Distribution by a function that is peaked around τ , $h(\tau)$, will be called a pseudo-Wigner Distribution (PWD) [3]. If the smoothing is carried out in both the time and frequency domains, the distribution will be called a smoothed Wigner Distribution (SWD) [6]. In addition to the Wigner Distribution, several others have been developed but all had the problem of cross terms [7-8]. In 1966, Cohen provided a general formula for generating different distributions [9]. Other distributions are obtained by changing an arbitrary function called the kernel. In his recent work, he gave a complete review of the time-frequency distributions [10].

Instead of smoothing the Wigner Distribution to eliminate the cross terms, Choi-Williams introduced a new kernel which can reduce the cross terms [11]. Unfortunately, the Choi-Williams Distribution does not completely satisfy the support properties in time and frequency. Recently, Jeong and Williams [12] defined the conditions which a kernel must satisfy to suppress the cross terms. This class of distribution is called the Reduced Interference Distributions (RID), and is an improved version of the exponential distribution.

It can be seen that each distribution has both advantages and disadvantages; the choice of distribution for a given practical application depends on the problem concerned. In Section 2, the necessary properties of a time-frequency distribution are summarized, time-frequency distributions are compared, and their advantages and disadvantages are given.

In Section 3, the history of time-frequency applications is presented; an in-house software developed for time-frequency distribution is discussed; and the effectiveness of the time-

frequency distribution is shown by analyzing signals measured from experimental and on-site tests.

2. TIME-FREQUENCY DISTRIBUTIONS

2.1 Time-Frequency Distribution Property Requirements

An ideal joint time-frequency function of signal $s(t)$ possesses a number of important properties, which form the basis for interpreting the function as a time-frequency distribution of the signal energy.

These properties discussed in [3] are summarized as follows:

a) the instantaneous signal power at a certain time is equal to the projection of the $P(t,\omega)$ on the time axis:

$$\frac{1}{2\pi}\int_{-\infty}^{\infty} P(t,\omega)d\omega = |s(t)|^2$$

b) the energy density spectrum of $s(t)$ at a certain frequency is equal to the projection of the $P(t,\omega)$ on the frequency axis:

$$\int_{-\infty}^{\infty} P(t,\omega)dt = |S(\omega)|^2$$

The ***a*** and ***b*** are called time and frequency marginal conditions.

c) the first-order moment of the $P(t,\omega)$ with respect to frequency may be expressed as follows

$$\Omega(t) = \frac{1}{P(t)} \int_{-\infty}^{\infty} \omega P(t,\omega) d\omega \quad \text{where} \qquad P(t) = \int_{-\infty}^{\infty} P(t,\omega) d\omega$$

The $\Omega(t)$ can be interpreted as the average frequency of the $P(t,\omega)$ at time t.

For real signals the average frequency provides no information. Let us therefore assume that $s(t)$ is complex-valued in the form $s(t) = v(t)e^{j\varphi(t)}$. Where $v(t)$ and $\varphi(t)$ are real functions, $v(t)$ is the envelope of $s(t)$, and $\varphi(t)$ is the phase of $s(t)$. Using this representation of $s(t)$, we find that $\Omega(t) = \varphi'(t)$. Therefore it can be concluded that the instantaneous frequency is an average frequency at a particular time.

d) the first moment of the $P(t,\omega)$ with respect to time at a particular frequency is

$$T(\omega) = \frac{1}{P(\omega)} \int_{-\infty}^{\infty} t P(t,\omega) dt \qquad \text{Where} \qquad P(\omega) = \int_{-\infty}^{\infty} P(t,\omega) dt$$

if we consider the complex spectrum $F(\omega) = A(\omega)e^{j\psi(\omega)}$ where $A(\omega)$ is its amplitude and $\psi(\omega)$ is its phase angle, we can prove that $T(\omega) = -\psi'(\omega)$.

Thus, the average time of the $P(t,\omega)$ at a particular frequency is equal to the negative of the derivative of the spectral phase of the signal.

e) the time shift: If $s(t) \rightarrow s(t-\tau)$ then $P(t,\omega) \rightarrow P(t-\tau,\omega)$

f) the frequency shift: If $s(t) \rightarrow s(t)e^{j\Omega t}$ then $P(t,\omega) \rightarrow P(t,\omega - \Omega)$

g) the time limited signal property.

If $s(t)$ is restricted to a finite time interval only and $s(t) = 0$ for $t \prec t_a$ or $t \succ t_b$

then the $P(t,\omega)$ is restricted to the same time interval $P(t,\omega) = 0$ for $t \prec t_a$ or $t \succ t_b$

h) the frequency limited signal property.

If $S(\omega) = 0$ for $\omega \prec \omega_a$ or $\omega \succ \omega_b$ then $P(t,\omega) = 0$ for $\omega \prec \omega_a$ or $\omega \succ \omega_b$

From a mathematical point of view, there is an infinite number of joint functions which satisfy these conditions since the conditions do not define the problem uniquely. Several distributions have been proposed over the last fifty years but in this section only certain distributions with desirable properties will be studied.

2.2 Time-Frequency Methods

The Wigner Distribution (WD) is one of the joint time-frequency distributions that is fundamentally different from the STFT. The original formulation was proposed by Wigner in 1932 and used in quantum mechanics. The Wigner Distribution of signal $s(t)$ is defined as

$$WD_s(t,\omega) = \int_{-\infty}^{\infty} s(t+\tau/2)s^*(t-\tau/2)e^{-j\omega\tau}d\tau \qquad (1)$$

where $s(t)$ is a continuous complex signal and "*" denotes the complex conjugate (unless otherwise indicated, the ranges of integrals are from $-\infty$ to ∞ throughout this paper.)

This representation may be interpreted as the Fourier Transform of

$$R_s(t,\tau) = s(t+\tau/2)s^*(t-\tau/2) \tag{2}$$

with respect to the lag variable τ where $R_s(t,\tau)$ is defined as the instantaneous auto correlation of a complex signal $s(t)$, Therefore :

$$WD_s(t,\omega) = \int R_s(t,\tau)e^{-j\omega\tau}d\tau \tag{3}$$

The Wigner Distribution possesses very high resolution in both time and frequency, and it has the properties ***a*** to ***h***. Despite the desirable properties of the Wigner Distribution, it has two major draw-backs: it is not necessarily non-negative and it is a bilinear function producing interferences or cross terms for multi-component signals. The Wigner Distribution of the sum of two signals $s_1(t)+s_2(t)$ is

$$WD_{s_1+s_2}(t,\omega) = WD_{s_1}(t,\omega) + 2Re\left[WD_{s_1s_2}(t,\omega)\right] + WD_{s_2}(t,\omega) \tag{4}$$

which has a cross term " $2Re\left[WD_{s_1s_2}(t,\omega)\right]$ ", in addition to the two auto terms. Cross terms lie between signal components in different regions in the time-frequency plane and are oscillatory. They can have a peak value as high as the auto terms and make the interpretation of the time-frequency representation of signals very difficult. Ville used the Wigner Distribution in signal analysis in 1948 when he replaced the continuous complex signal with the analytical

This representation may be interpreted as the Fourier Transform of

$$R_s(t,\tau) = s(t+\tau/2)s^*(t-\tau/2) \tag{2}$$

with respect to the lag variable τ where $R_s(t,\tau)$ is defined as the instantaneous auto correlation of a complex signal $s(t)$, Therefore :

$$WD_s(t,\omega) = \int R_s(t,\tau)e^{-j\omega\tau}d\tau \tag{3}$$

The Wigner Distribution possesses very high resolution in both time and frequency, and it has the properties ***a*** to ***h***. Despite the desirable properties of the Wigner Distribution, it has two major draw-backs: it is not necessarily non-negative and it is a bilinear function producing interferences or cross terms for multi-component signals. The Wigner Distribution of the sum of two signals $s_1(t)+s_2(t)$ is

$$WD_{s_1+s_2}(t,\omega) = WD_{s_1}(t,\omega) + 2Re\left[WD_{s_1s_2}(t,\omega)\right] + WD_{s_2}(t,\omega) \tag{4}$$

which has a cross term " $2Re\left[WD_{s_1s_2}(t,\omega)\right]$ ", in addition to the two auto terms. Cross terms lie between signal components in different regions in the time-frequency plane and are oscillatory. They can have a peak value as high as the auto terms and make the interpretation of the time-frequency representation of signals very difficult. Ville used the Wigner Distribution in signal analysis in 1948 when he replaced the continuous complex signal with the analytical

signal. $s(t)$ is an analytical signal if the imaginary part of $s(t)$ is equal to the Hilbert transform of the real part of $s(t)$, so that

$$s_I(t) = \frac{1}{\pi} \int \frac{s_R(t)}{t-\tau} d\tau \tag{5}$$

In the case where $s(t)$ is an analytical signal, the Wigner Distribution is termed the Wigner-Ville Distribution (WVD). By using the analytical signal in the Wigner Distribution: firstly, the negative frequencies which have no physical significance for a real signal are eliminated and, consequently, the cross terms between the negative and positive parts of the spectrum are eliminated; secondly, the Nyquist frequency can be applied to the sampling frequency of the signal. However, although the analytical signal eliminates some cross terms, there are still cross terms between multiple components which make interpretation difficult.

In practical applications, the Wigner Distribution requires some smoothing in order to suppress the cross terms. The pseudo-Wigner Distribution (PWD) is defined by:

$$PWD_s(t,\omega) = \int s(t+\tau/2)s^*(t-\tau/2)h(\tau)e^{-j\omega\tau} d\tau \tag{6}$$

where $h(\tau)$ is a window function or a low pass filter in order to reduce cross terms which have oscillations of relatively high frequencies. The pseudo-Wigner Distribution can be considered as a frequency-domain variation of the Wigner Distribution.

$$PWD_s(t,\omega) = WD_s(t,\omega) *_\omega H(\omega) \tag{7}$$

filter is $\Phi(t,\omega) = \frac{1}{2\pi} WD_w(-t,\omega)$.

The spectrogram has the non-negativity property which facilitates the interpretation of the spectrogram as the signal energy distribution, but does not preserve the time and frequency energy marginals of a signal. In general, the non-negativity property often conflicts with other desirable properties. However, a major drawback of the STFT is that it requires a trade-off between the time and frequency resolutions. Although, the Short-Time Fourier Transform with a window that conforms to the signal components provides maximum resolution in the smoothed Wigner Distribution, the STFT has less concentration than the Wigner Distribution. Moreover, for unknown signals, how can appropriate windows be found without *a priori* knowledge of the signal components?

Apart from the Wigner Distribution, several other distributions have been proposed. These are similar to the Wigner Distribution in that they satisfy the marginal, the instantaneous frequency condition, and various other properties. The Rihaczek [7] and the Page [8] Distributions are two of those proposed.

The Rihaczek distribution, which gives a complex energy spectrum, is defined as

$$e(t,\omega) = \frac{1}{\sqrt{2\pi}} s(t) S^*(\omega) e^{-j\omega t} \tag{12}$$

The real part of the Rihaczek distribution, which is called Margenau-Hill distribution, lacks many desirable properties such as instantaneous frequency, but does satisfy the marginal conditions.

Page considered only the signal up to the present time t and abandoned the future because it is

unknown. A new signal is defined as follows :

$$\begin{cases} s_t(t') = s(t') & for \quad t' \le t \\ s_t(t') = 0 & for \quad t' \succ t \end{cases}$$

The Page Distribution for the above signal definition may be written as follows :

$$P^{-}(t,\omega) = 2Re\frac{1}{\sqrt{2\pi}} s^{*}(t)\, S_t^{-}(\omega)\, e^{j\omega t} \tag{13}$$

where $S_t^{-}(\omega) = \frac{1}{2\pi}\int_{-\infty}^{t} s(t')e^{-j\omega t'}dt'$

The Page Distribution satisfies the marginal conditions but is unable to show correctly a multi-components signal in the time-frequency plane. Figure 1 shows a representation of a multi-components signal by the Wigner, Rihaczek and Page distributions. The signal is a sine with frequency ω_1 started at $t = 0$ and stopped at $t = t_1$, restarted again at $t = t_2$ with another frequency ω_2 , and ended at $t = t_3$. Each of the three distributions displays energy density where one does not expect to find it.

In 1966, a method was derived that could generate an infinite number of new distributions in a very simple way. This general distribution formula is obtained by replacing $\phi(\theta,\tau)$ with $\Phi(t,\omega)$ in the formula (8):

$$WD_s(t,\omega) = \iiint e^{j(-\theta t-\tau\omega+\theta u)}\varphi(\theta,\tau)s(u+\tau/2)s^*(u-\tau/2)du\,d\tau\,d\theta \qquad (14)$$

where $\varphi(\theta,\tau)$ is the two dimensional inverse Fourier transform of $\Phi(t,\omega)$ and θ and τ are respectively the frequency lag and the time lag. Formula (14) is referred to as Cohen's class of time-frequency distributions and characterizes time-frequency distributions by an auxiliary function, called the kernel function $\varphi(\theta,\tau)$. The properties of a distribution are reflected by simple constraints on the kernel, and by examining the kernel one can readily be assured of the properties of the distribution. This allows one to pick and choose those kernels that produce distributions with prescribed, desirable properties. By using this general formula we can find the kernel function for each of the distributions which have been defined, such as the Wigner, Rihacezk, Margenau-Hill and Page. The kernel function for the Wigner, Rihacezk, Margenau-Hill and Page distributions are respectively 1, $e^{j\theta\tau/2}$, $\cos\frac{\theta\tau}{2}$ and $e^{j\theta|\tau|/2}$.

In 1980, Choi and Williams presented a new kernel for reducing cross terms in the Wigner Distribution. Their kernel is defined as

$$\varphi(\theta,\tau) = e^{-\theta^2\tau^2/\sigma} \qquad (15)$$

where σ is a parameter which trades off auto-term resolution for cross term suppression or vice

$$CWD_s(t,\omega) = \frac{1}{4\pi^{3/2}}\int\int\frac{1}{\sqrt{\tau^2/\sigma}}\exp(-\frac{(u-t)^2}{4\tau^2/\sigma})\,s^*(u-\tau/2)\,s(u+\tau/2)\,e^{-j\omega\tau}du\,d\tau \qquad (16)$$

versa. By increasing σ, we achieve a distribution similar to the Wigner Distribution and by decreasing σ, we eliminate the cross terms but we lose resolution in the time and frequency domains. The Choi-Williams distribution may be written as follows :

Figure 2 shows the Choi-Williams representation with a different value of σ for a sinusoidal signal with two constant frequencies. Although, the Choi-Williams Distribution satisfies the marginal conditions, it violates the support properties ***g*** and ***h***. It attenuates the cross terms equally in the time and the frequency domains and provides a higher resolution than the smoothed Wigner Distribution. Although, the Choi-Williams Distribution is the best choice for analyzing mutli-component signals in which the components have a constant frequency content, its resolution for signal components with significant frequency modulation or time-varying signals is very poor. However, the Choi-Williams Distribution is insensitive to the time-scale of the components, due to the shape of its kernel.

By generalizing from Choi-Williams' work, a broader class of exponential distribution (ED) defined by Diethorn [13] induces a kernel of the following form:

$$\varphi(\theta,\tau) = e^{\frac{-|\theta|^p|\tau|^q}{\sigma}} \tag{17}$$

By carefully selecting parameters p, q and σ, we may obtain the desired properties.

To reduce the cross terms and preserve simultaneously the properties ***a*** to ***h***, Jeang and Williams [12] introduced a new class of time-frequency distribution, called the Reduced Interference Distributions (RID). The RID satisfies properties ***a*** to ***h***, as does the WD. The RID kernel should be not only a low-pass filter but also a function of $\theta\tau$ which satisfies

$$|\varphi(\theta,\tau)| \prec\prec 1 \qquad \text{for} \quad |\theta\tau| \succ\succ 0$$

where θ and τ are respectively the frequency lag and the time lag.

The kernel of the RID is defined as follows :

$$\varphi_{RID}(\theta,\tau) = H(\theta\tau) \tag{18}$$

where H is a two dimensional low-pass filter type. The WD is not a member of the RID because its kernel does not have the reduced interference property. Although the RID satisfies many properties, it has many disadvantages. First, the RID may or may not satisfy the regularity property and it does not have the unitary property. Secondly, the RID only reduced the height of the cross terms and spread them over a larger time-frequency area. In particular, the RID is not able to suppress the cross term which is located on the θ or the τ axis.

In 1966, Born and Jordan [14] used a sinc kernel which is defined as

$$\varphi(\theta,\tau) = \frac{\sin(a\theta\tau)}{a\theta\tau} \tag{19}$$

with $a = 1/2$. But its property of reducing interference distributions was derived from the work of Jeang and Williams in 1992.

In 1990, a new time-frequency distribution with very interesting features, called the cone-shaped kernel, was developed by Zhoa, Atlas and Marks (ZAM) [15]. This distribution not only suppresses the cross terms, but also produces good resolution in both time and frequency. Their kernel is defined as

$$\varphi_{ZAM}(\theta,\tau)=g(\tau)\,|\tau|\frac{\sin(a\theta\tau)}{a\theta\tau} \tag{20}$$

where $g(\tau)=1$, $a=1/2$.

Figure 3 shows the comparison between the Spectrogram and the ZAM Distribution. This distribution hides the cross terms by placing them under the auto terms.

In 1993, Louglin et al. [16] studied a general method for placing cross terms under auto terms. They used a kernel in the form of

$$\varphi(\theta,\tau)=f(\theta,\tau)\,\sin(a\theta\tau) \tag{21}$$

Depending on the choice of $f(\theta,\tau)$ these kernels may or may not satisfy other desirable properties. In 1994, a new kernel function called the "compound kernel" was presented by Zhang and Sato [17]. This kernel is the product of the Choi-Williams and Margenau-Hill kernels.

$$\varphi_{zs}=\exp(-2\pi^2\theta^2\tau^2/\sigma^2)\cos(2\pi\beta\theta\tau) \tag{22}$$

Where σ and β are two parameters which may be identified as follows:

When $\sigma\to\infty$, $\beta\to 1/2$, we obtain the Margenau-Hill Distribution;

When $\beta\to 0$, we have the Choi-Williams Distribution, and

When $\sigma\to\infty$, $\beta\to 0$ we get the Wigner-Ville Distribution.

In this distribution, the cross terms are transposed with the auto terms. Consequently, the correct value of the auto terms is slightly modulated due to cross terms. Figure 4 illustrates the cross-sectional features of both distributions for various values of the parameter σ.

3. THE APPLICATION OF TIME-FREQUENCY ANALYSIS TO MACHINERY DIAGNOSTICS

3.1 Brief Historical Perspective

From an application point of view, Boashash [20] was the first to use the time-frequency technique for real problems. He applied it to geophysical exploration. The Wigner Distribution was used by Bazelaire and Viallix [21] to obtain data to measure the absorption and dispersion coefficients of the ground and to formulate a new understanding of seismic noise. Forrester [22] has made a great contribution to machinery diagnostics by using the WVD in the vibration analysis of defective helicopter gearboxes. He showed that signal enhancement techniques are not capable of distinguishing tooth cracking from spalling and can be misleading in their indications of the extent of damage, but WVD can detect both the type and extent of faults. Meng and Qu [23] presented the effectiveness of using WVD in rotating machinery fault diagnosis.

In a series of reports, McFadden and Wang [24-27] reviewed several definitions of the continuous and the discrete WVD, implemented WVD for the detection of gear damage, and compared the results with those from existing narrow band enhancement techniques. In another application of time-frequency analysis, Rohrbaugh [28] used the time-frequency method to find defects in different elements of several sets of marine machinery, such as fans and motor-generators. Rao, Taylor and Harrison [29] used the Wigner Distribution in the diagnosis of faults in a high-power gas turbine. They described the advantages of WD in providing high-resolution estimates of non-stationary, narrow-band signals in the time-frequency domain. Another application of time-frequency analysis to the detection of faults in a gearbox is described by Oehlmann et al. [30].

Williams [31] used the Reduced Interference Distributions (RID) time-frequency technique in the analysis of signals measured from bearings. He showed that the spectrogram and Waterfall Plot do not adequately represent time-varying signals.

The detection of faults in reciprocating machines such as internal combustion engines and pumps is particularly difficult. Rohrbaugh and Cohen [32] applied time-frequency methods to the analysis of a cam-operated pump. They showed that time-frequency methods can provide more detail about the signal, thus facilitating the detection of faults. In comparing time-frequency analysis with the STFT and traditional methods, they found time-frequency methods to be superior. In another work, Samimy and Rizzoni [33] presented the application of time-frequency analysis to the detection of internal combustion engine knock. The transient nature and time-varying characteristics of the signal mean that only time-frequency methods will give a satisfactory result.

Another application of time-frequency methods is in machine tool monitoring. Zheng and Whitehouse [34] described the potential of the Wigner Distribution for the detection of incipient chatter. Loughlin et al. [35] discussed the application of time-frequency analysis to drilling and grinding operations. They demonstrated how a new technique can reveal features that do not appear in the Short-Time Fourier Transform.

The Wigner-Ville Distribution has been applied in various fields : as an indicator of drill attrition in industry or surface-fault in a diesel engine. Changes in the dynamic characteristics of ground using seismic analysis were presented by Bigret et al. [36]. Atlas, Bernard and Narayanan [37] gave a review of the application of time-frequency analysis to different elements of rotating machine monitoring and machine tool monitoring.

In 1992, Boashash [38] published a book about time-frequency analysis and its application. In this book, he reviewed several articles on different methods of time-frequency analysis and applications of the analysis in several different domains.

All of the above papers show the potential of time-frequency analysis in different fields of mechanical engineering. They demonstrate the applicability of time-frequency analysis to the solution of problems in machine monitoring. In the next section we will compare some of the time-frequency analyses by applying these methods in experimental and real cases.

3.2 Software for Time-Frequency Analysis of Signals

An in-house user-friendly software program has been developed for time-frequency analysis. This program is capable of calculating and demonstrating the different time-frequency transforms in two and three dimensions. The program includes the Fourier spectrum analysis, the Short-Time Fourier Transform, the Wigner-Ville Distribution, the smoothed Wigner-Ville Distribution, the Choi-Williams Distribution, the Rihaczek-Margenau Distribution, the Born-Jordan-Cohen Distribution, and many other time-frequency methods. In this section, the performance of each method is illustrated by a test signal generated by computer. The test signals are similar to those which are often observed in machine diagnosis.

The first example, which is called a sum of sines, is a multi-component signal with constant frequencies. This kind of signal is generated by faults such as imbalance, misalignment, looseness, and resonance which cause the constant frequencies at $N \times RPM$. The signal consists of three sines with frequencies 100 Hz, 300 Hz and 1000 Hz. In the time-frequency plane, one sees three lines at 100 Hz, 300 Hz and 1000 Hz parallel with the axis of time and, in time-frequency-energy,

the three sines are shown in the form of three peaks constant in time. Figure 5 shows the signal and its Fourier spectrum. As shown in Fig. 6, the STFT of the signal presents exactly what we expected. Figure 7 shows the Wigner-Ville distribution of the signal, and we can see that the autoterms are contaminated by the interference terms. It is very difficult to identify the three frequencies without advance knowledge of the signal.

The SWV (smoothed Wigner-Ville) shows the three peaks clearly in Figure 8. In the Choi-Williams Distribution of the signal, by changing the value of σ, we can obtain a good representation of the three frequencies, as shown in Figure 9. In the Born-Jordan-Cohen Distribution of the signal, shown in Figure 10, resolution is lost due to the elimination of the cross-terms.

The second example is an amplitude-modulated cosine at 1000 Hz with frequency modulation equal to 15 Hz, as shown in Figure 11. Cases such as a damaged gearbox and a defective bearing usually generate amplitude-modulated signals. Whilst it is not always possible to identify these by the Fourier spectrum or time waveform, with time-frequency analysis it is relatively simple. Figures 12 to 17 show the different time-frequency representations of the signal, and all these methods give a clear representation of the signal with varying resolution. It must be noted that the STFT requires an adjustment of the window and the Choi-Williams method requires an appropriate value of σ in order to provide satisfactory resolution. Among these representations, the Wigner-Ville Distribution provides the best result.

Certain types of gearbox problem may result in a frequency-modulated signal that is extremely difficult to identify. Such a signal is represented by a frequency-modulated cosine at 1000 Hz with frequency modulation equal to 20 Hz, as shown in Figure 18. As shown in Figure 18, it is not

possible to determine the characteristics of the signal using its Fourier spectrum. On the other hand, time-frequency methods clearly demonstrate the time-varying characteristic of the signal, as shown in Figures 19 to 24 . The Wigner-Ville, the smoothed Wigner-Ville, and the Choi-Williams Distributions give better representations of the signal than the others.

The last example is a frequency and amplitude modulated cosine at 1000 Hz, as shown in Figure 25. This case is more complicated than the others but time-frequency methods provide clear representations of the signal, as shown in Figures 26 to 31. In this case, the Wigner-Ville, the smoothed Wigner-Ville, and the Choi-Williams Distributions again give better representations of the signal than do the others.

3.3 Experimental Study of Time-Frequency Methods

3.3.1 Experimental Apparatus

In this section, an experimental installation which enables us to simulate different defect configurations in rotating machinery is presented. The experimental prototype (see Figure 32) consists of three distinct parts: part I, motor; part II, journal, and part III, receptor.

Part I is a three-phase asynchronous motor (550-575 V, power 2 HP). The rotating speed can vary from 0-1725 r.p.m. Part II consists of an interchangeable rotating shaft which is supported by two journal bearings (SKF 1210 EKTN9 self aligning double row) labeled A and B. There are three shafts on which bearings with different defects are mounted. And Part III consists of a reducing gearbox with a ratio of 40:1 and a brake that can produce a variable resistance torque. Parts I, II, and III are connected by two couplings. An accelerometer is mounted on the experimental installation and is connected to an analyser.

3.3.2 Tests and Results

We examined the time-frequency methods to pin-point defects of known characteristics and location on the rolling bearing. There was a small defect on the inner raceway of the bearing. The defect was created by scratching the bearing raceway with an electric pen. Figures 32 to 39 show the signal measured on bearing A, its spectrum and all other distributions. The results for the defective bearing were also verified by calculating the frequency at which the rolling elements passed over the defects [39]. The geometric characteristics of the bearing are as follows:

pitch diameter D=69 mm

Diameter of the rolling body d=10.32 mm

Contact angle α =7.87 deg

Number of rolling elements N =17 (per row)

Bearing frequency of rotation F_r=12.2 Hz

On the inner raceway, the frequency of rolling body defect impact is:

$$F_i = \frac{F_r N}{2}\left[1 + \frac{d}{D}\cos(\alpha)\right] \tag{24}$$

The pass frequency on a point of the inner raceway is calculated and is equal to 238 Hz. The spectrum in Figure 32 shows the default frequency, along with other frequencies. However, the spectrum can be misleading [23]: we cannot be certain which is the default frequency unless we know its special characteristics. In this case, the default frequency should be an amplitude-modulated wave at approximately 238 Hz with the frequency of modulation being equal to the rotating frequency.

The amplitude-modulated signal at the default frequency and at $2 \times$ default frequency in the STFT is shown, and we calculate the frequency of modulation and verify that it is correct and equal to the rotating frequency.

Among time-frequency methods, the Wigner-Ville cannot provide a good representation of the signal due to the cross terms which are generated between the signal components. The smoothed Wigner-Ville shows the signal even better than the STFT and we can clearly see the amplitude modulation and easily calculate the frequency of the modulation. The Choi-Williams gives a representation which is not as satisfactory as that produced by the smoothed Wigner-Ville as it is necessary to choose an appropriate value of σ. The Born-Jordan-Cohen gives a good appearance of the signal but, again, the resolution in time and frequency is not as satisfactory as that produced by the smoothed Wigner-Ville or the Choi-Williams. The Rihaczek-Margenau cannot even give a good appearance of the signal.

Therefore, after comparing the different time-frequency transforms of this signal we conclude that the SWV gives the best representation of the signal in this case.

3.4 Application of Time-Frequency Methods to Industrial Problems

3.4.1 Gearbox Test

The first set of data is obtained from a defective gear train of a hoist drum in a large shovel operating at an open pit iron mine. The data are measured by International Measurement Solutions company in order to find the problem in the machine.

Gears generate a mesh frequency equal to the number of teeth on the gear multiplied by the rotational speed of the shaft driving it. A high vibration level at the mesh frequency is often

caused by tooth error, wear of the meshing surfaces, or any other problem that would cause the profiles of meshing teeth to deviate from their ideal geometry. Sidebands at the mesh frequency, on the other hand, are typically due to a failure of mating teeth. Imagine a cracked tooth which is not yet broken, and will consequently not be noticed by the operating personnel. However, it will, due to its weakened mechanical condition, deflect more under load than the other (healthy) teeth when it goes into mesh. This results in a signal with amplitude modulation. Thus, an increasing level in the sidebands spaced with rotation speed in the frequency spectrum results from the cracked tooth.

A minimum length of time is required to perform an FFT analysis of each process. Here, the time resolution required will depend on the period of each tooth mesh and the desired level of accuracy. Sometimes, it is not possible to measure the signal for long enough to provide the periodicity of shock in FFT spectrum. In our case, the process does not even last one revolution of the driven gear.

Figures 40 to 46 show respectively the spectrum, the STFT, the Wigner-Ville, the smoothed Wigner-Ville, the Choi-Williams, the Born-Jordan-Cohen and the Rihaczek-Margenau representation of the signal (SPEC1). The FFT spectrum of the signal shows some peaks around 200 Hz and other smaller peaks at 400 Hz, 800 Hz and 1200 Hz. However, it is very difficult to find the problem without more information, and we are unable to visualise the pattern of the signal in the time-frequency plane. It is possible to see the amplitude-modulated signal in the STFT of the signal. The gear-meshing frequency is seen to be at approximately 200Hz and three large impacts due to three partially broken teeth at approximately 400 Hz. It is possible to find the frequency of the periodicity of the peaks on the STFT. However, the smoothed Wigner-Ville

gives a better representation than the STFT. The frequency of the periodicity is found with more precision in the smoothed Wigner-Ville representation than in the STFT representation. The Choi-Williams, with an appropriate value of σ, gives a representation of the signal in which a part of the energy of the first peak is dispersed between the second peak and the third peak. In the Born-Jordan-Cohen, the second peak is almost invisible and it is difficult to obtain satisfactory information about the signal. The Rihaczek-Margenau does not give a clear representation of the signal and the second peak has completely vanished. Here, again the SWV gives the best representation of the signal.

3.4.2. Bearing Test

The second test was carried out on the dryer of a paper machine at the Abitibi-Consolidated Company in Quebec. A typical dryer section consists of about 60 paper-drying cylinders which are divided into five top and five bottom sections, as shown in Fig. 47. The standard paper dryer is a four- or five-foot diameter hollow cylinder of cast iron. The dryer journals must support the dryer which is extremely heavy and rugged. The drive of the dryer section has a critical function and any undesirable vibration in one of the cylinders can affect the passage of the paper over this section. Therefore, a precise and periodic diagnosis of the dryer bearing is essential. An efficient diagnostic method can recognize the problem before damage has occurred. For this reason, time-frequency methods are used in this particular case to show their capacity, potential and credibility. Figure 48 shows the measured signal on dryer # 27 and its spectrum. From the individual impacts which appear at regular intervals in the spectrum, one can conclude that there is a problem in the dryer. The low-level intense noise in the spectrum makes it impossible to see the amplitude

modulations associated with the impacts. Time-frequency analysis makes the detection of this fault a straight-forward matter. Figures 49 to 52 show the different time-frequency representations of the signal. The constant impacts in time lead us to the defects which cause frequency constants components such as the defect on the outer race of a bearing. In this machine, bearings play an important role and it is to be expected that we first verify the bearing defaults. From the characteristics of the bearings, it is possible to calculate the different frequency of the bearing defaults. The frequency of the first impact corresponds to the BPFO (*ball-pass frequency on the outer race*) of the bearing and the other impacts are $2 \times BPFO, 3 \times BPFO, \ldots$. After replacing the bearing by a new one, this diagnosis is confirmed by an inspection of the old bearing. In this case, there is not a great difference between the time-frequency distributions, and the STFT with an appropriate window may provide a clear representation. Thus, it is not possible, in this instance, to choose one method as being superior to the others, because the choice of method depends on the signal and the resolution requirement in the analysis.

4. DISCUSSION AND CONCLUSION

By comparing the results obtained from time-frequency analysis of different mechanical signals, we can conclude that :

Time-frequency analysis has definite advantages over time-based vibration analysis or frequency-based vibration analysis and these advantages make it a powerful tool in machine monitoring.

The STFT can give a satisfactory representation of a signal in the time-frequency plane provided that an appropriate length of window for cutting the signal is chosen. The resolution in time or

frequency is always dependent on the length of window.

The Wigner-Ville is not able to produce a satisfactory representation of multi-component signals due to the presence of cross terms. It is valid only for mono-frequency signals.

The smoothed Wigner-Ville is the most appropriate among the transforms which we have studied in this paper. It gives not only a clear representation of the signal but also satisfactory resolution in time and in frequency.

The Choi-Williams may give a representation of the signal which is as satisfactory as that of the SWV but it is necessary to find a suitable value of σ . By the Born-Jordan-Cohen, we can obtain an image of the signal in the time-frequency plane; however, the resolution in time and in frequency are not always accurate and it is not possible to calculate exactly the frequency of modulation or the frequency and the time of a transient peak in a time-frequency plane.

The Rihaczek-Margenau may not provide a satisfactory representation of the signal when the signal comes from a real case, but for theoretical signals it gives a good representation.

In summary, the choice of a distribution in a practical application depends on the problem concerned, and none of these distributions provides us with complete and conclusive results, thus we cannot rank one above the others. For this reason, we recommend that researchers consider all distributions and compare the results in each case studied.

5. REFERENCES

1. E.P. Wigner 1932 Phys. Rev. 40, 749-759, On the Quantum Correction for Thermodynamic Equilibrium.

2. J. Ville 1948 Cables et Transmission 2A, 61-74, Théorie et Applications de la Notion de Signal Analytique.

3. T.A.C.M. Classen and W.F.G. Mecklenbrauker 1980 Philips J. Res. 35, 217-250, The Wigner Distribution - A Tool for Time-Frequency Signal Analysis Part I: Continuous Time Signals.

4. F. Hlawatsch 1984 Proc. Int. Conf. Signal Processing (Florence, Italy), 363-367, Interference terms in the Wigner distribution.

5. P. Flandrin Mar. 1984 Proc. IEEE 1984 Int. Conf. Acoust., Speech, Signal Processing (San Diego, CA), 41.B.4.1-4.4, Some features of time-frequency representation of multicomponent Signals.

6. L.Jacobson and H. Wechsler 1983 Proc. IEEE ICASSP-83 (Boston, MA), 254-256, The Composite Pseudo Wigner Distribution (CPWD): A Computable and Verstaile approximation to the Wigner distribution (WD).

7. W. Rihaczek 1986 IEEE Trans. Informat. Theory IT-14, 369-374, Signal Energy Distribution in Time and Frequency.

8. C.H. Page 1952 J. Appl. Phys. 23, 103-106, Instantaneous Power Spectra.

9. T.A.C.M. Classen and W.F.G. Mecklenbrauker 1980 Philips J. Res. 35, 276-300, The Wigner Distribution - A Tool for Time-Frequency Signal Analysis Part II: Discrete Time Signals.

10. L. Cohen 1989 Proc. IEEE 77(7), 941-981, Time-Frequency Distribution - A Review.

11. H.I. Choi and W.J. Williams 1989 IEEE Trans. Acoust., Speech, Signal Processing 37(6), 862-871, Improved Time-Frequency Representation of Multicomponent Signals Using Exponential Kernels.

12. J. Jeong and W. Williams IEEE Trans. Sig. Proc. 40, 402-412, Kernel Design for Reduced Interference Distributions.

13. E.J. Diethorn 1994 IEEE Trans. Signal Processing 42(5), The Generalized Exponential Time-Frequency Distribution.

14. L. Cohen 1966 J. Math. Phys. 7, 781-786, Generalized Phase-Space Distribution Functions.

15. Y. Zhao, L.E. Atlas and R.J. Marks 1990 IEEE Trans. Acoust., Speech, Signal Process. 38(7), 1084-1091, The Use of Cone Shaped Kernels for Generalized Time-Frequency Representations of Non stationary Signals.

16. P. Loughlin, E.L. Atlas and J. Pitton 1993 Advanced Time-Frequency Representations for Speech Processing, Visual Representations of Speech Signals, M. Cooke, S. Beete and M. Crawford (eds.), John Wiley & Sons.

17. B. Zhang and S. Sato 1994 IEEE Trans. Signal Processing 42(1), A Time-Frequency Distribution of Cohen's Class With a Compound Kernel and Its Application to Speech Signal Processing.

18. G. Zhonyu, L. Daurand and C.L. Howard 1994 IEEE Transactions on Signal Processing 42(7), 1700-1706, The Time-Frequency Distributions of Non stationary Signals Based on a Bessel Kernel.

19. R.G. Baraniuk and D.L. Jones 1993 IEEE Trans. Signal Processing 41(4), 1589-1602, A Signal-dependent Time-Frequency Representation: Optimal Kernel Design.

20. B. Bouachache 1978 Représentation Temps-Fréquence, Soc. Nat. ELF Aquitaine, Pau, France, Publ. Recherches, No. 373-378.

21. E. Bazelaire and J.R. Viallix 1987 Proc. 49th Eur. Ass. Explor. Geophys. Mtg. (Belgrade, Yugoslavia), 1-2, Theory of Seismic Noise.

22. B.D. Forrester 1989 Proc. ASSPA89, 78-82, Use of the Wigner-Ville Distribution in Helicopter Fault Detection.

23. Meng Qingfeng and Qu Liangsheng 1991 Mechanical Systems and Signal Processing 5(3), 155-166, Rotating Machinery Fault Diagnosis Using Wigner Distribution.

24. P.D. Mcfadden and W. Wang 1990 Report No. : OUEL-1859/90; ETN-91-98957, Department of Engineering Science, Oxford University, Time-Frequency Domain Analysis of Vibration Signals for Machinery Diagnostics. 1: Introduction to the Wigner-Ville Distribution.

25. P.D. Mcfadden and W. Wang 1991 Report No. : OUEL-1891/91; ETN-92-91087, Department of Engineering Science, Oxford University, Time-Frequency Domain Analysis of Vibration Signals for Machinery Diagnostics. 2: The Weighted Wigner-Ville Distribution.

26. P.D. Mcfadden and W. Wang 1992 Report No. : OUEL-1911/92; ETN-92-92063, Department of Engineering Science, Oxford University, Time-Frequency Domain Analysis of Vibration Signals for Machinery Diagnostics. 3: The Present Power Spectral Density.

27. P.D. Mcfadden and W. Wang 1992 Report No. : OUEL-1953/92; ETN-94-95148, Department of Engineering Science, Oxford University, Time-Frequency Domain Analysis of Vibration Signals for Machinery Diagnostics. 4: Interpretation Using Image Processing Techniques.

28. R. Rohrbaugh 1993 Soc. Proceedings of the 27th Asilomar Conference on Signal, Systems

& Computer 2, 1455-1458, Application of Time-Frequency Analysis to Machinery Condition Assessment.

29. P. Rao, T. Fred and G. Harrison 1990 Sound and Vibration 24(5), 22-25, Real-Time Monitoring of Vibration Using the Wigner Distribution.

30. H. Oehlmann, D. Brie, V. Begotto and M. Tomczak 1995 2nd International Symposium Acoustical and Vibratory Surveillance Methods and Diagnostic Techniques 1(10), 243-253, Analyse Temps-Fréquence de l'Ecaillage d'Engrenage de Boîtes de Vitesses.

31. W.J. Williams, C.K.H. Koh and J. Ni 1995 Life Extension of Aging Machinery and Structures: Proc. Of the 49th Meet. of MFPT Soc. 49(4), Vibration Inst.: Virginia Beach, 315-326, Bearing Monitoring Using Reduced Interference Distributions.

32. R.A. Rohrbaugh and L. Cohen 1995 Life Extension of Aging Machinery and Structures: Proc. Of the 49th Meet. of MFPT Soc. 49(4), Vibration Inst.: Virginia Beach, 349-361, Time-Frequency Analysis of a Cam Operated Pump.

33. B. Samimy and G. Rizzoni 1996 Proceeding of the IEEE 84(9). 1330-13343, Mechanical Signature Analysis Using Time-Frequency Signal Processing: Application to Internal Combustion Engine Knock Detection.

34. K. Zheng and D.J. Whitehouse 1992 Proceedings of the Mechanical Engineers. Part C, Journal of Mechanical Engineering Science 206(C4), 249-264. The Application of the Wigner Distribution Function to Machine Tool Monitoring.

35. P. Loughlin, L. Atlas, G. Bernard and J. Pitton 1995 Life Extension of Aging Machinery and Structures: Proc. Of the 49th Meet. of MFPT Soc., 49(4). Vibration Inst.: Virginia Beach, 305-314, Application of Time-Frequency Analysis to the Monitoring of Machining.

36. R. Bigret, P. De Sloovere, G. Hays and M. Lassoued 1995 2nd International Symposium Acoustical and Vibratory Surveillance Methods and Diagnostic Techniques 1(10), 315-

326, Application Industrielles de la Transformée de Wigner-Ville.

37. L. Atlas, G. Bernard and S.B. Narayanan 1996 Proceedings of the IEEE 84(9), 1319-1329, Applications of Time-Frequency Analysis to Signal From Manufacturing and Machine Monitoring Sensors.

38. B. Boashash 1992 Time-Frequency Signal Analysis, John Wiley & Sons.

39. J.E. Berry 1991 Sound and Vibration 25(11), 24-35, How to Track Rolling Element Bearing Health with Vibration Signature Analysis.

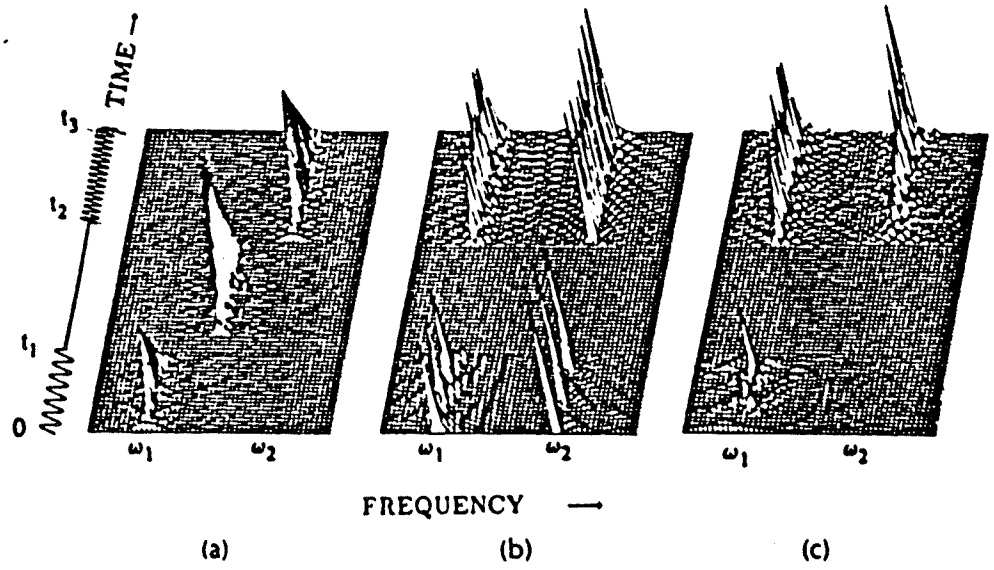

Figure 1: Representation of a multi components signal by (a) Wigner, (b) Rihaczek and (c) Page distribution [14].

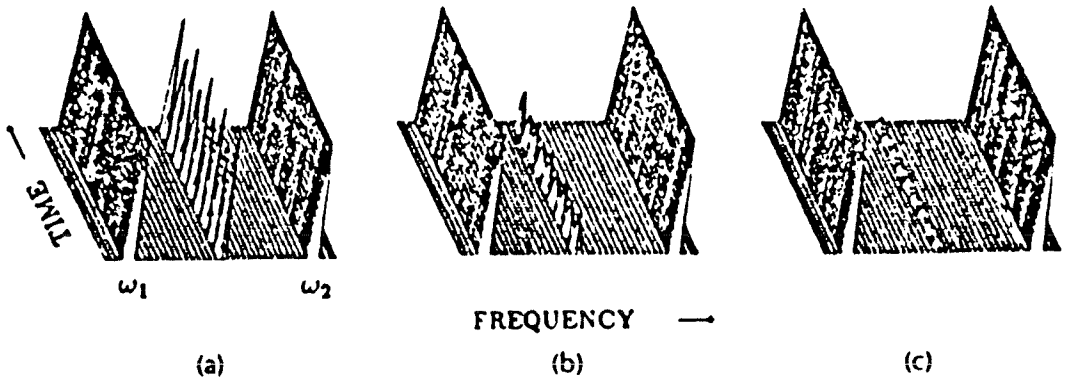

Figure 2: (a) Wigner and (b), (c) Choi-Williams distributions for the sum of two sine waves with (b) $\sigma = 10^6$ and (c) $\sigma = 10^5$ [15].

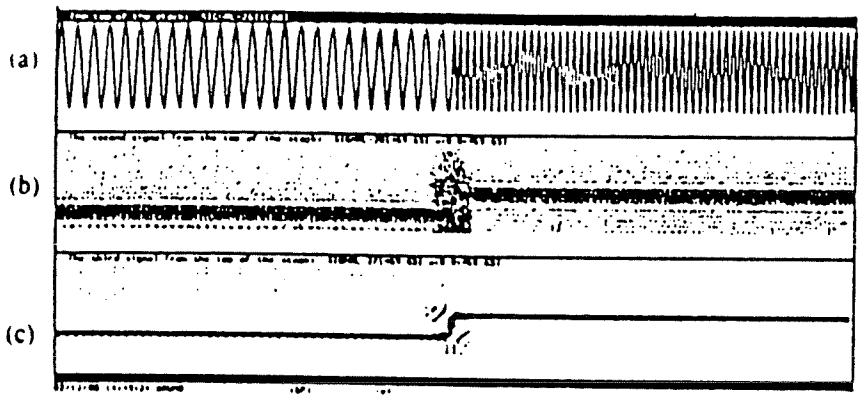

Figure 3: The comparison between (b) the STFT and (c) the ZAM distribution of a signal with a rapid frequency change.[16].

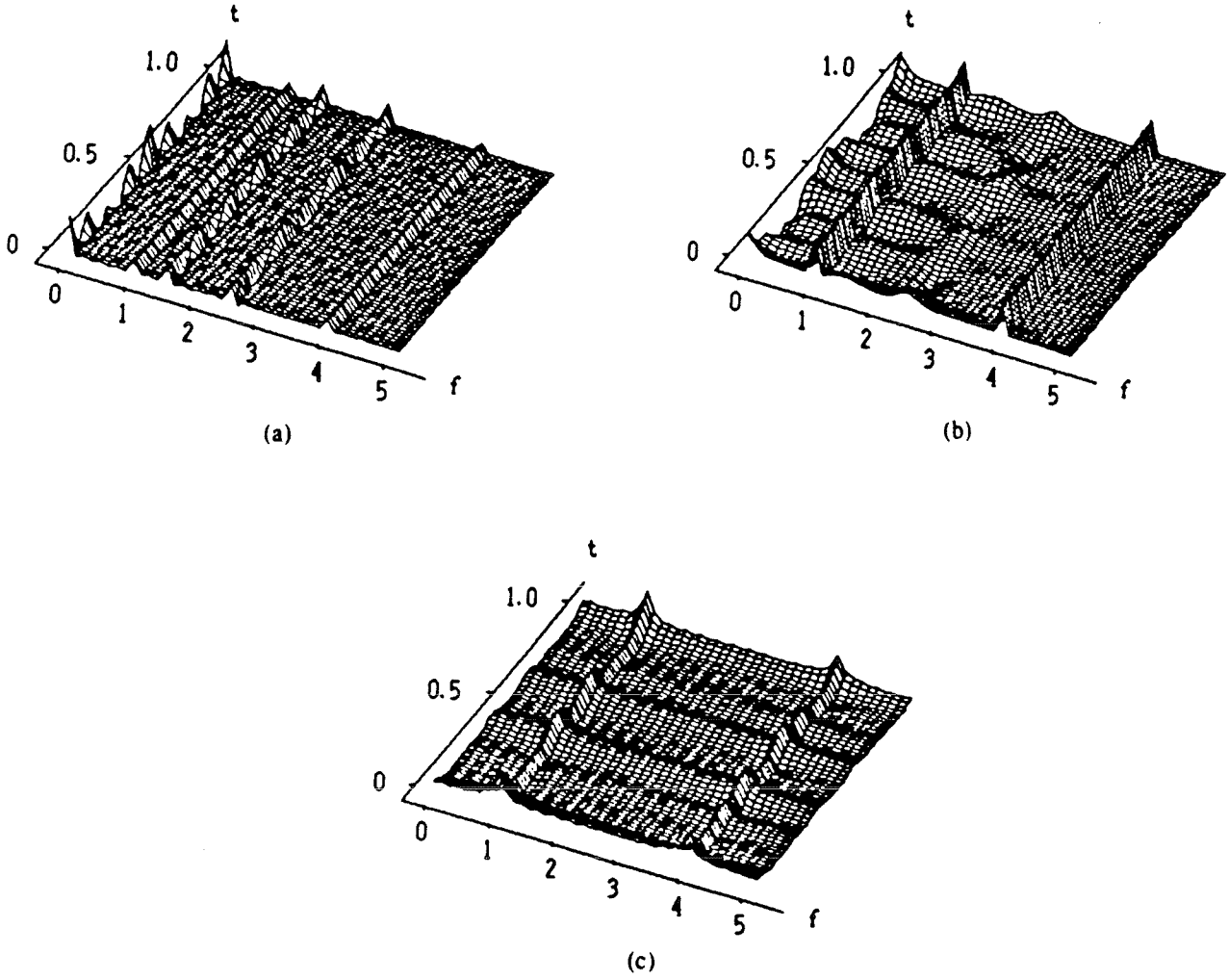

Figure 4: A comparison among (a) the Wigner-Ville (b) the Choi-Williams with σ =10 and (c) the Zhang-Sato with σ =10 for a sinusoidal signal with two and three components [18].

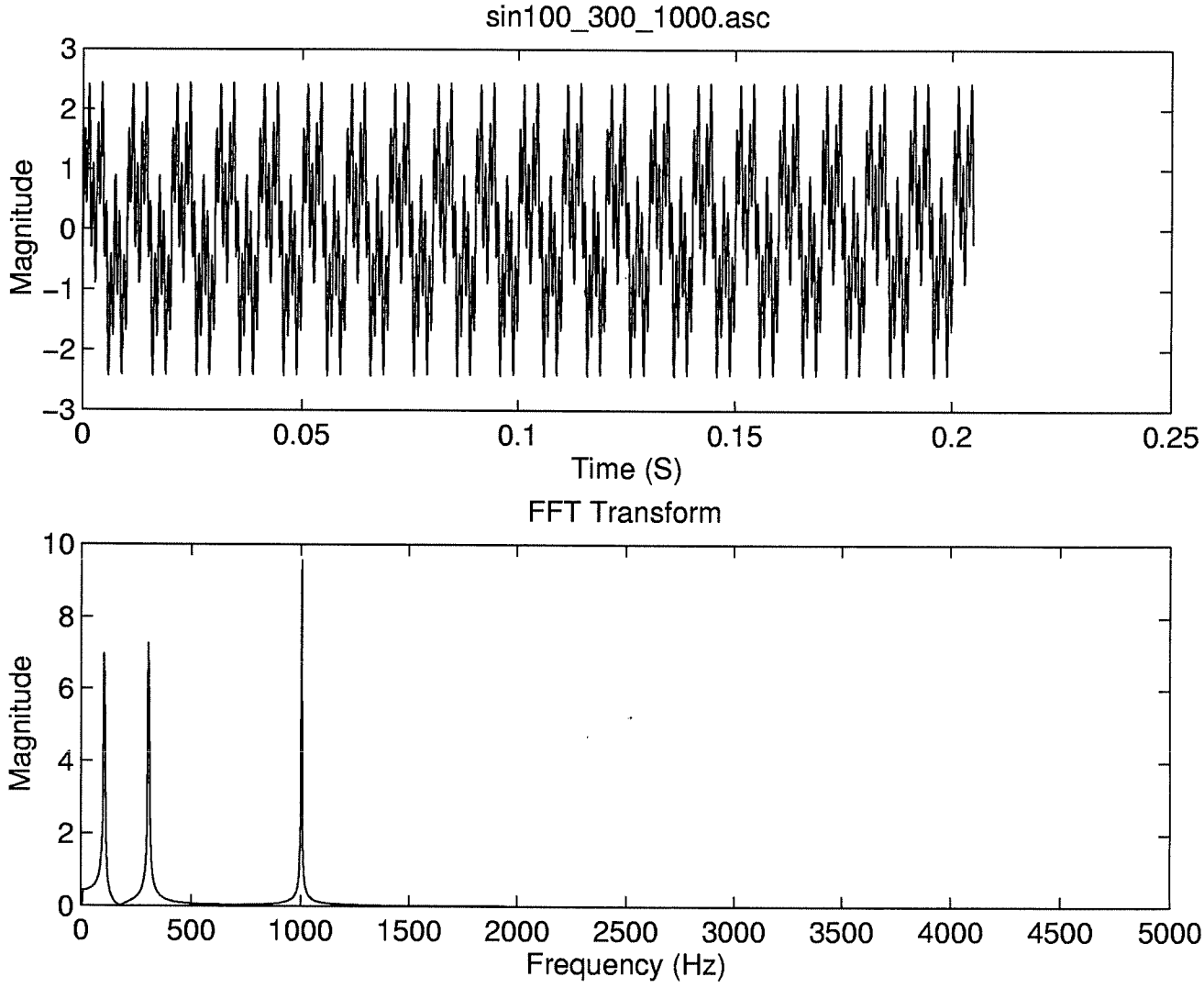

Figure 5: Time and spectrum representation of a sum of sines.

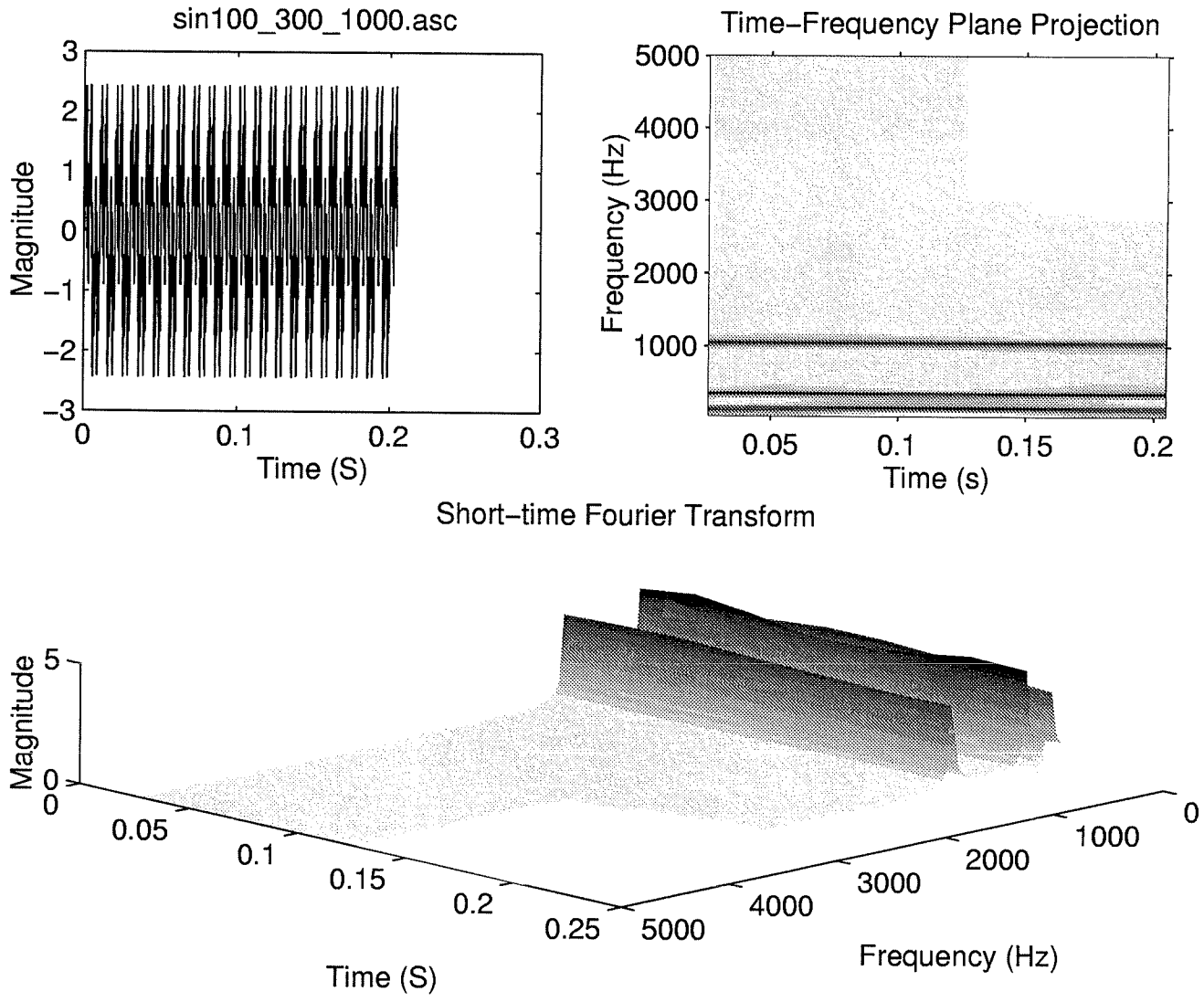

Figure 6: Spectrogram representation of a sum of sines.

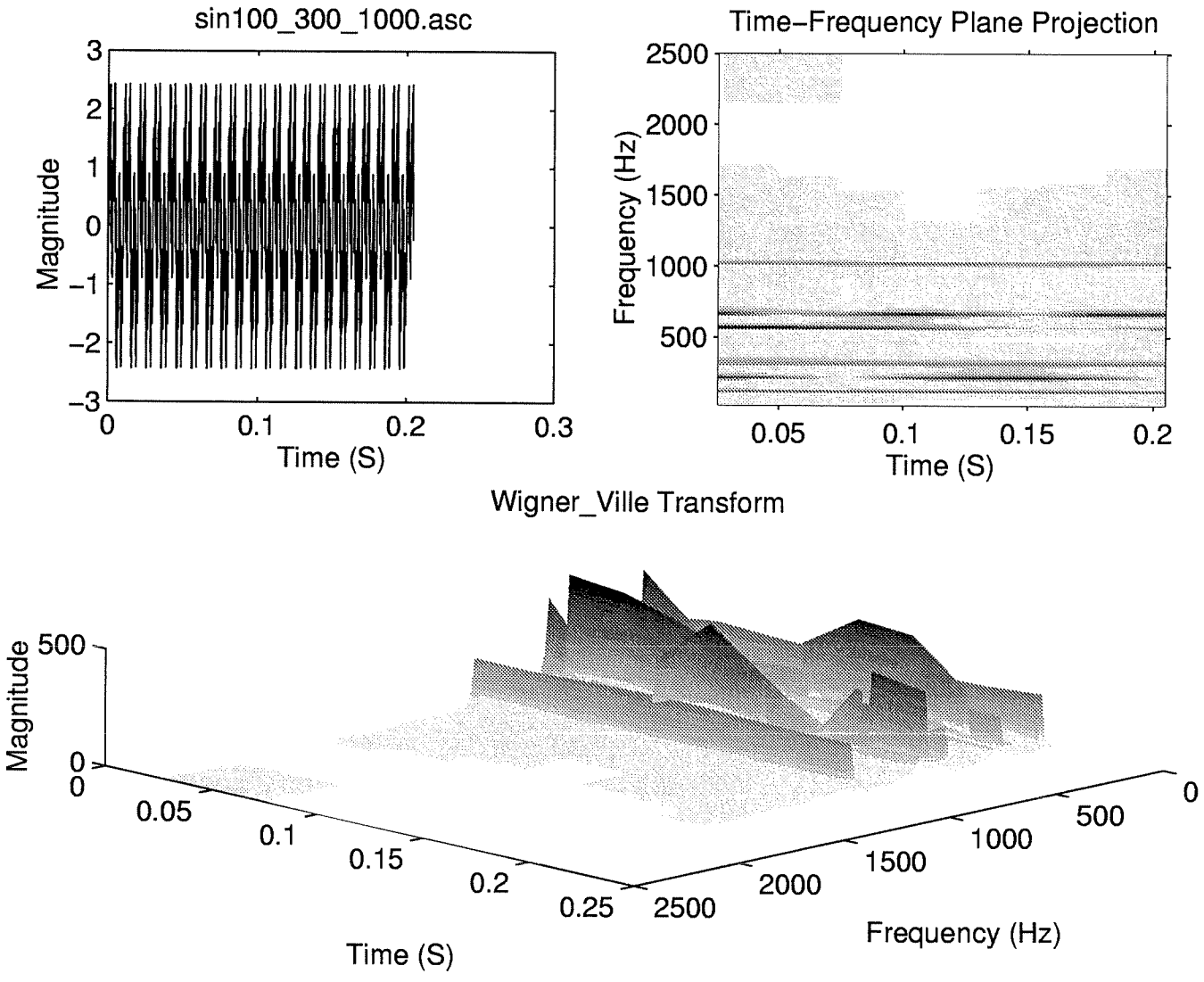

Figure 7: Wigner-Ville representation of a sum of sines.

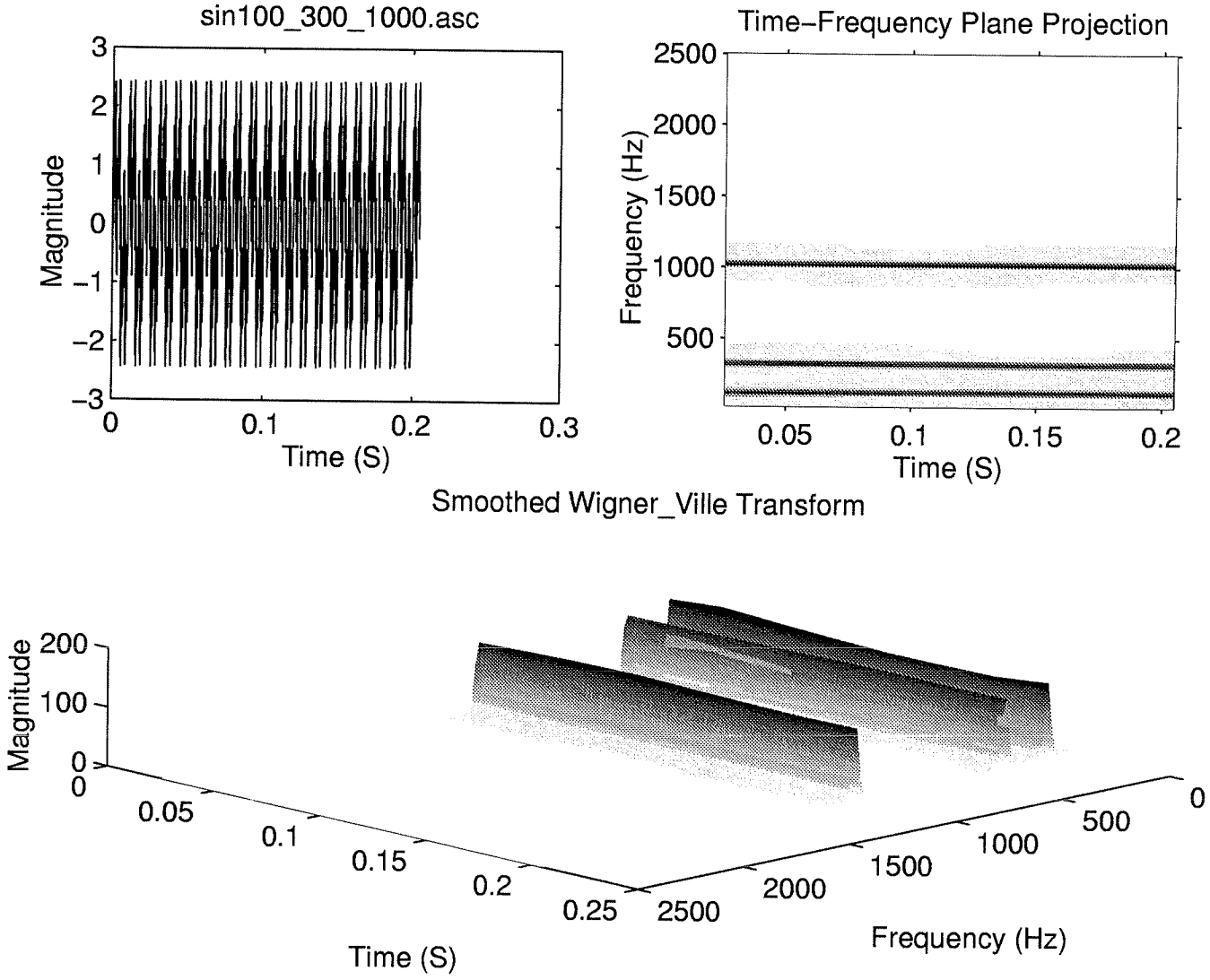

Figure 8: Smoothed Wigner-Ville representation of a sum of sines.

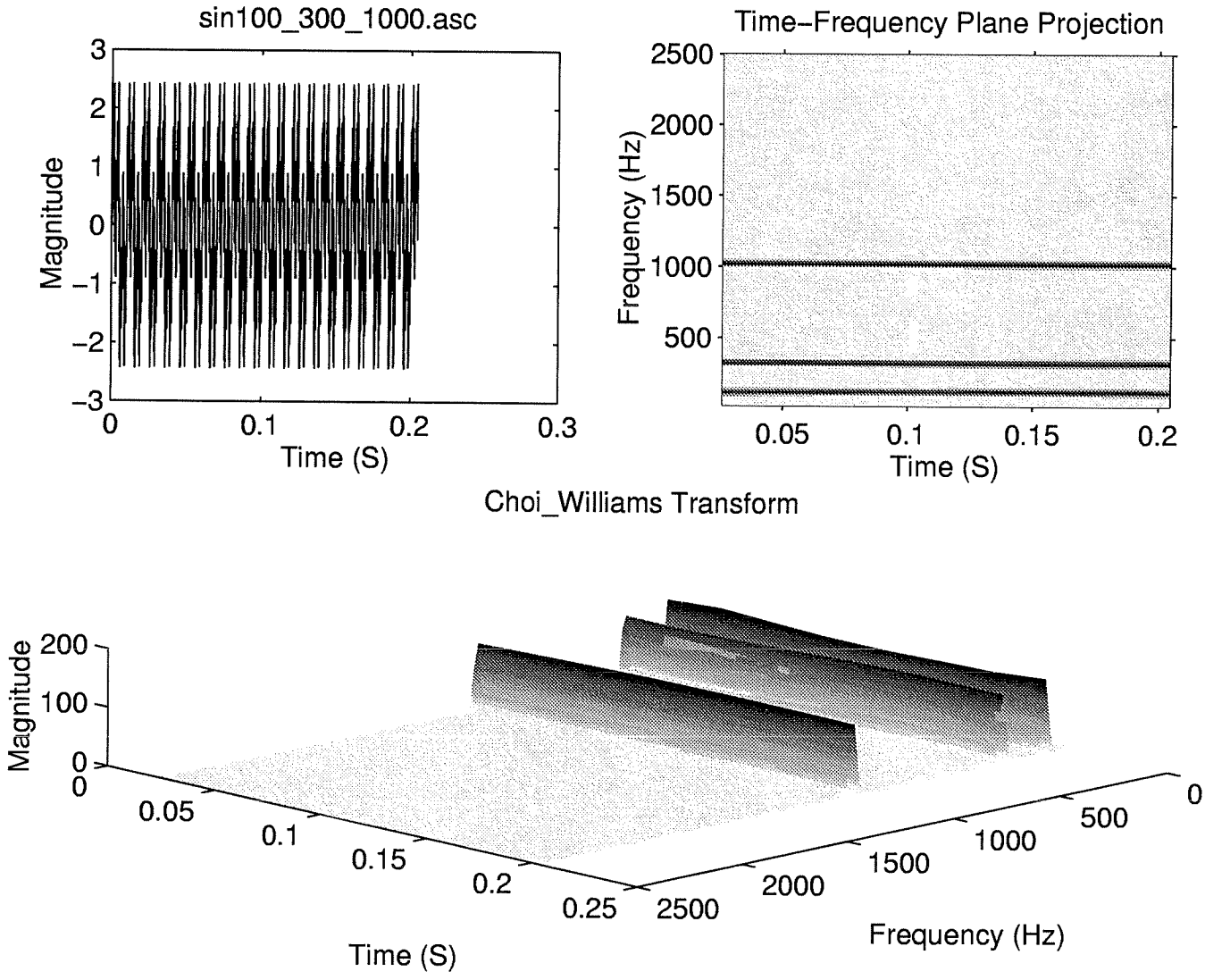

Figure 9: Choi-Williams representation of a sum of sines.

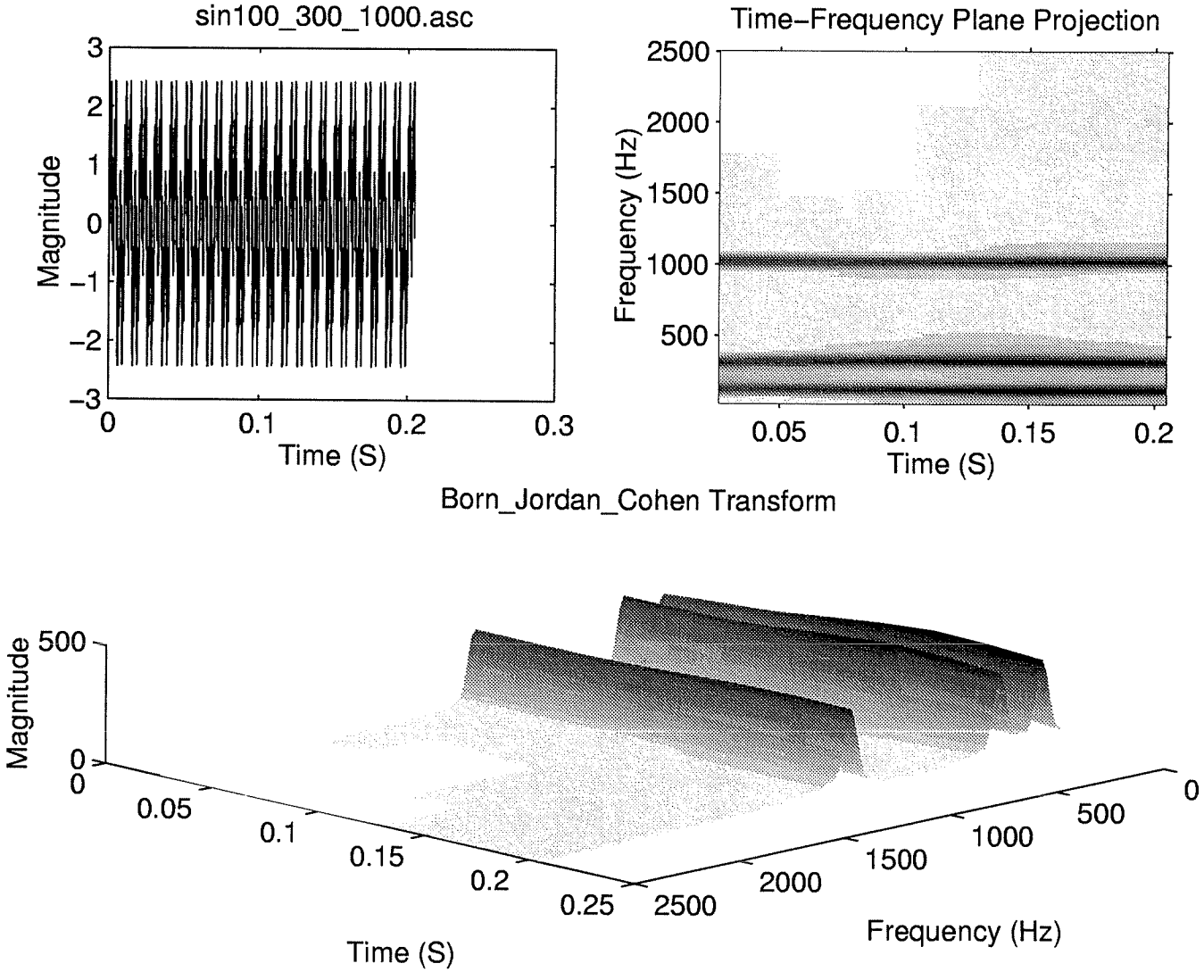

Figure 10: Born-Jordan-Cohen representation of a sum of sines.

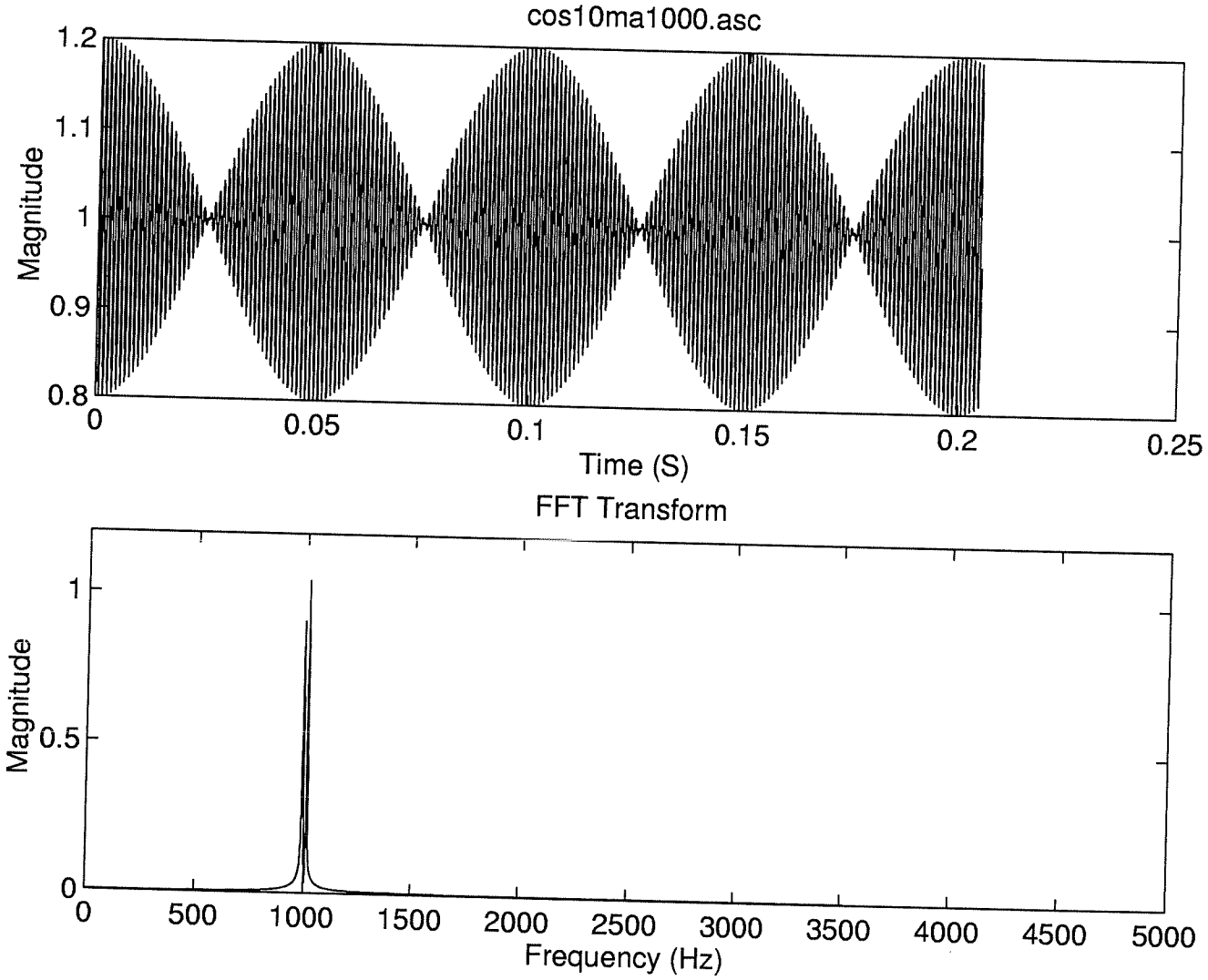

Figure 11: Time and spectrum representation of an amplitude-modulated wave.

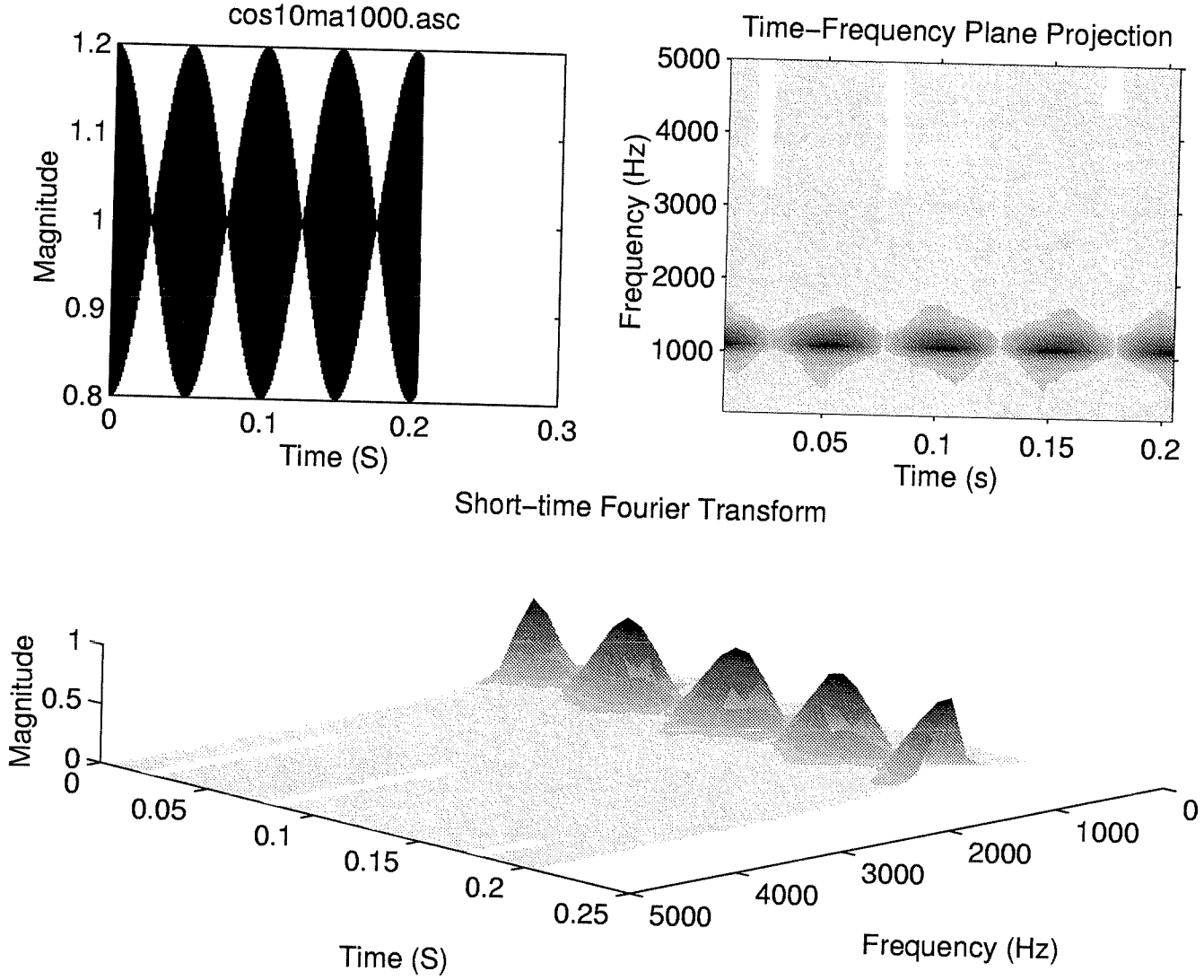

Figure 12: Spectrogram representation of an amplitude-modulated wave.

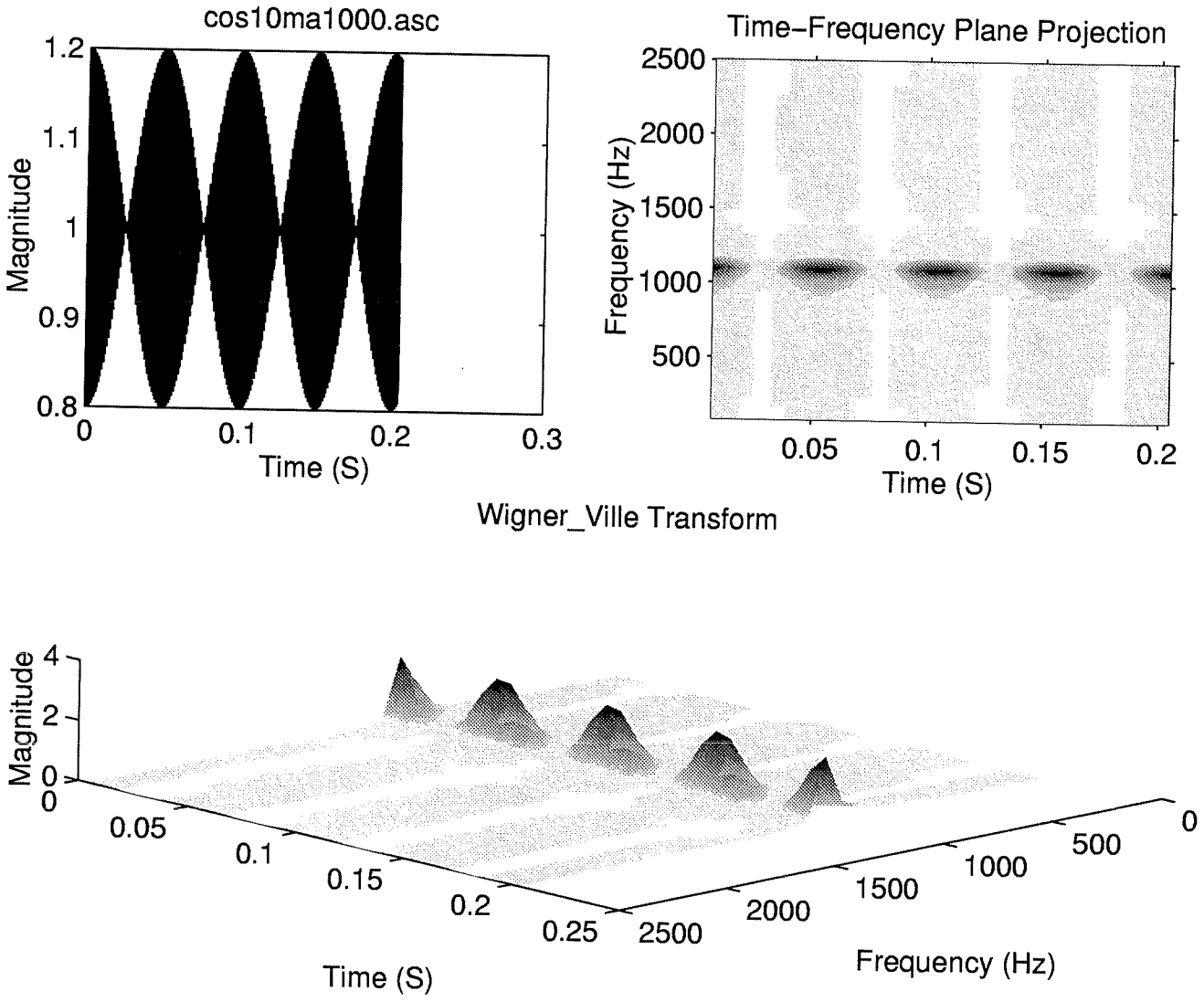

Figure 13: Wigner-Ville representation of an amplitude-modulated wave.

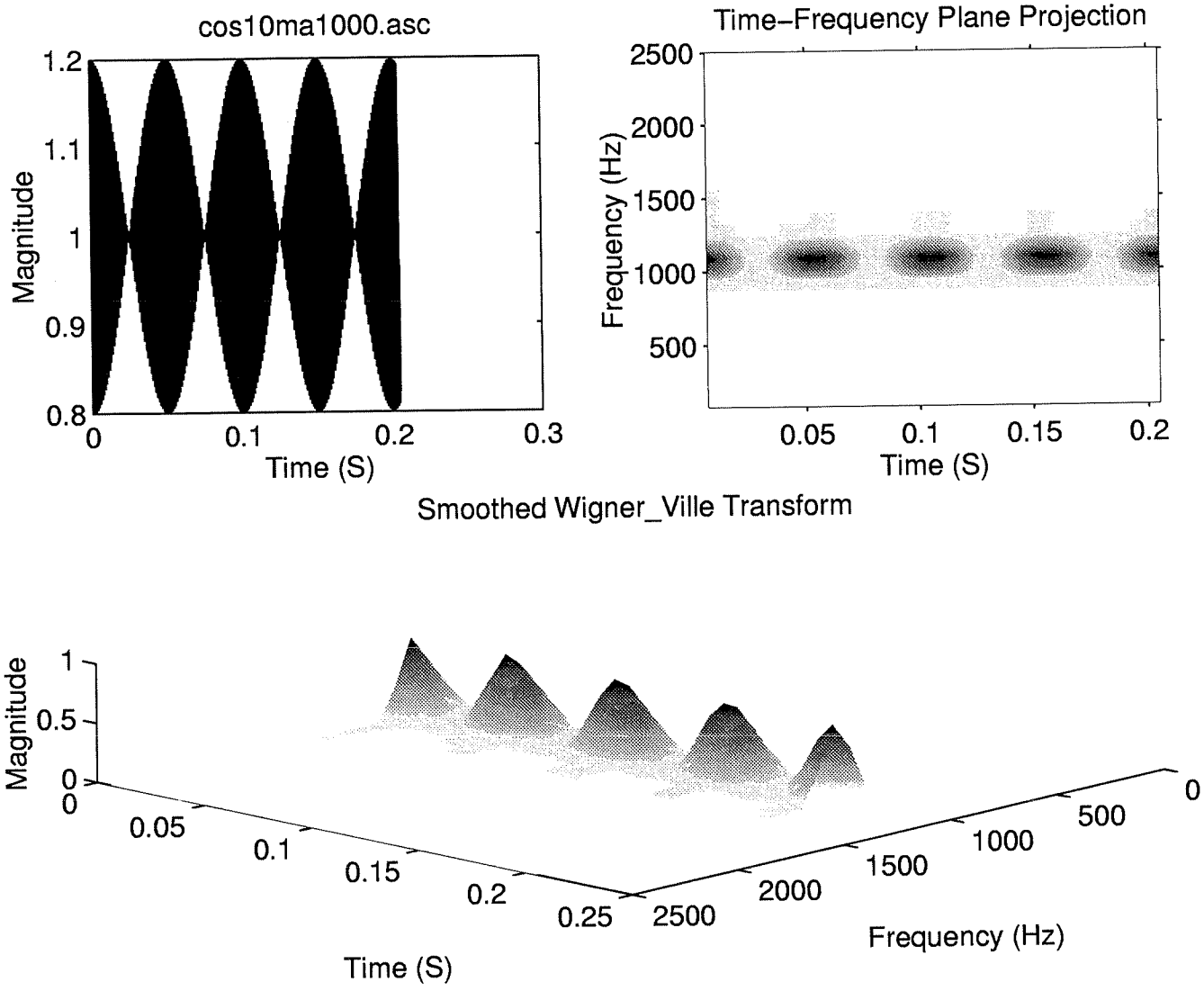

Figure 14: Smoothed Wigner-Ville representation of an amplitude-modulated wave.

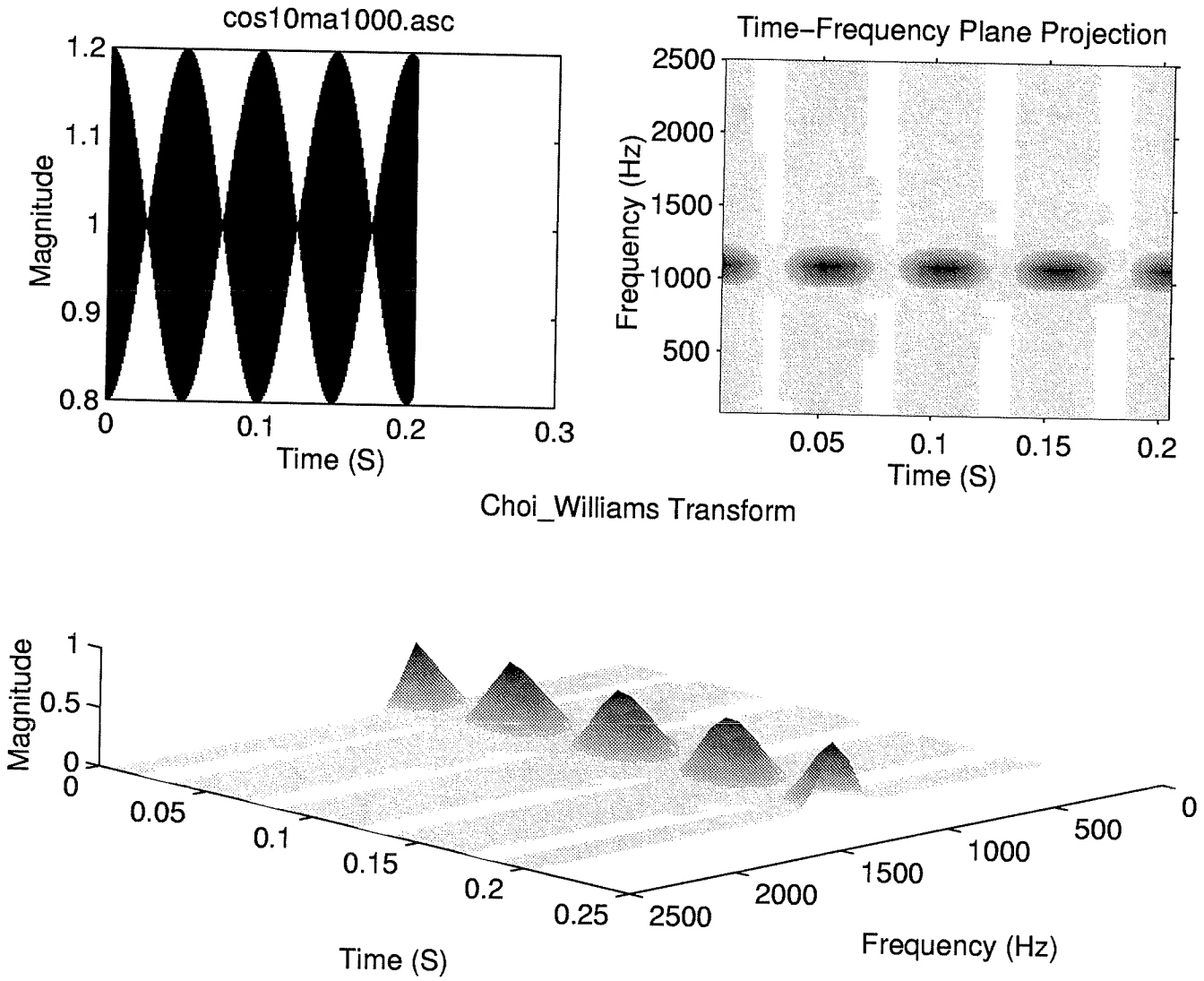

Figure 15: Choi-Williams representation of an amplitude-modulated wave.

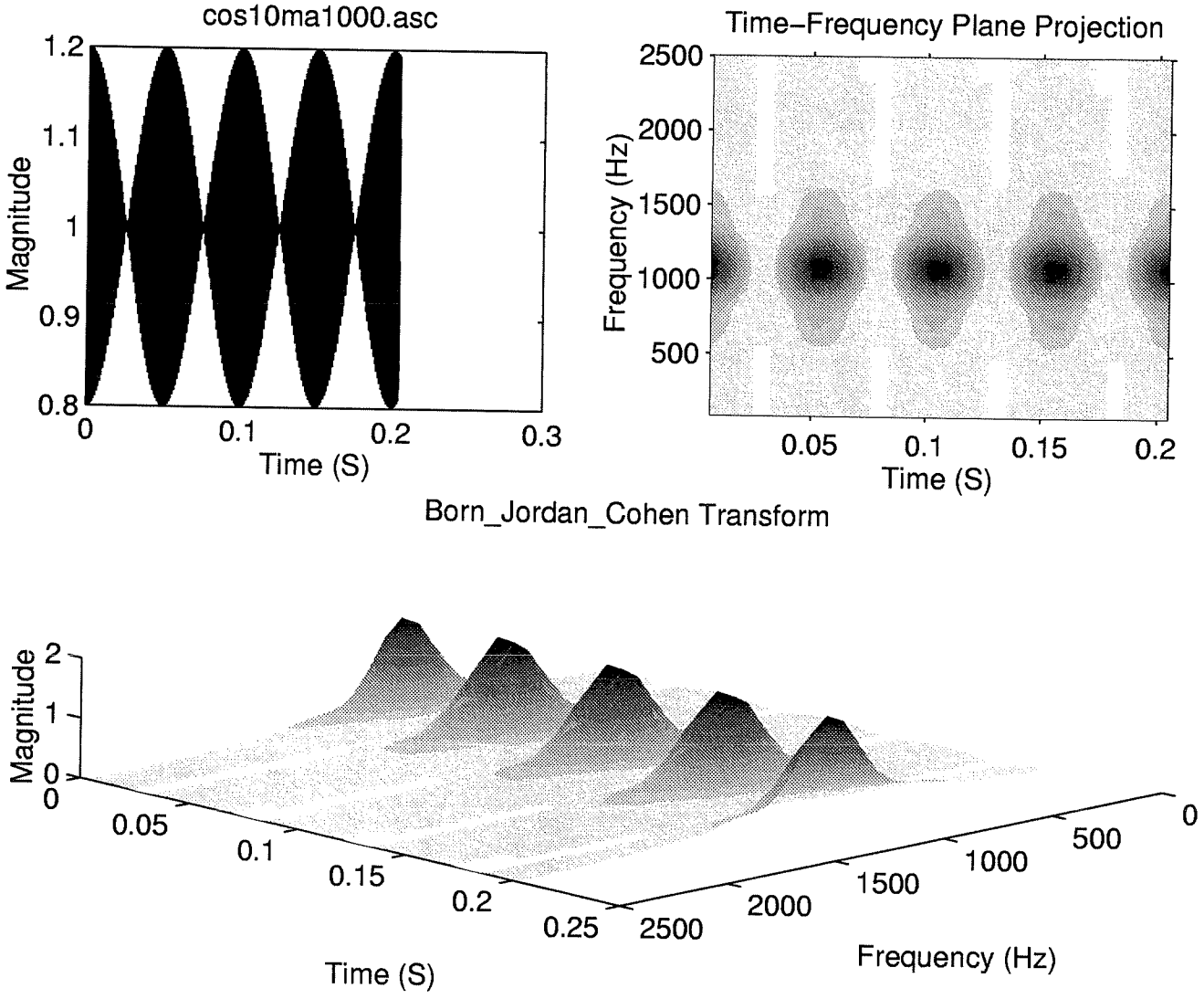

Figure 16: Born-Jordan-Cohen representation of an amplitude-modulated wave.

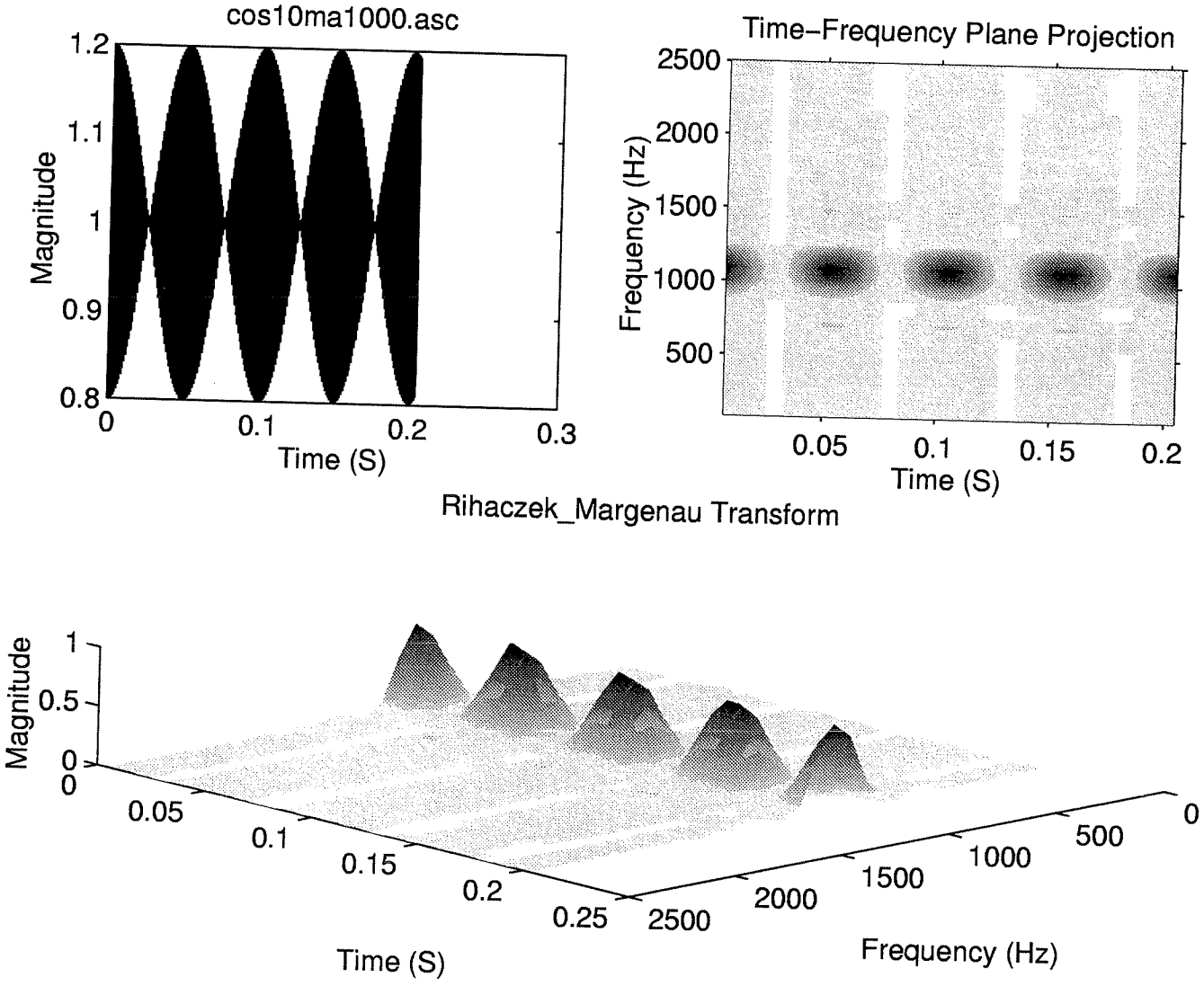

Figure 17: Rihacezk-Margenau representation of an amplitude-modulated wave.

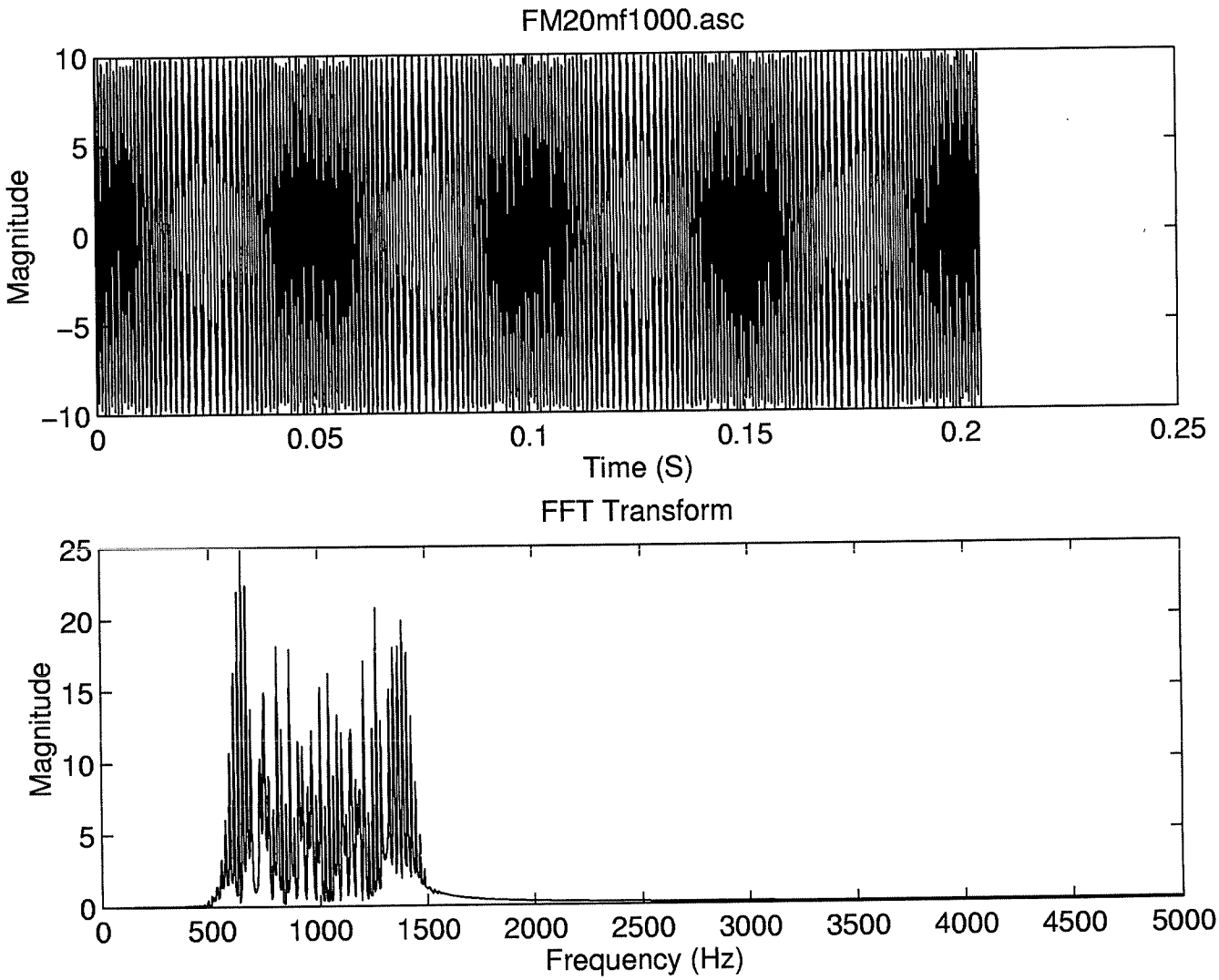

Figure 18: Time and spectrum representation of a frequency-modulated wave.

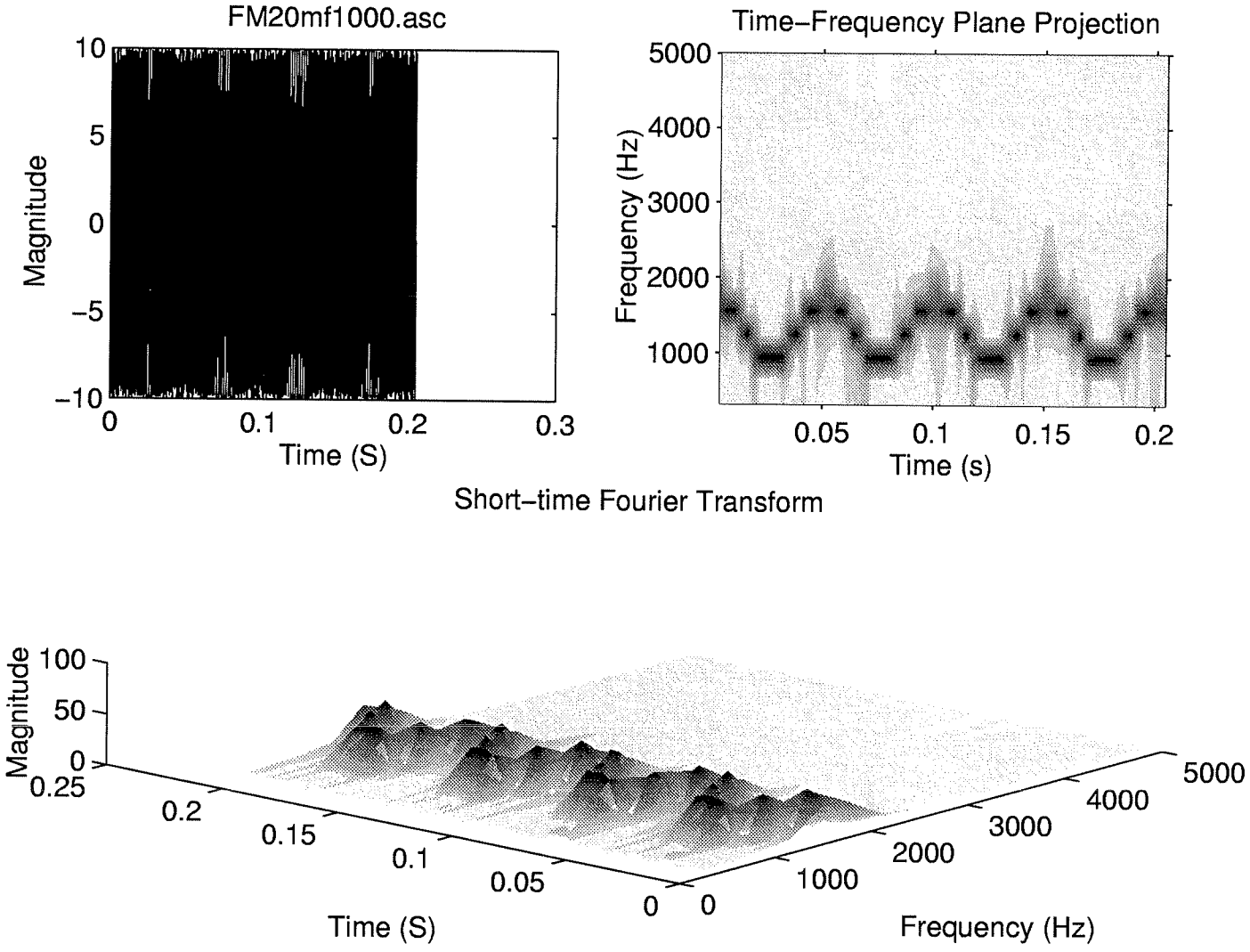

Figure 19: Spectrogram representation of a frequency-modulated wave.

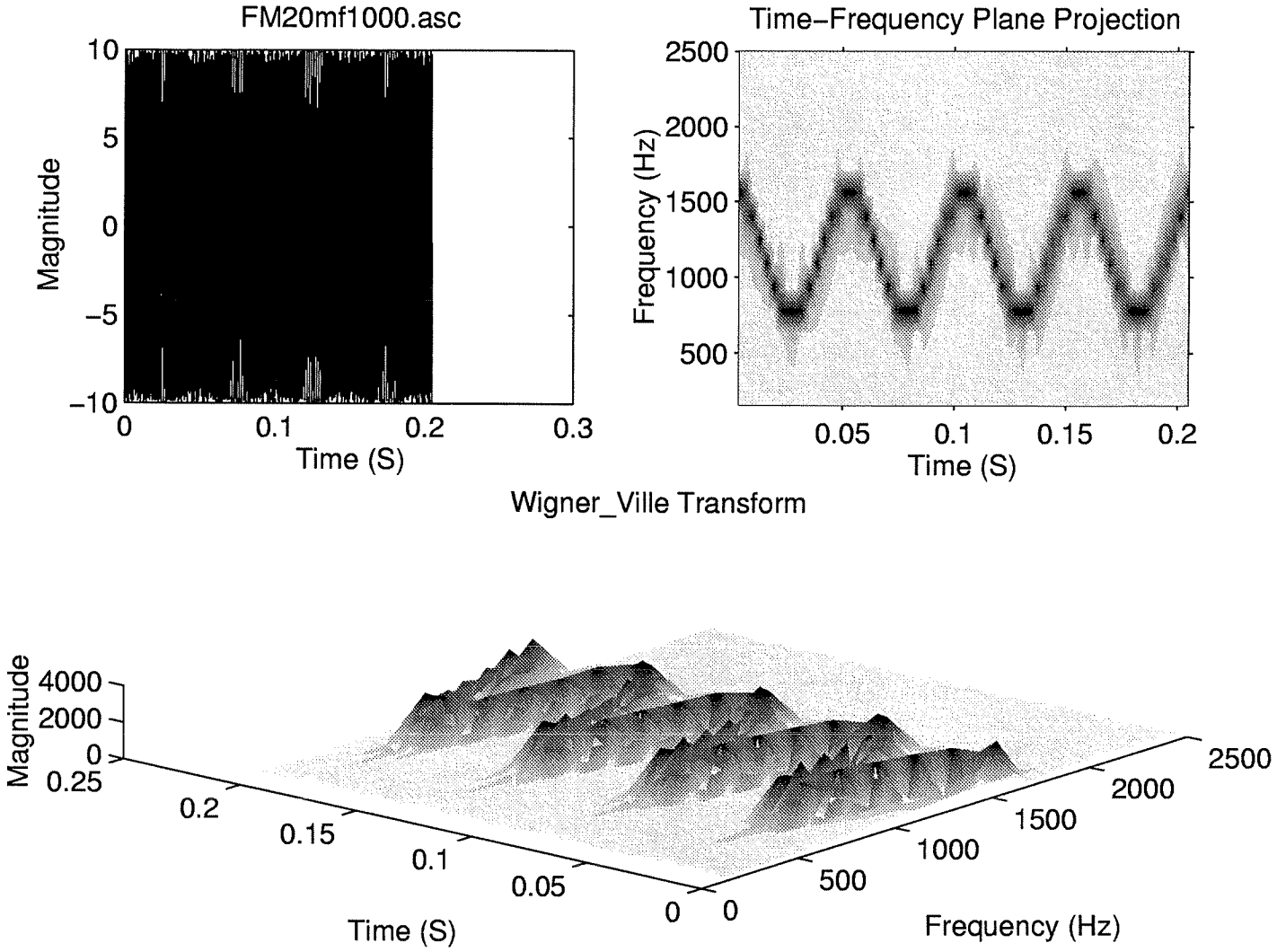

Figure 20: Wigner-Ville representation of a frequency-modulated wave.

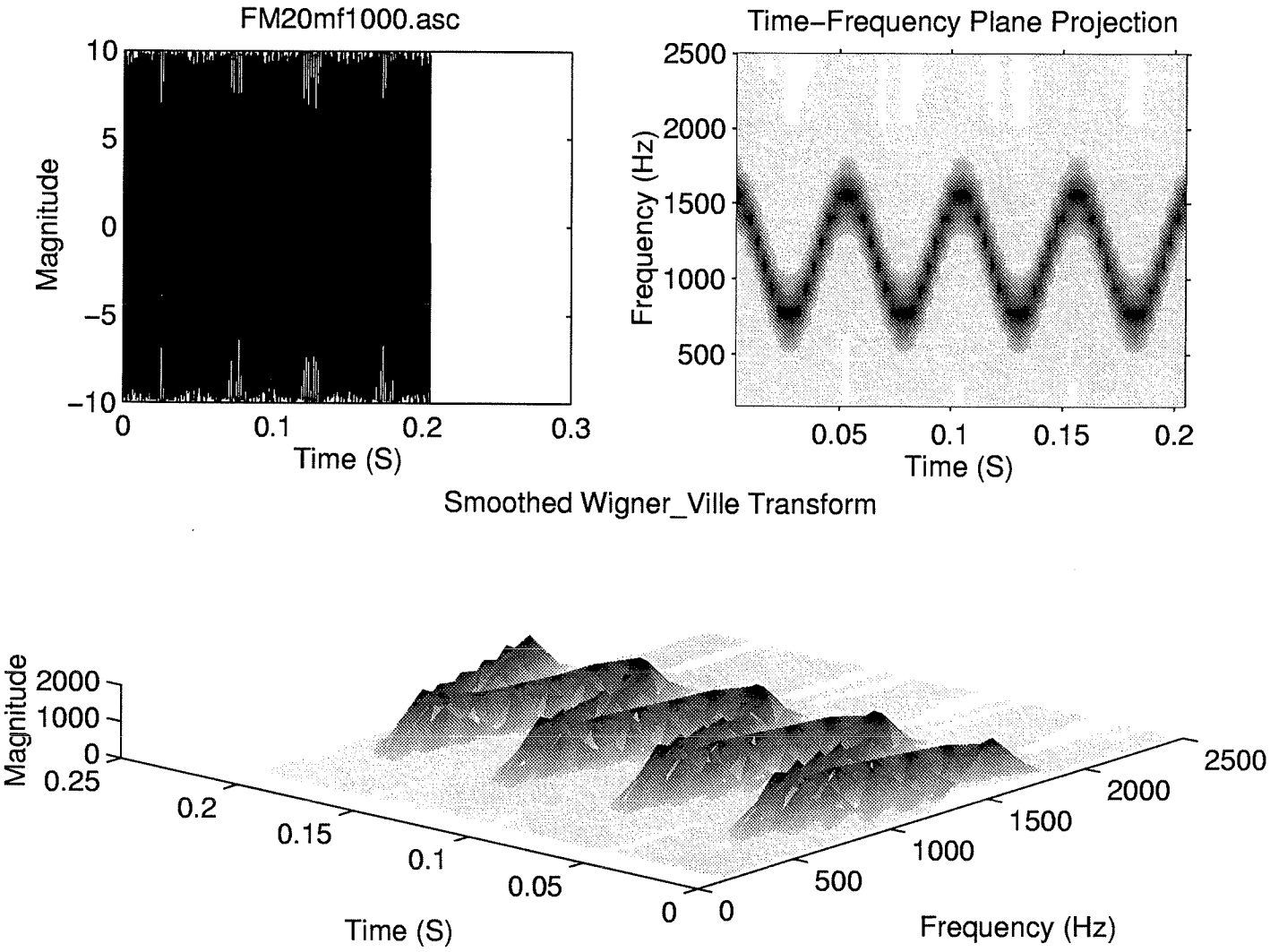

Figure 21: Smoothed Wigner-Ville representation of a frequency-modulated wave.

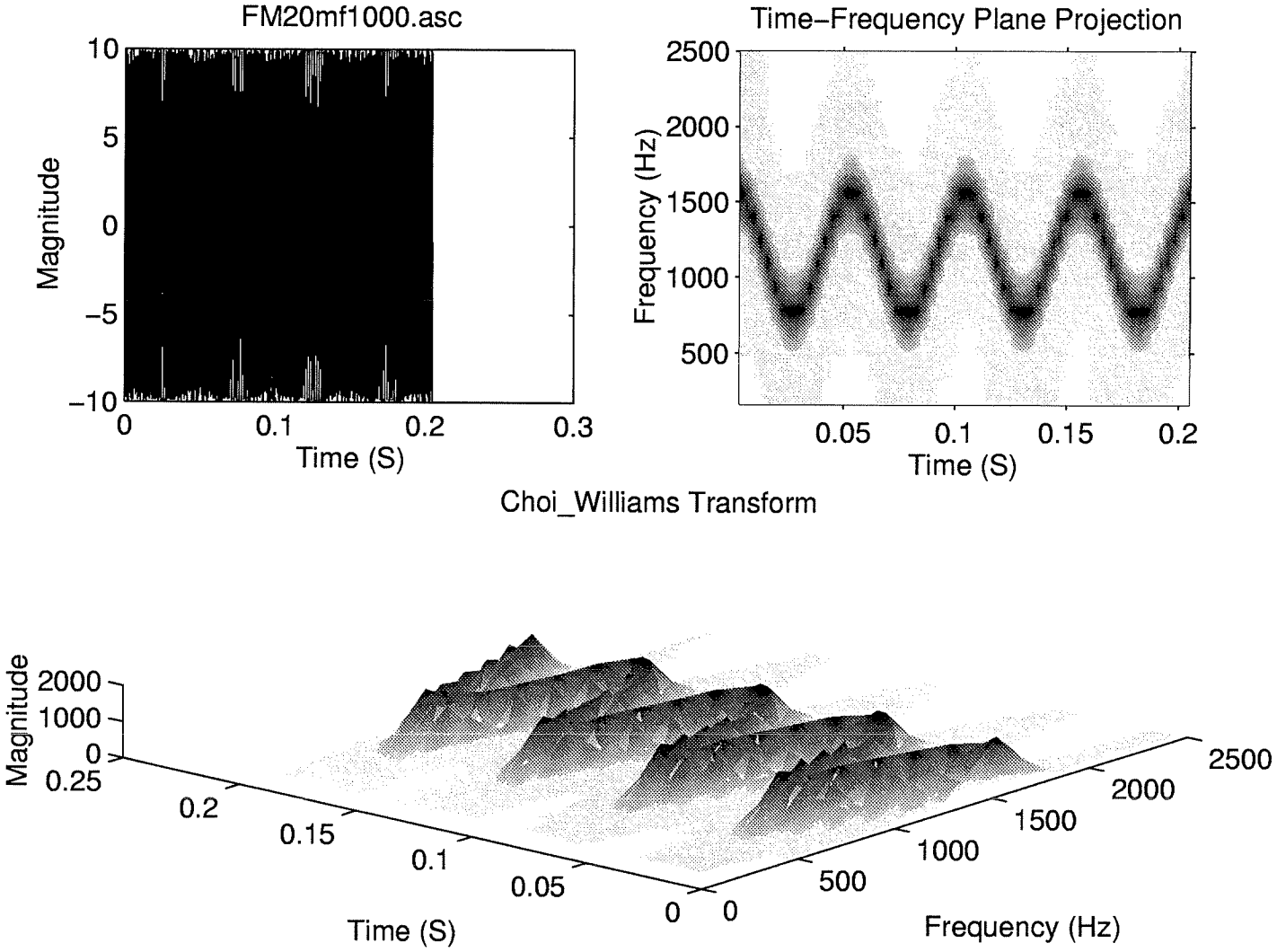

Figure 22: Choi-Williams representation of a frequency-modulated wave.

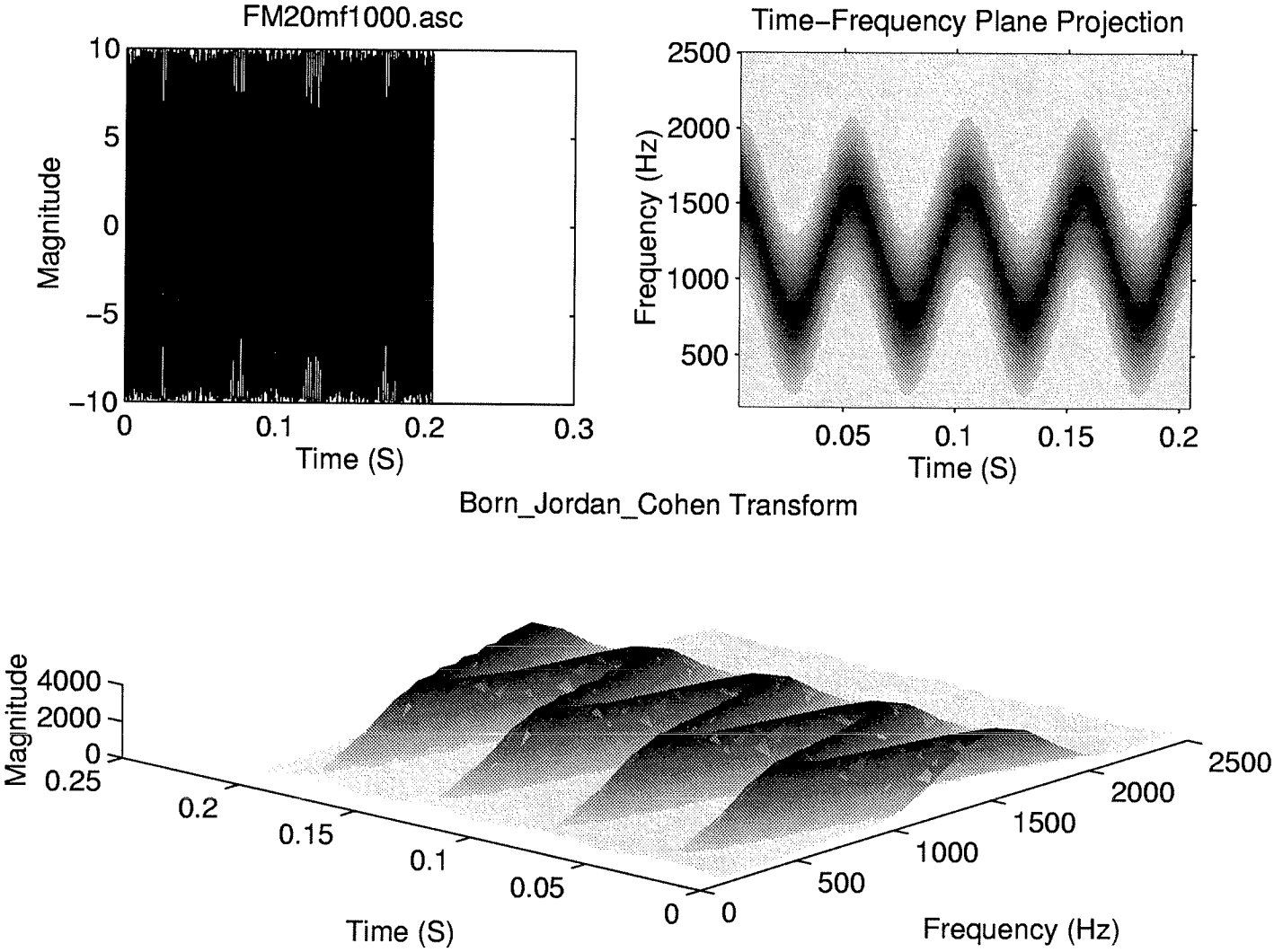

Figure 23: Born-Jordan-Cohen representation of a frequency-modulated wave.

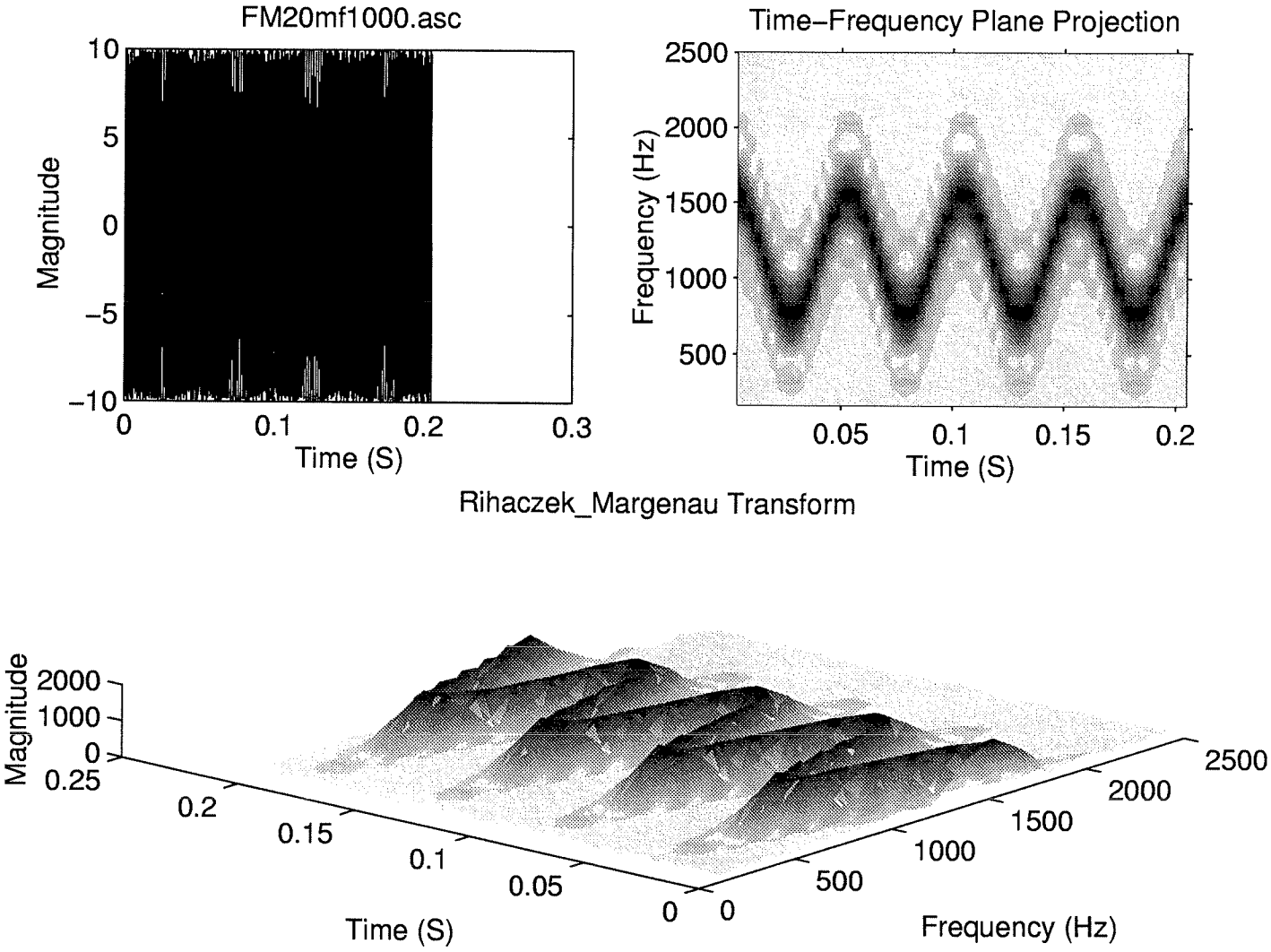

Figure 24: Rihacezk-Margenau representation of a frequency-modulated wave.

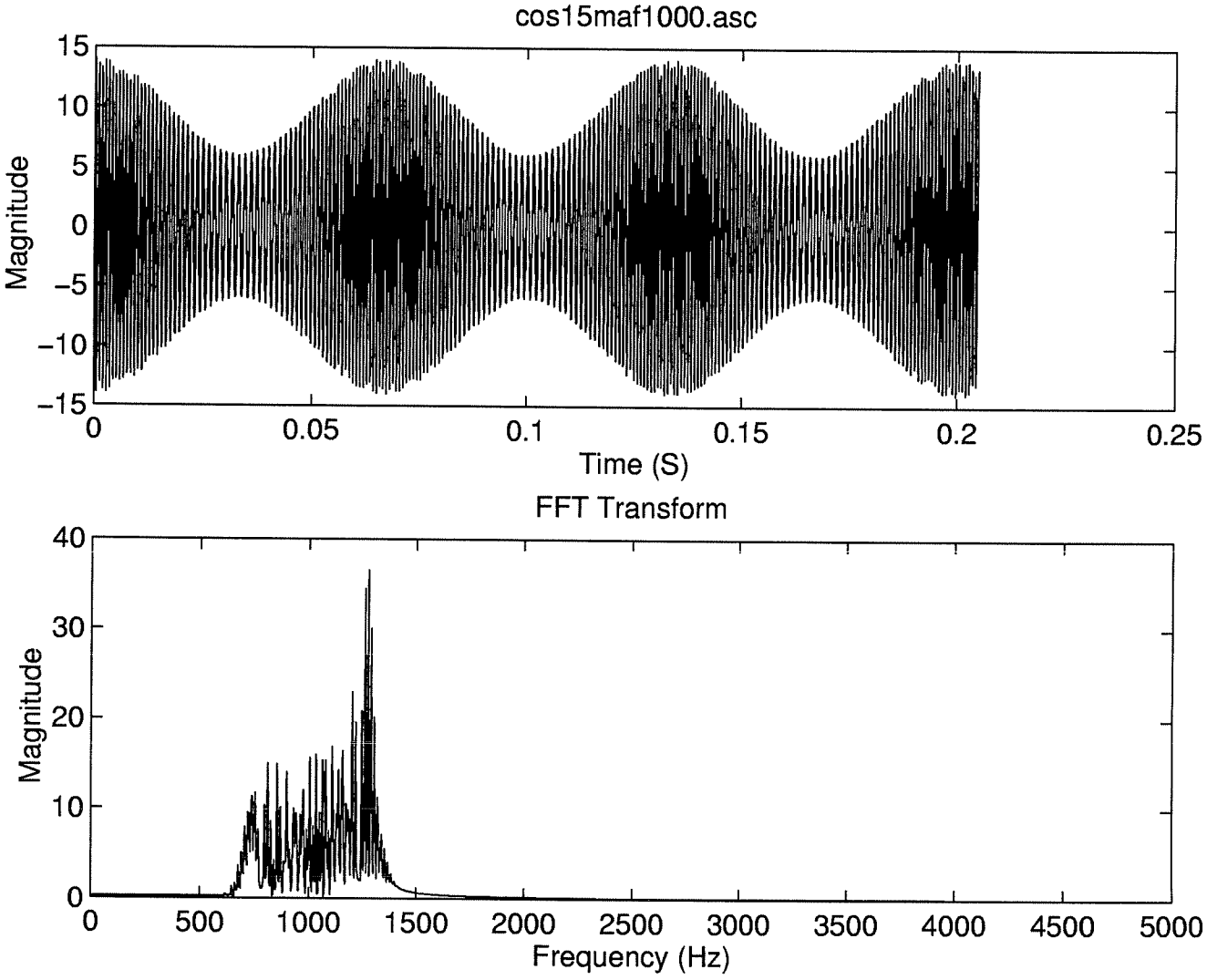

Figure 25: Time and spectrum representation of a frequency and amplitude modulated wave.

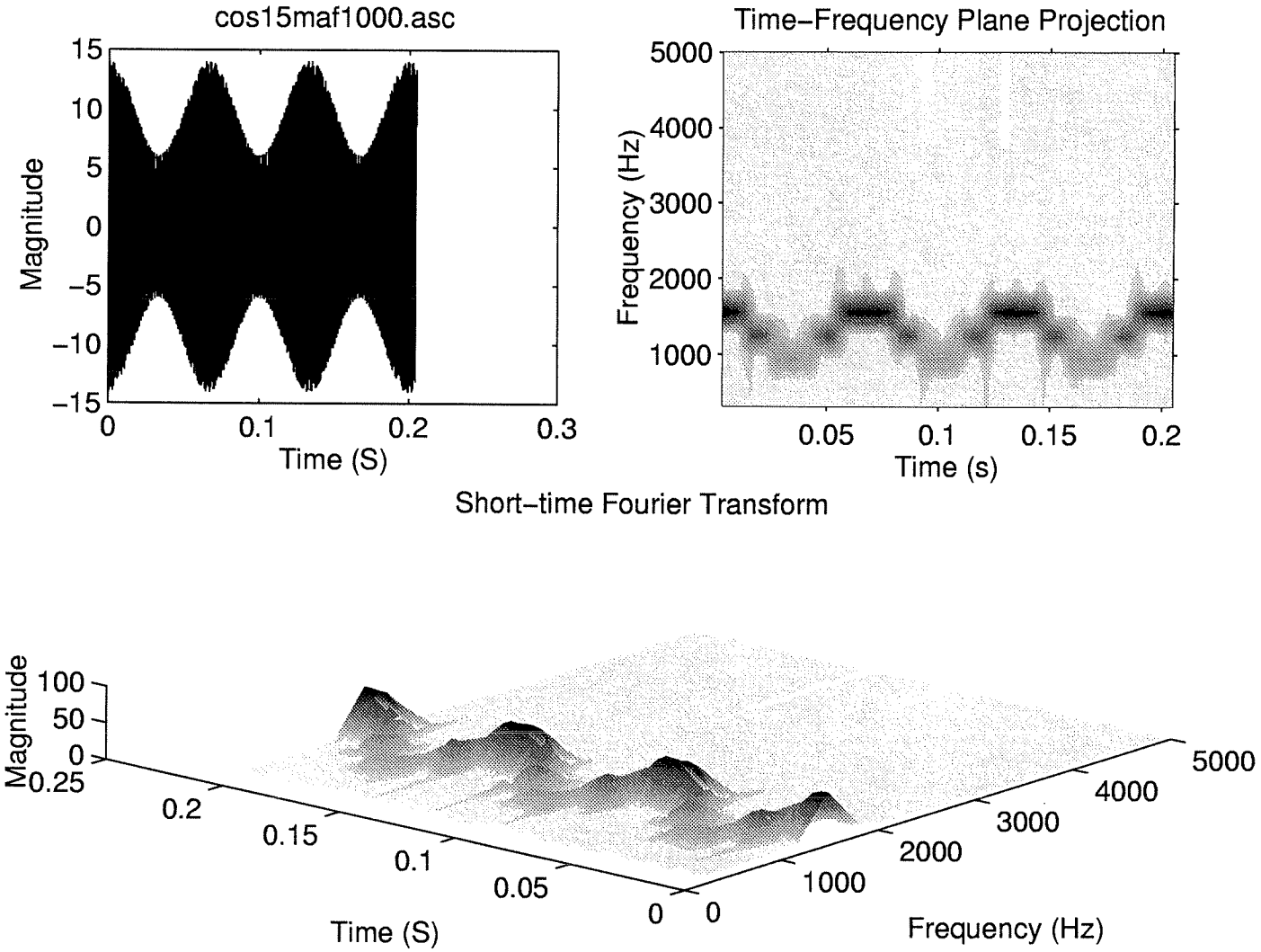

Figure 26: Spectrogram representation of a frequency and amplitude modulated wave.

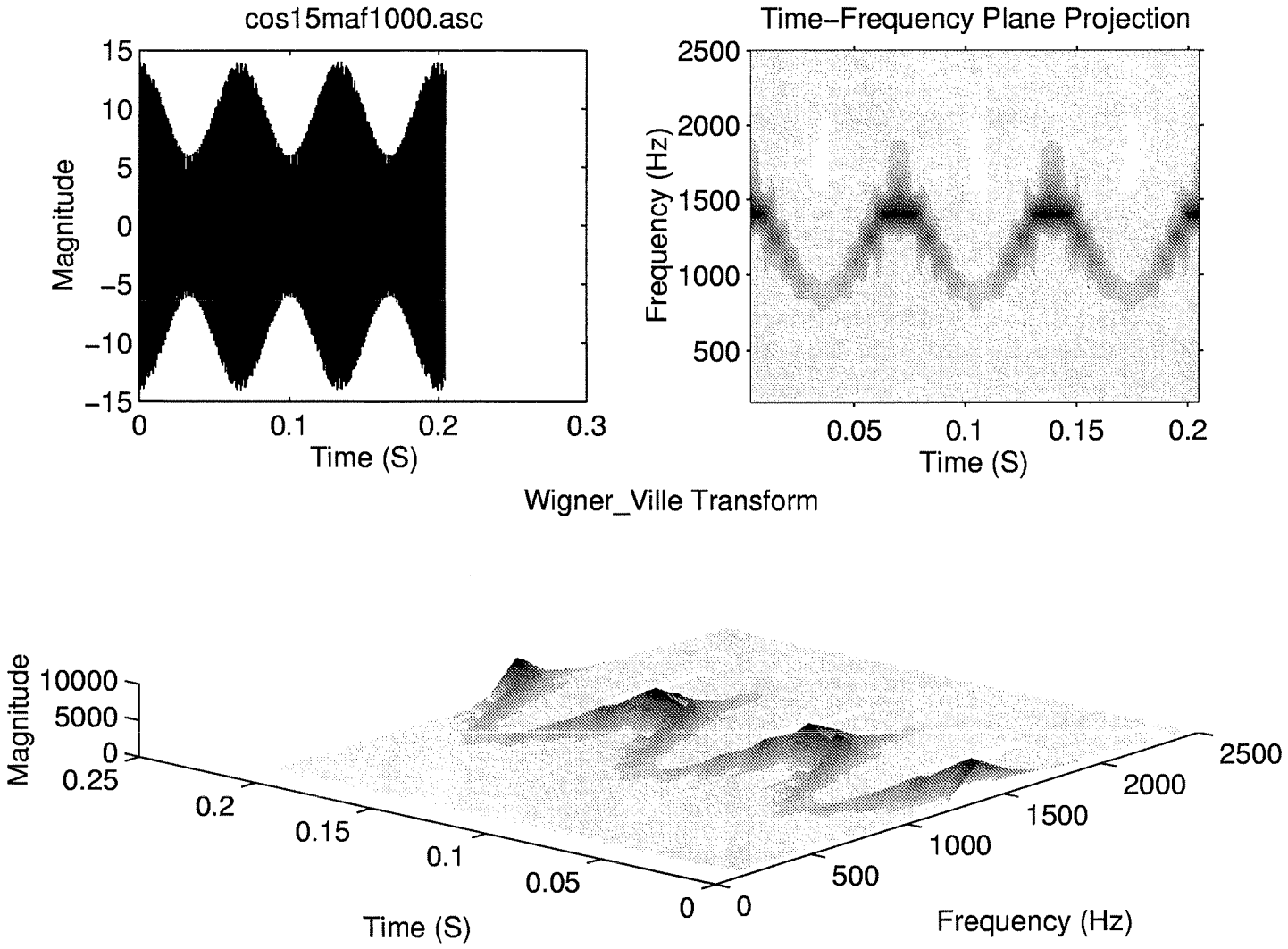

Figure 27: Wigner-Ville representation of a frequency and amplitude modulated wave.

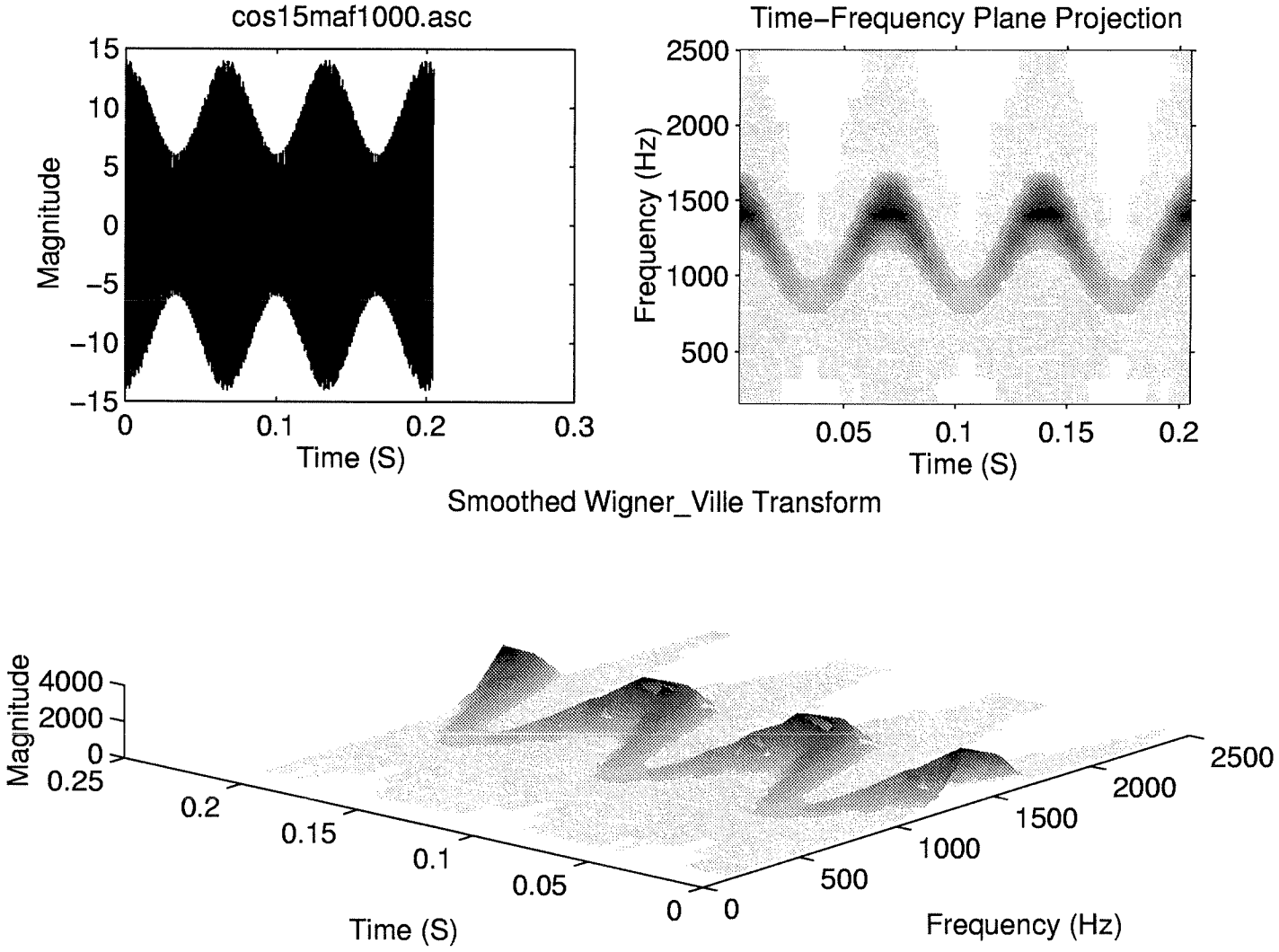

Figure 28: Smoothed Wigner-Ville representation of a frequency and amplitude modulated wave.

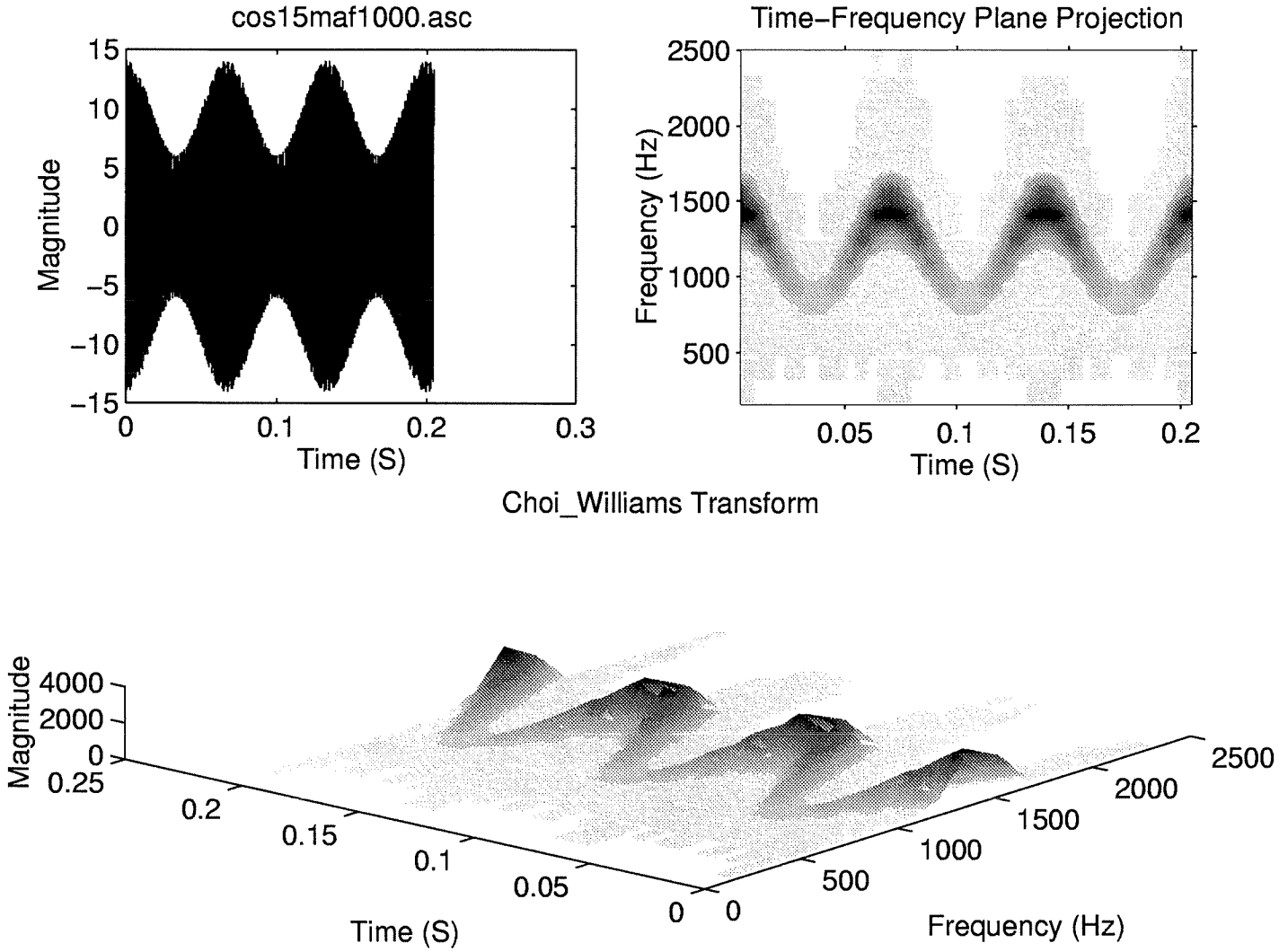

Figure 29: Choi-Williams representation of a frequency and amplitude modulated wave.

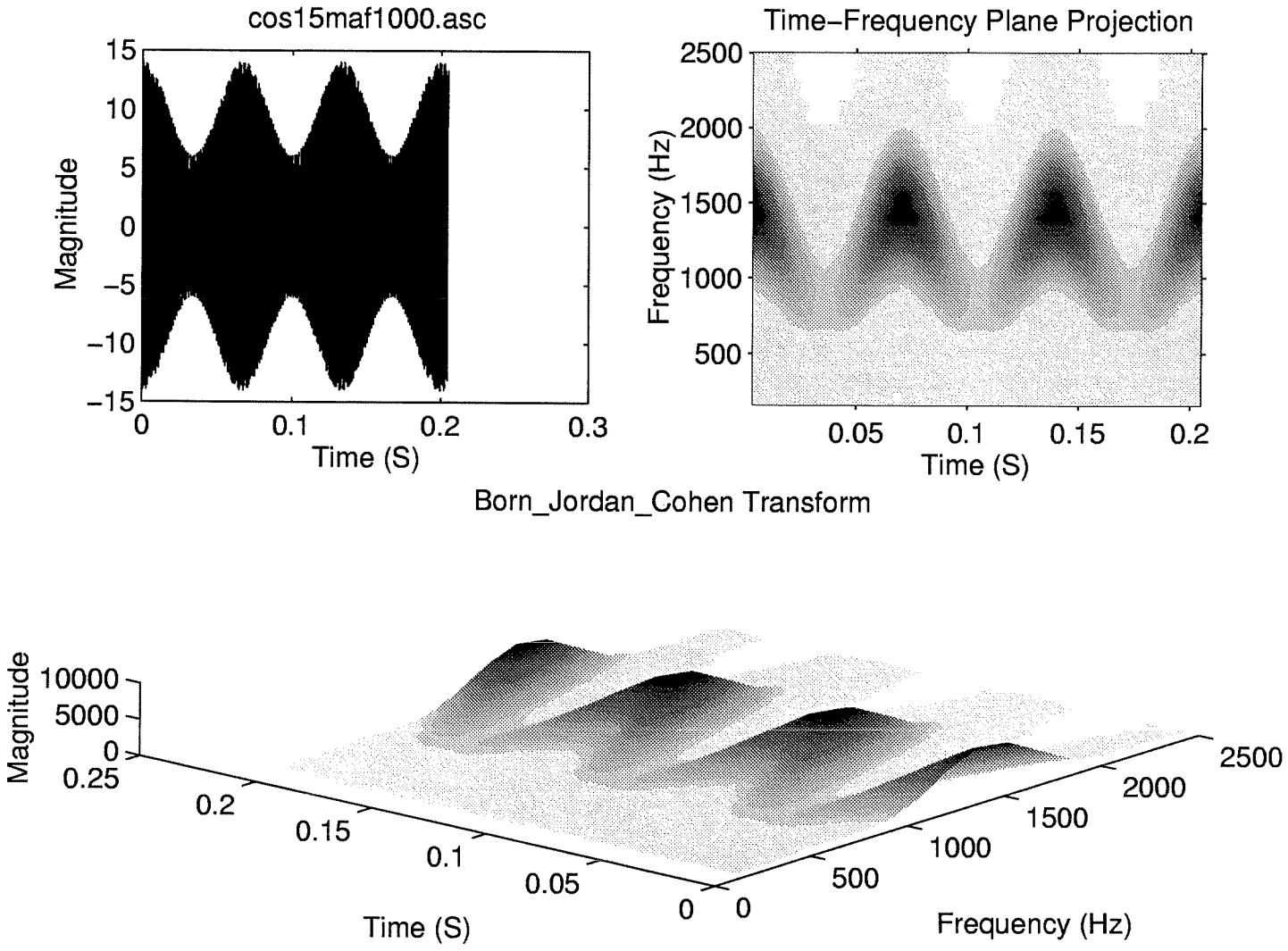

Figure 30: Born-Jordan-Cohen representation of a frequency and amplitude modulated wave.

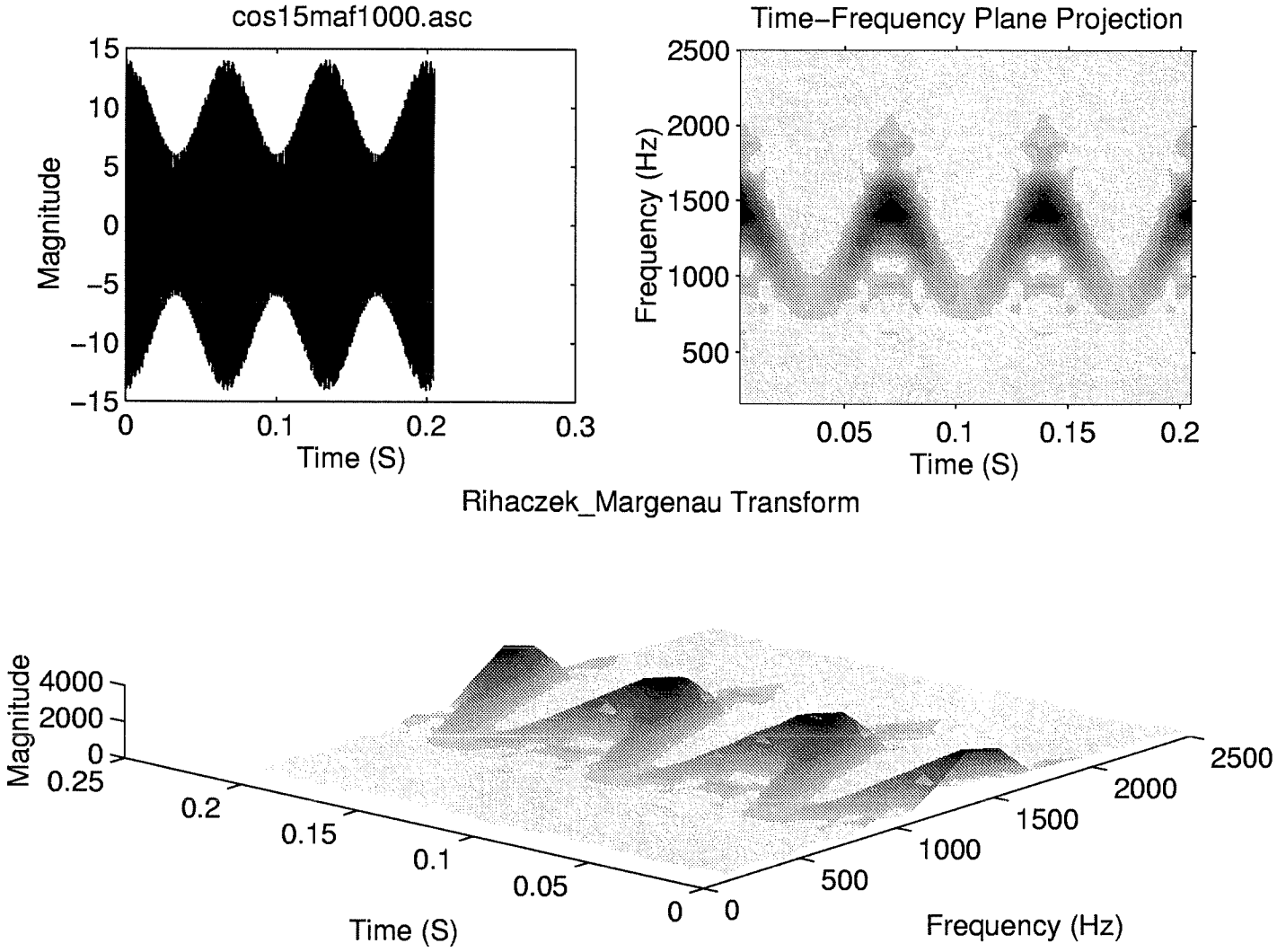

Figure 31: Rihacezk-Margenau representation of a frequency and amplitude modulated wave.

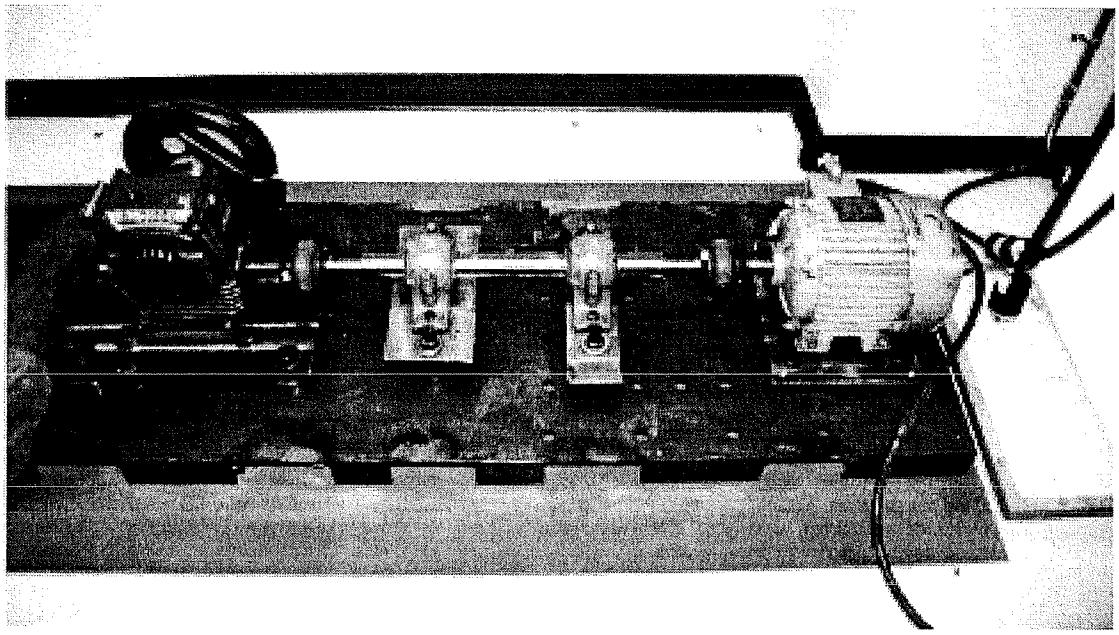

Figure 32: Setup test.

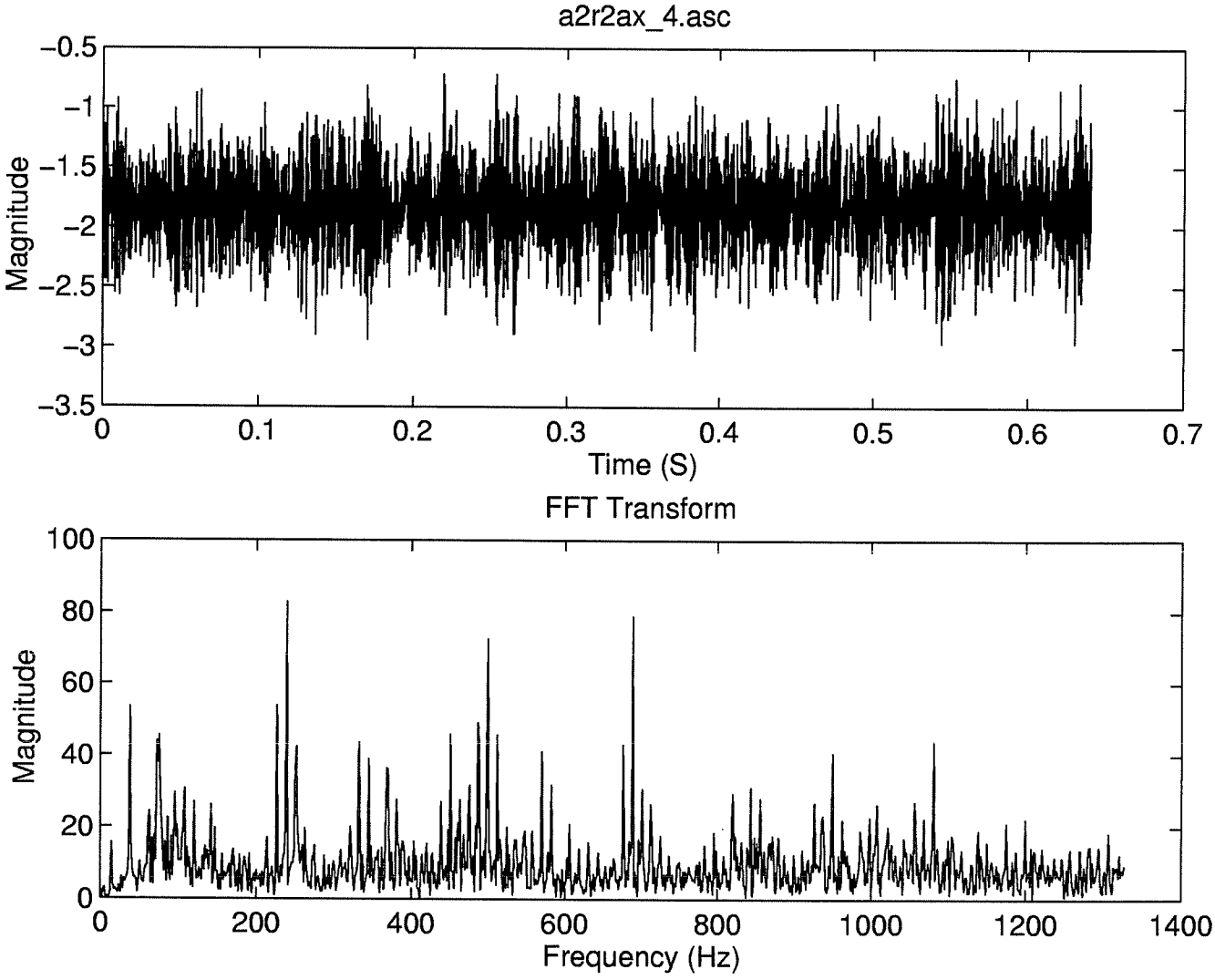

Figure 33: Time and spectrum representation of the signal measured on a defective bearing.

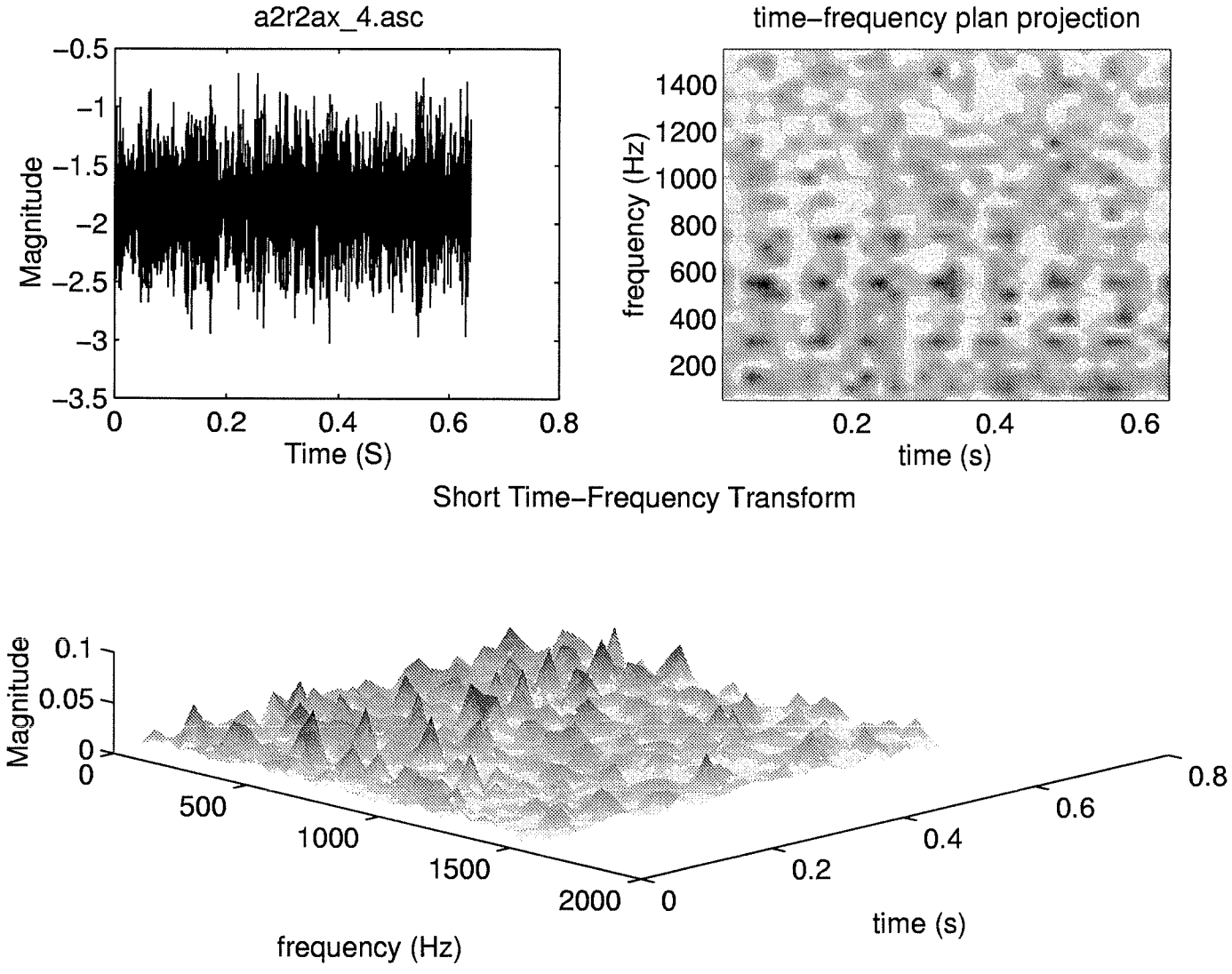

Figure 34: Spectrogram representation of the signal measured on a defective bearing.

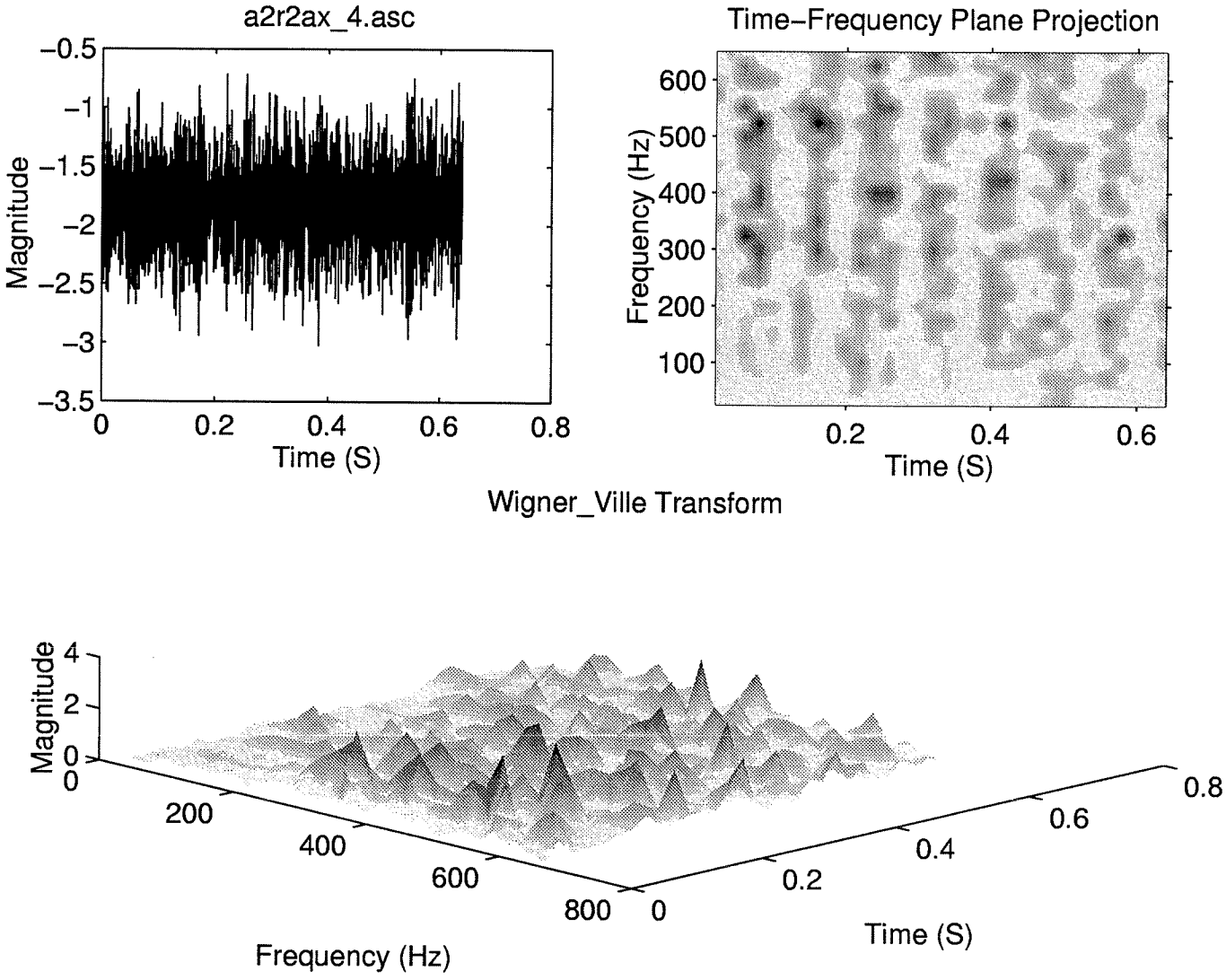

Figure 35: Wigner-Ville representation of the signal measured on a defective bearing.

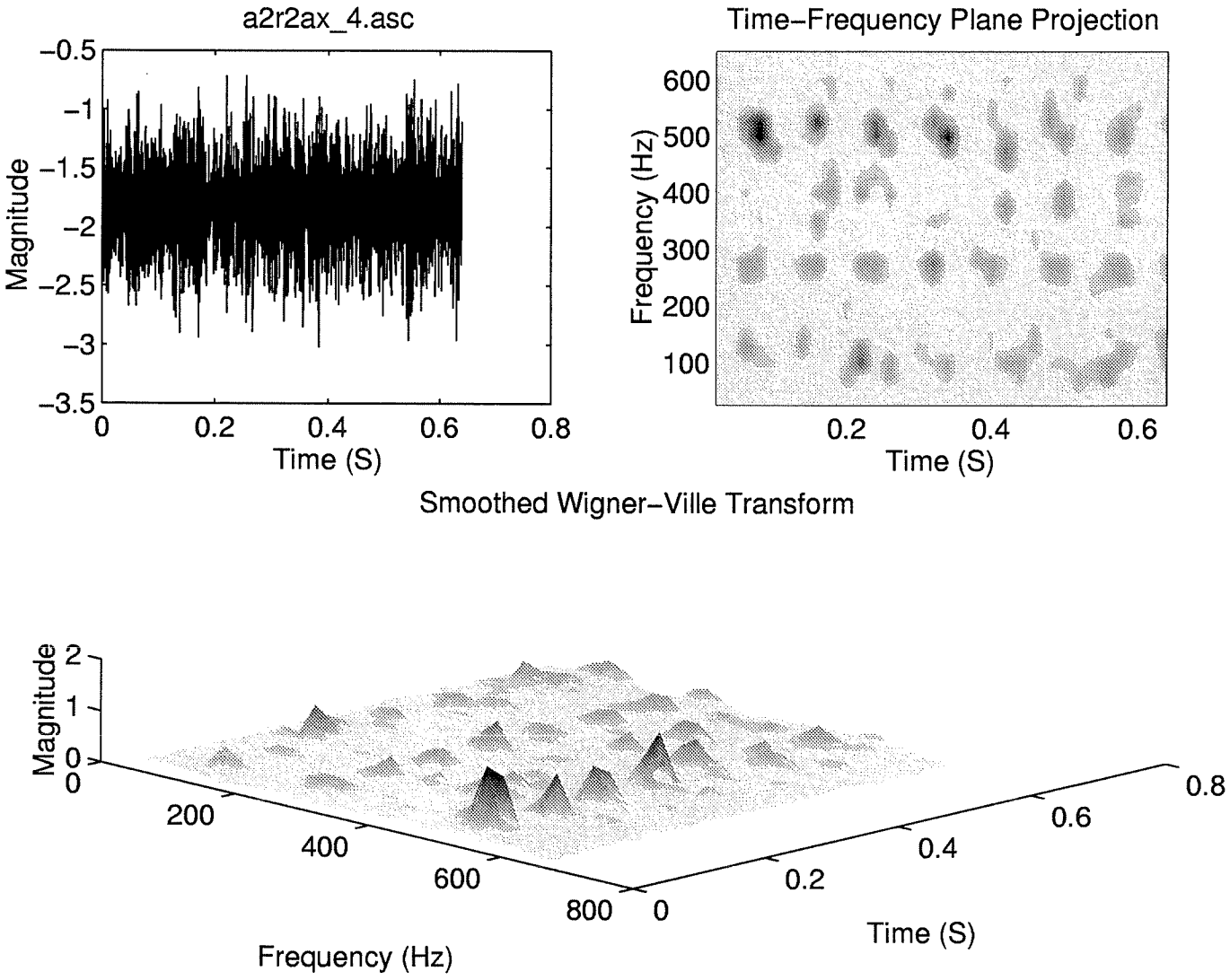

Figure 36: Smoothed Wigner-Ville representation of the signal measured on a defective bearing.

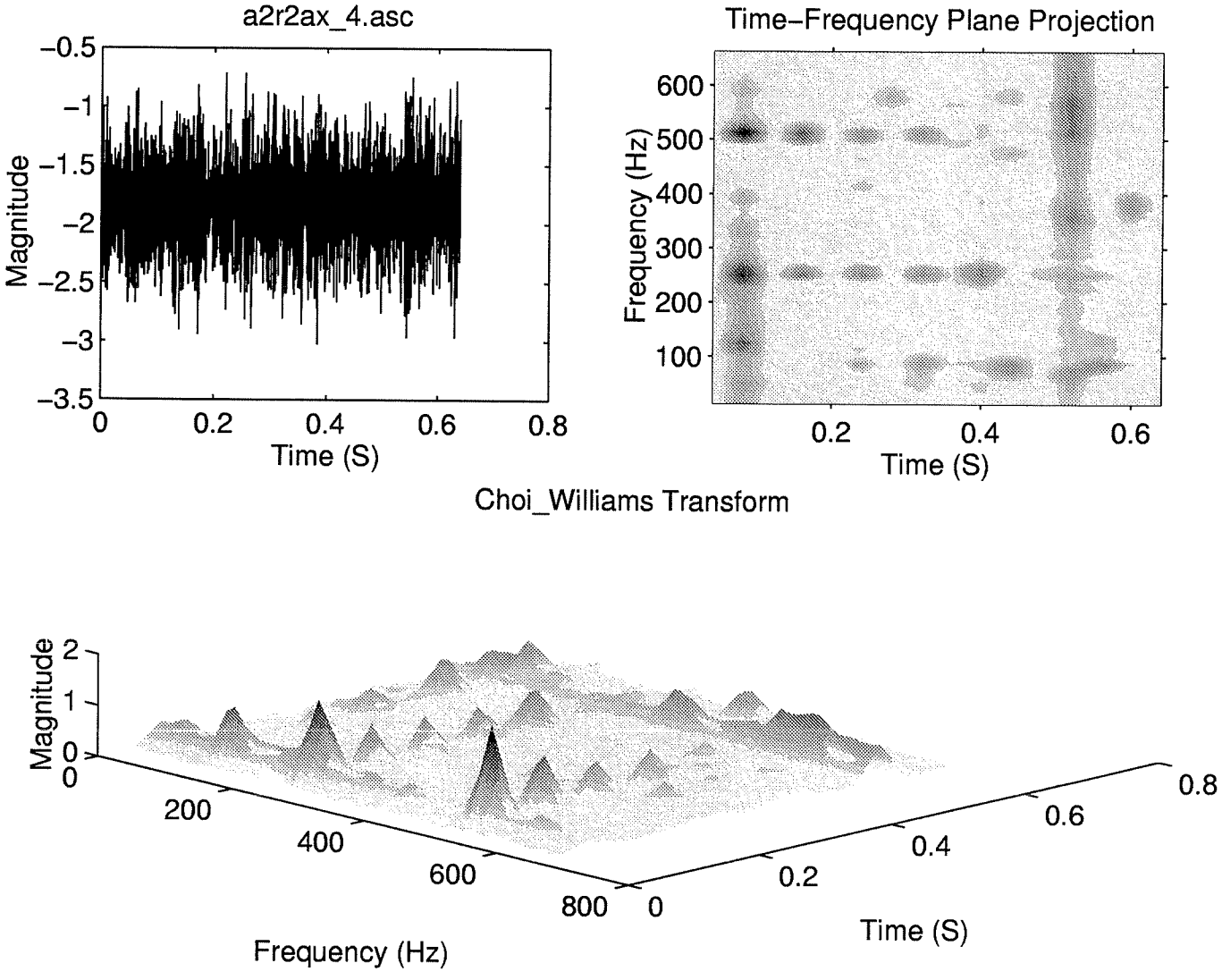

Figure 37: Choi-Williams representation of the signal measured on a defective bearing.

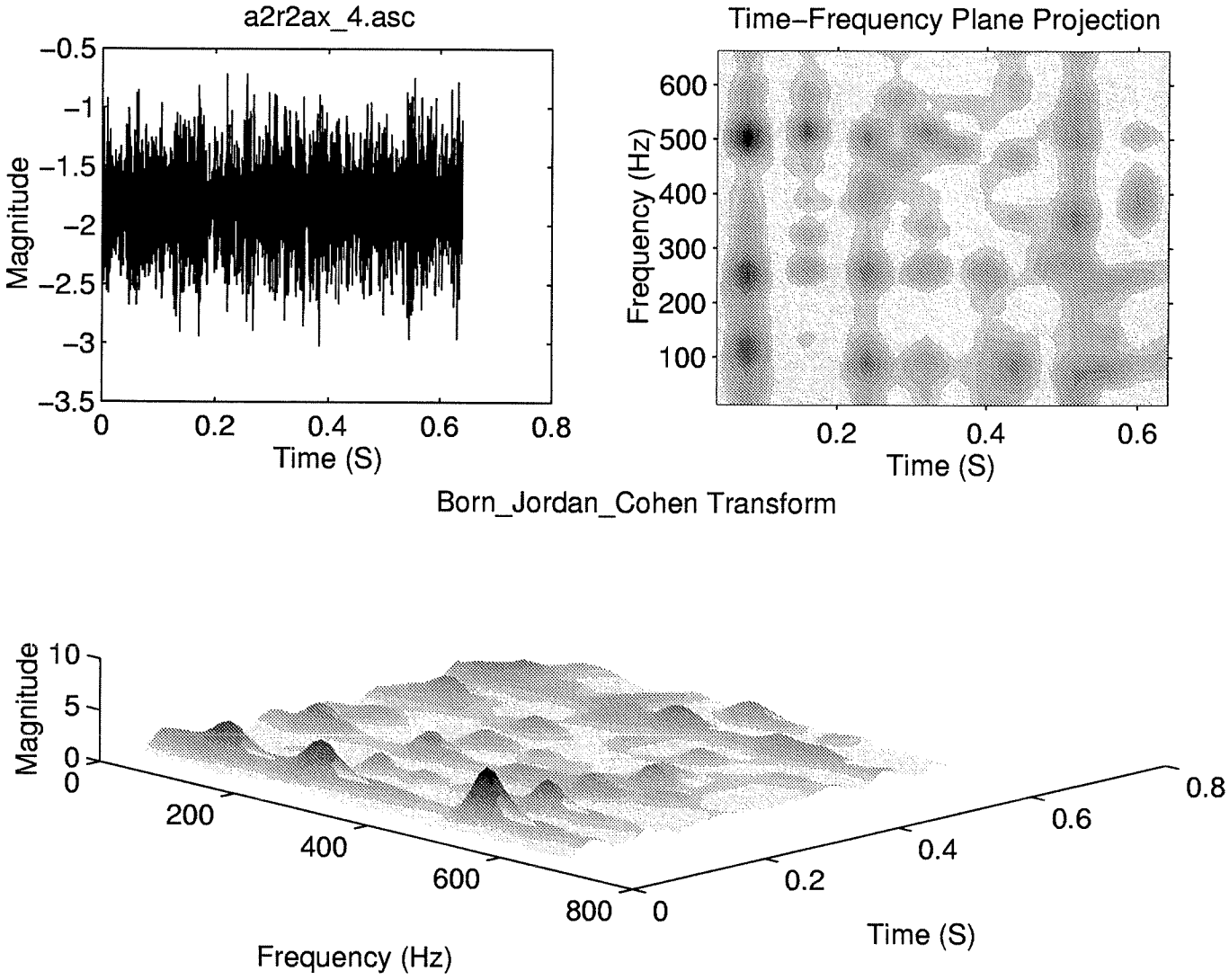

Figure 38: Born-Jordan-Cohen representation of the signal measured on a defective bearing.

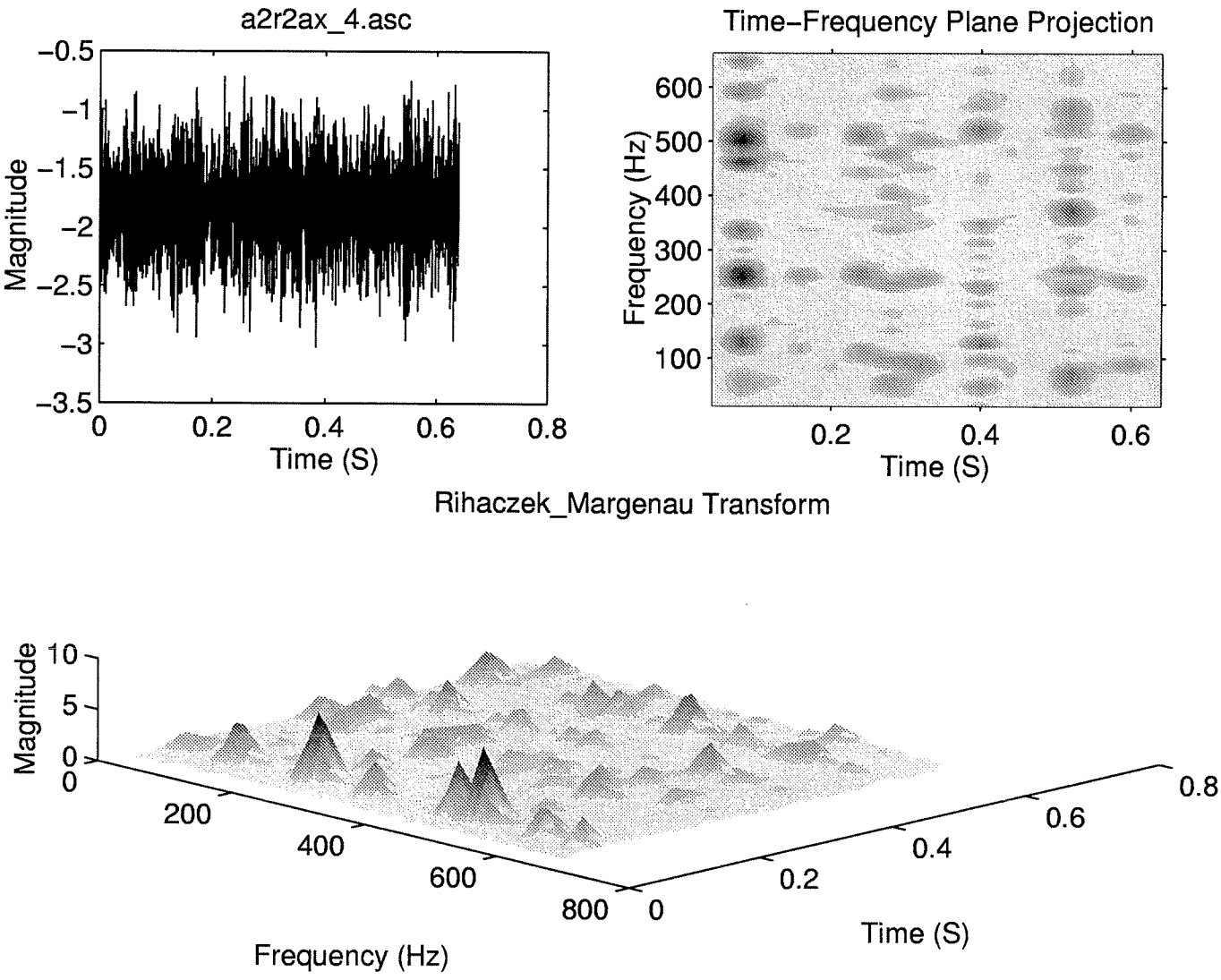

Figure 39: Rihacezk-Margenau representation of the signal measured on a defective bearing.

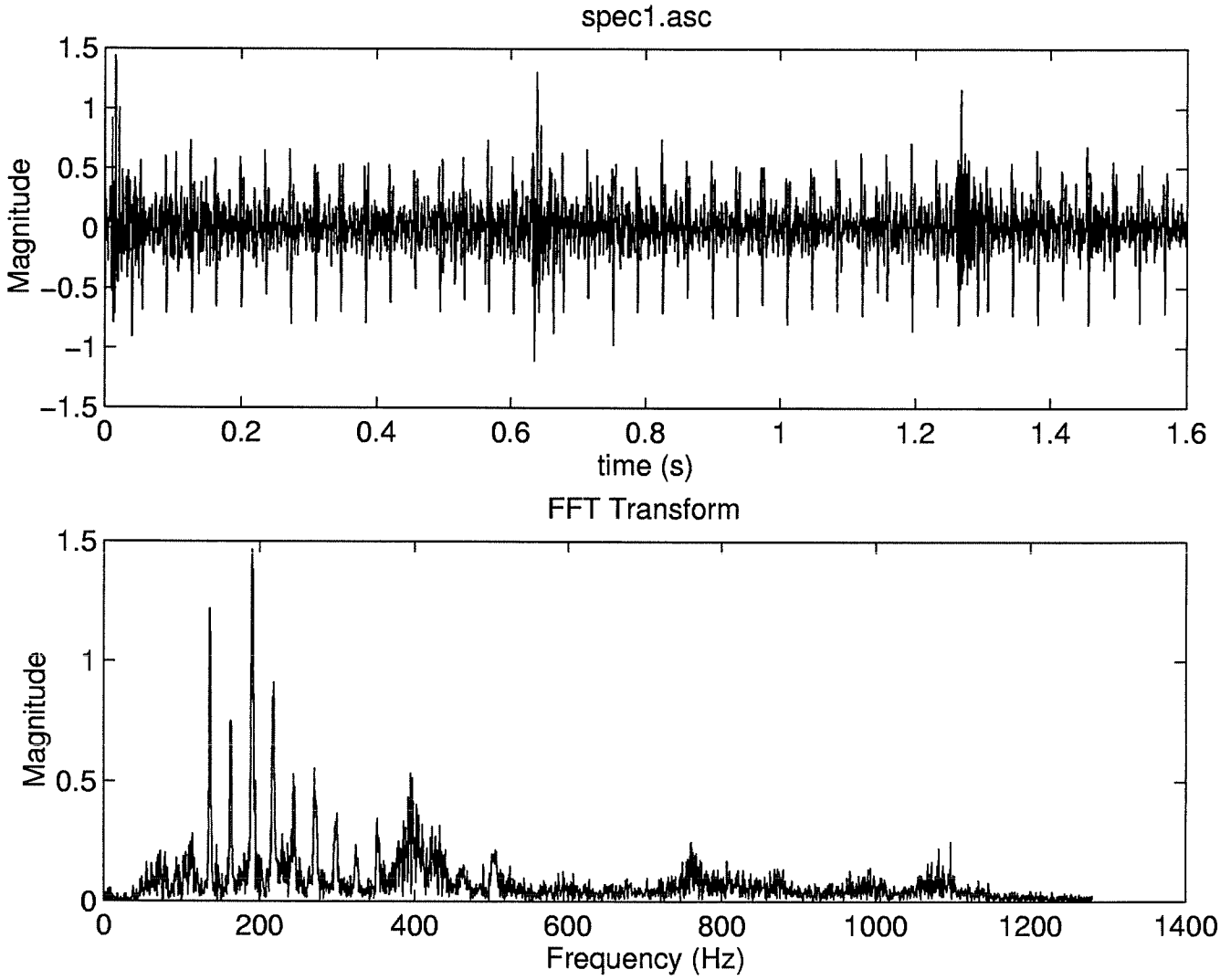

Figure 40: Time and spectrum representation of the signal measured on a defective gearbox.

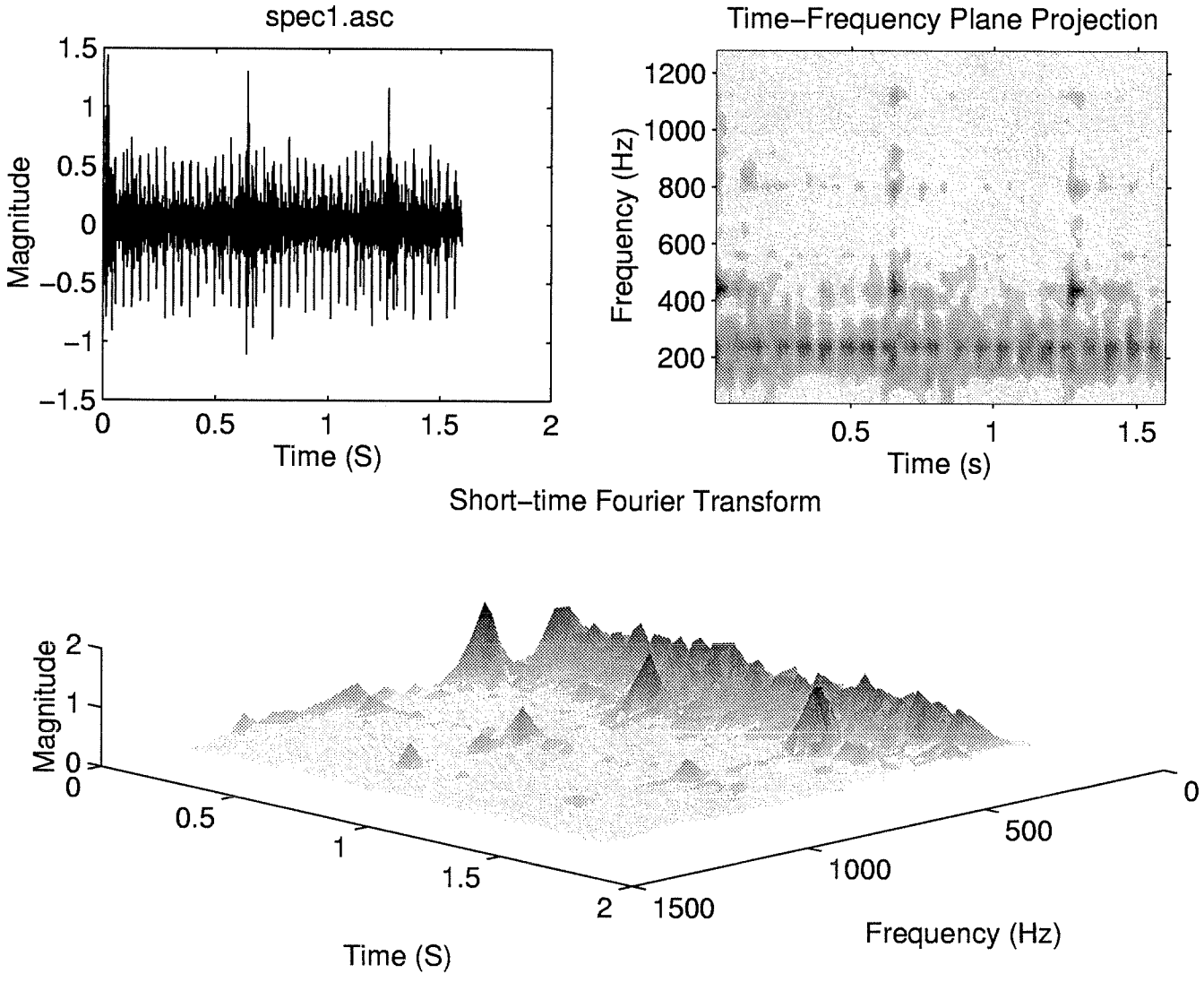

Figure 41: Spectrogram representation of the signal measured on a defective gearbox.

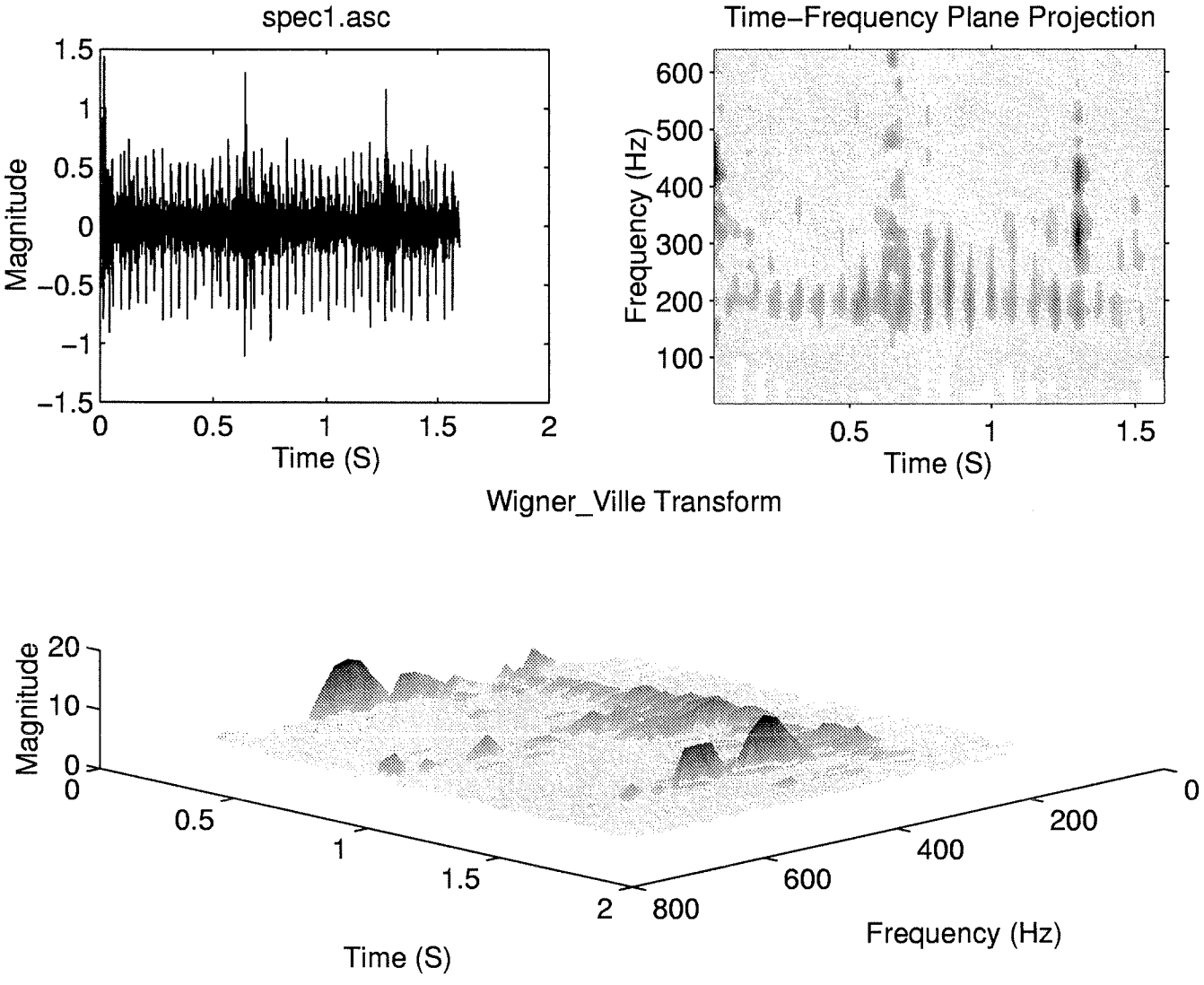

Figure 42: Wigner-Ville representation of the signal measured on a defective gearbox.

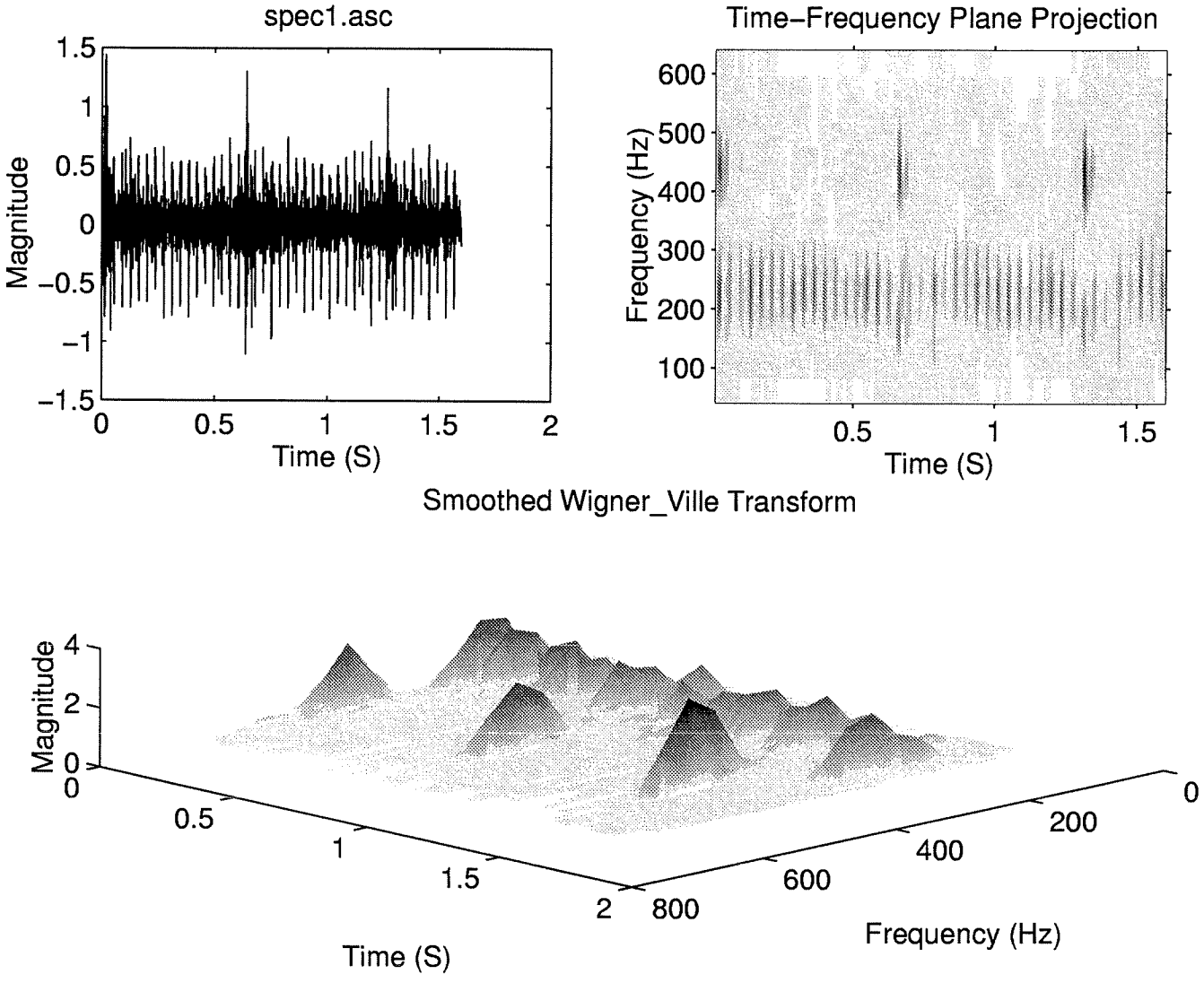

Figure 43: Smoothed Wigner-Ville representation of the signal measured on a defective gearbox.

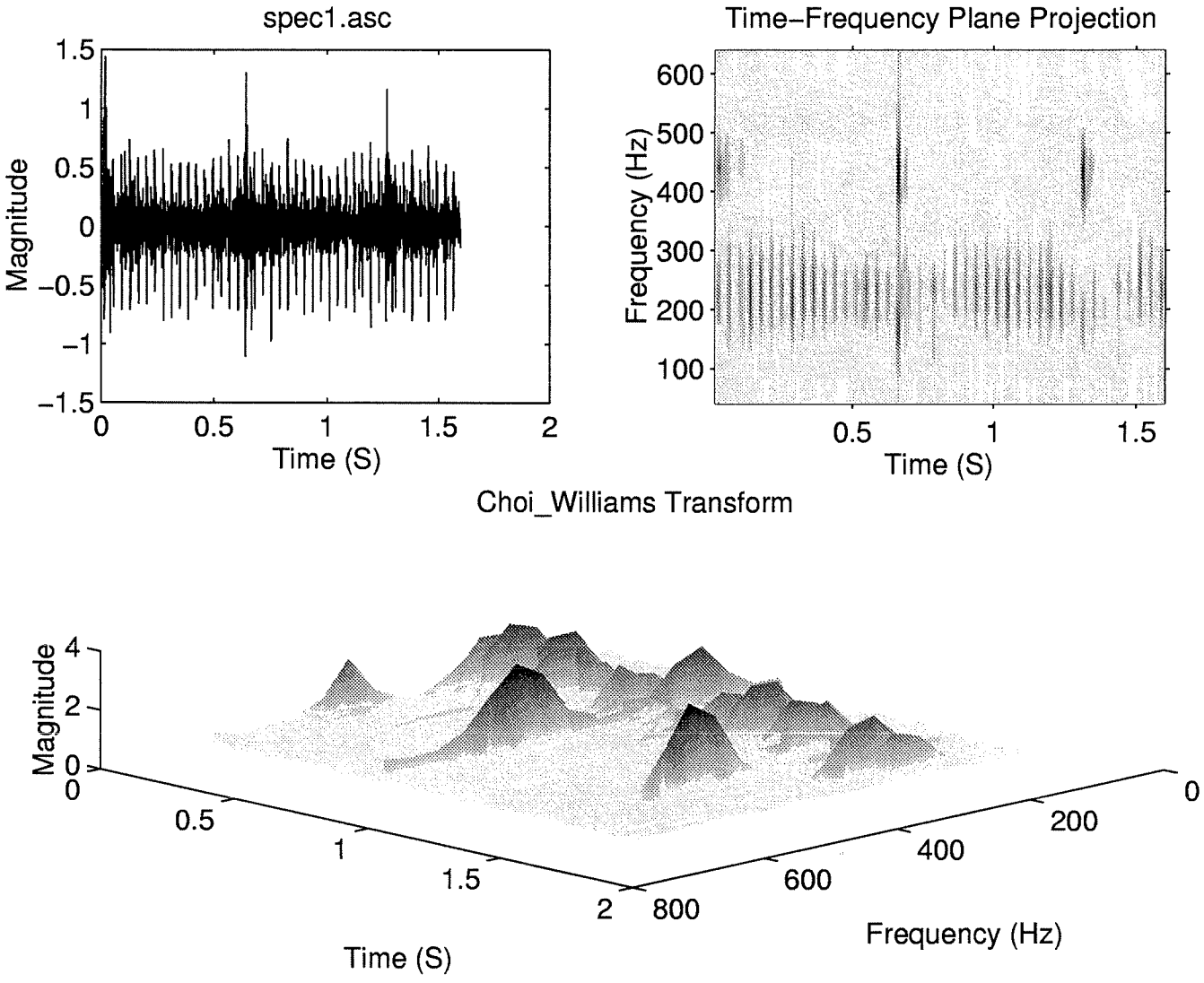

Figure 44: Choi-Williams representation of the signal measured on a defective gearbox.

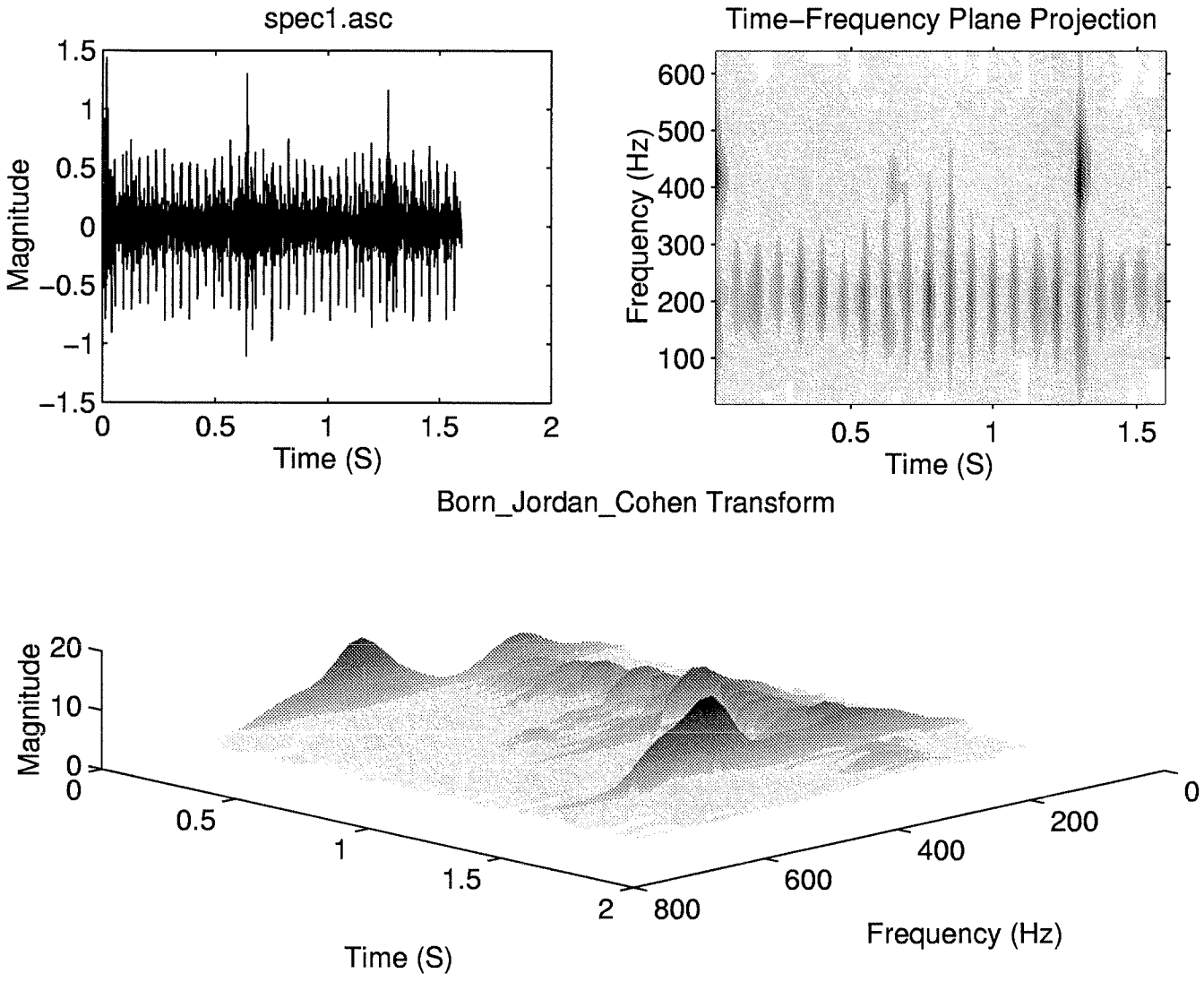

Figure 45: Born-Jordan-Cohen representation of the signal measured on a defective gearbox.

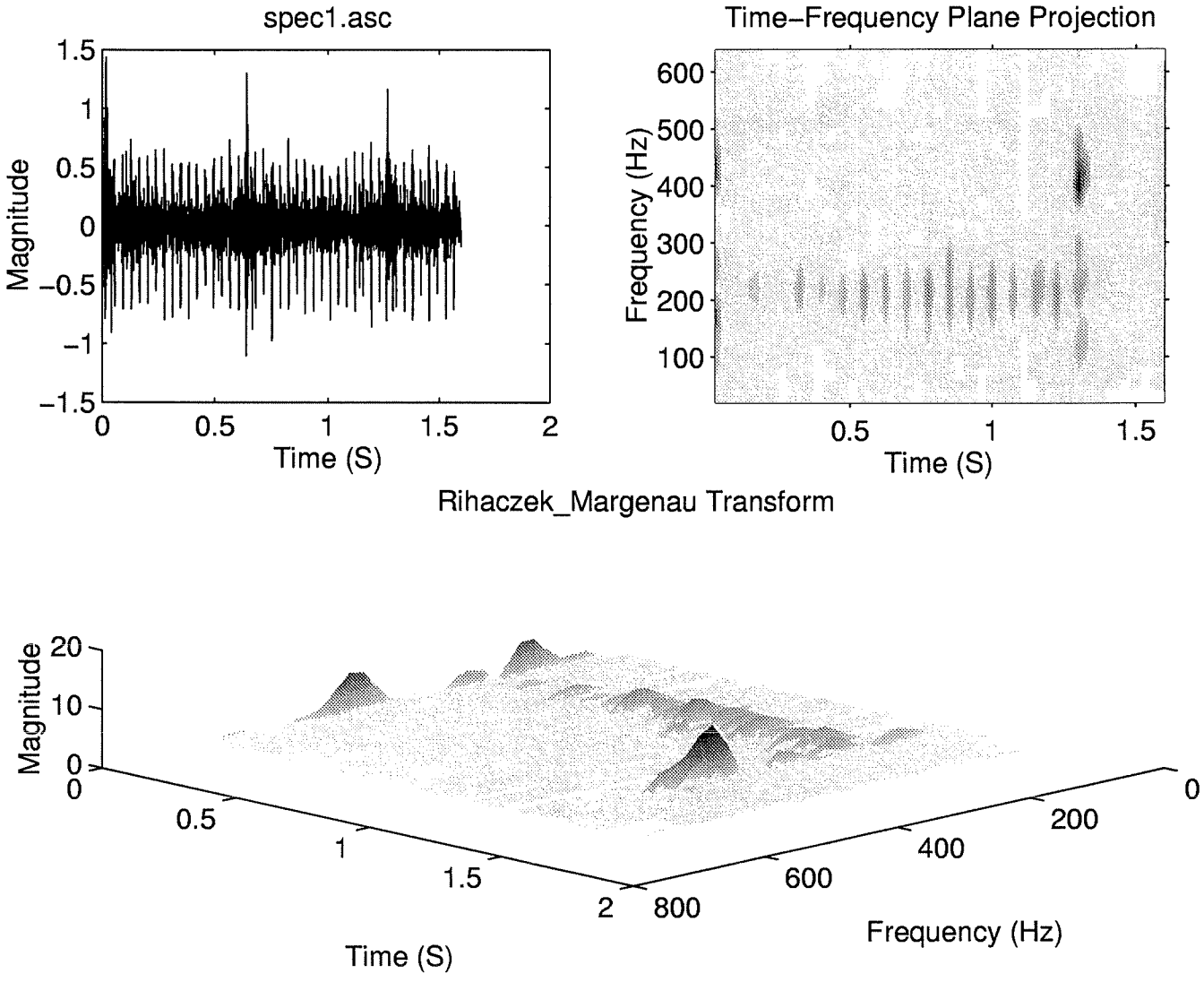

Figure 46: Rihacezk-Margenau representation of the signal measured on a defective gearbox.

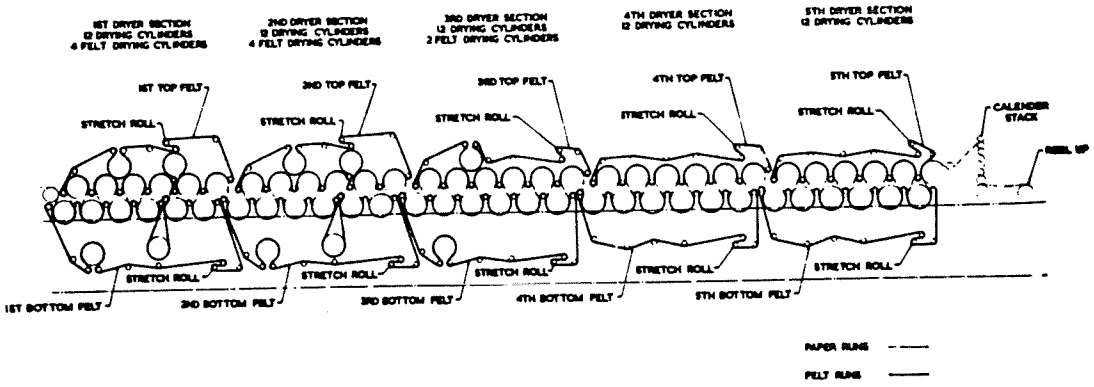

Figure 47: Paper machine dryer part.

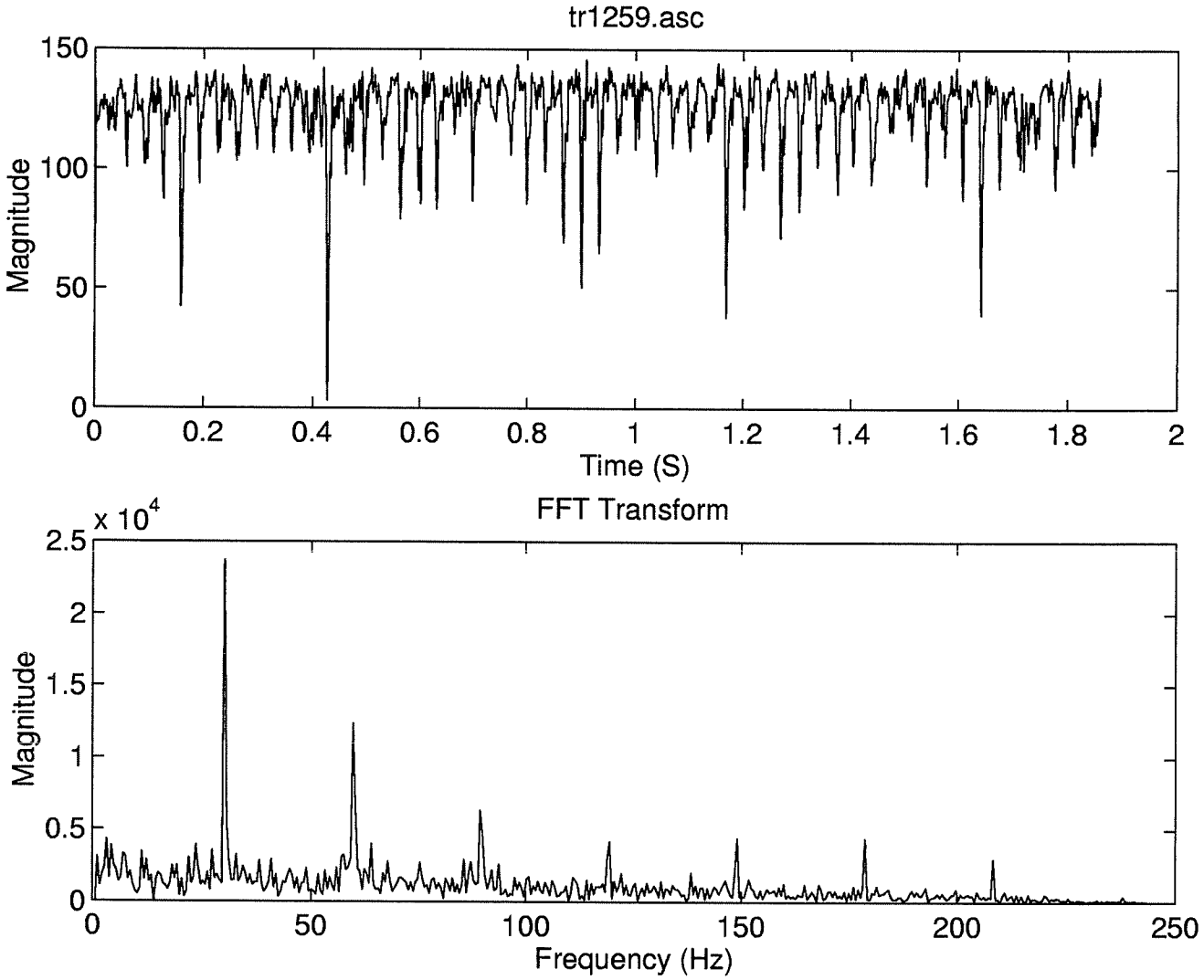

Figure 48: Time and spectrum representation of the signal measured on a defective dryer machine.

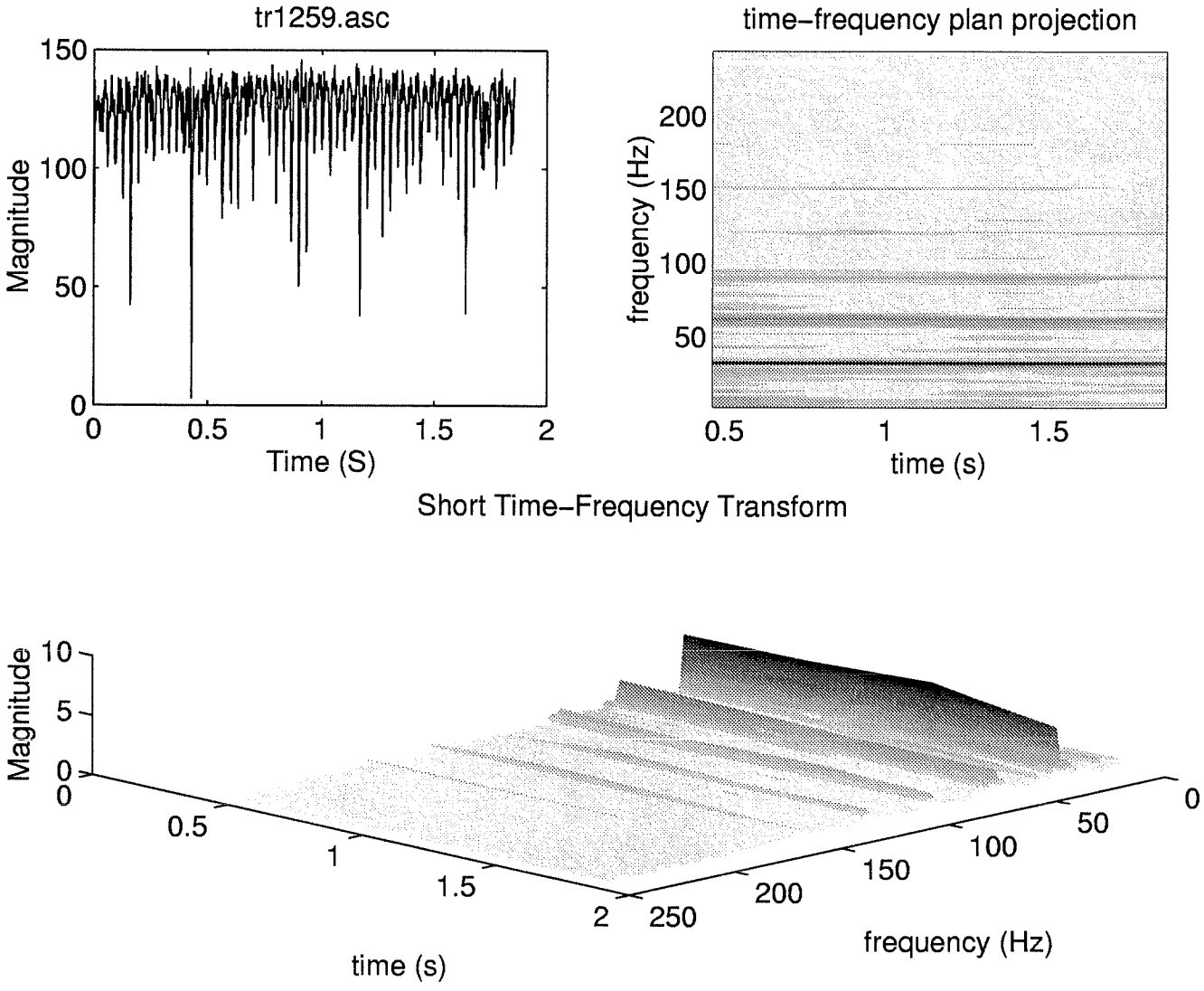

Figure 49: Spectrogram representation of the signal measured on a defective dryer machine.

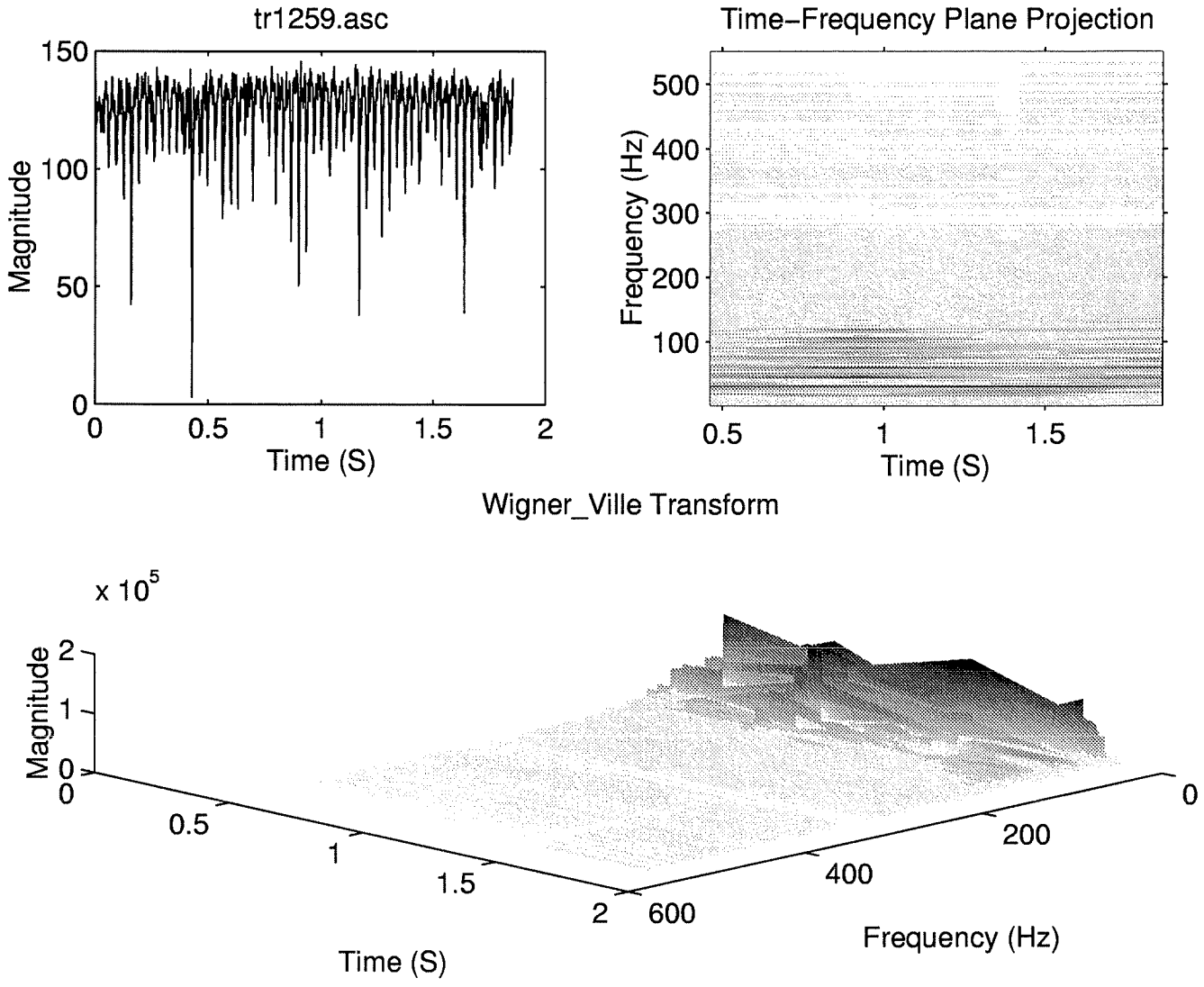

Figure 50: Wigner-Ville representation of the signal measured on a defective dryer machine.

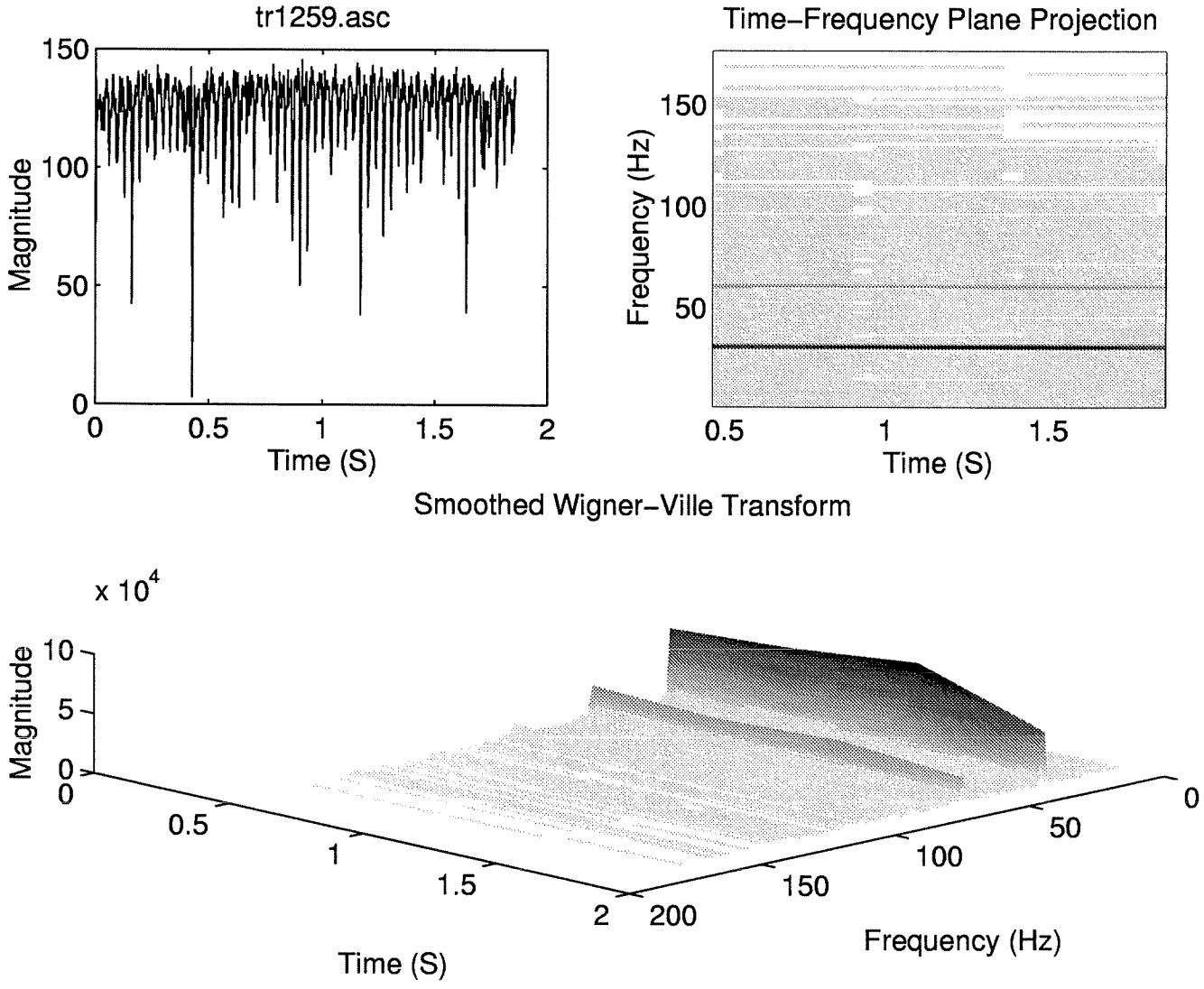

Figure 51: Smoothed Wigner-Ville representation of the signal measured on a defective dryer machine.

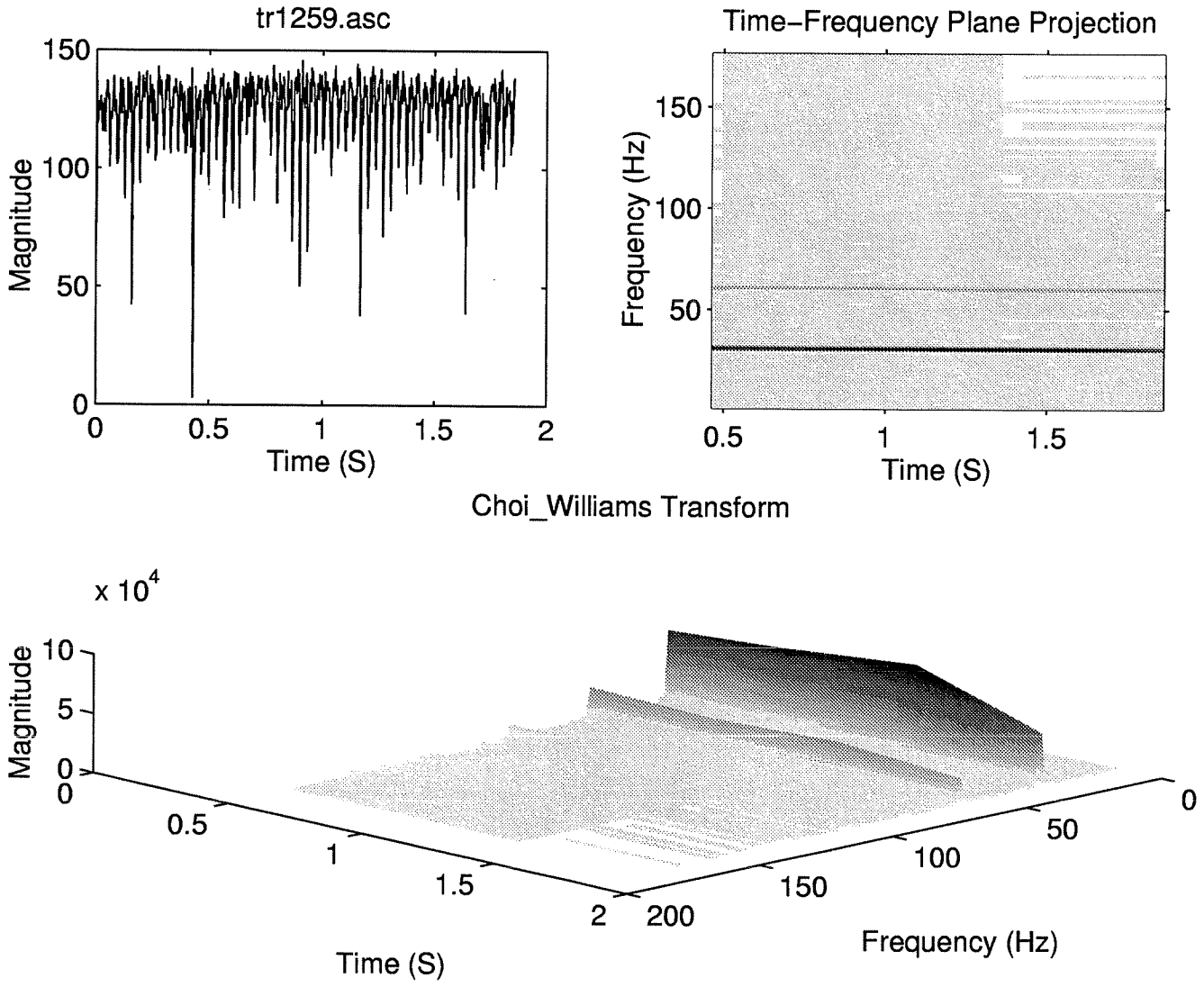

Figure 52: Choi-Williams representation of the signal measured on a defective dryer machine.